



Cand.Scient.Thesis in Physics

Stellar CCD Photometry in the Auroral Zone

Robert Kamben

December, 2000

University of Tromsø

Faculty of Science

Department of Physics

Astrophysics Group

Abstract

Observing pulsating stars in the auroral zone, seemed for many years to be an impossible task. Due to the aurora, the sky is bright and rapidly changing. Precise photometry could only be performed on stars down to 7th. magnitude.

A new instrument for continuous photometry, with the use of CCD technology, and windowed readout, is developed by the Astrophysics group at the University of Tromsø. The Tromsø CCD Photometer (TCP), has been tested for stellar photometry in the auroral zone during the winter 1999/2000.

The windowed readout makes it possible to have sampling time down to 5 seconds, and this open the possibility to use CCD's for fast photometry. The data reduction package developed for the system has proven to work perfectly for reducing the photometric data obtained under aurora conditions. Using individual sky background close to each star observed, for correcting the sky level in front of the star, was specially useful.

The observations was done at the Skibotn Observatory with the 50 cm telescope. In the thesis we present the observations and reductions of the white dwarf GD 358, and the cataclysmic variable star AM CVn.

The performance of the instrument was excellent, and we obtained good photometric data on variable stars down to magnitude 14.5, under aurora conditions. This opens the possibility to use the long arctic and antarctic nights to obtain long continuous light curves.

Contents

preface	vi
1 Introduction	1
1.1 Photometry	2
1.2 Previous Photometry at Skibotn Observatory	3
1.3 Skibotn Observatory	5
1.3.1 The Telescope	5
1.3.2 Auto guiding	6
1.3.3 Telescope control	7
2 Aurora	8
2.1 Frequency and appearance of the aurora.	8
2.1.1 Auroral prediction and space weather forecast	9
2.2 Emission lines	10
2.3 Intensity	12
2.3.1 The auroral substorm.	14
2.4 Filters for observing through the aurora	14

3	Tromsø CCD photometer	17
3.1	Camera head	17
3.2	Filter and shutter unit.	18
3.3	Controller for the camera (Copenhagen controller)	21
3.4	Controller for the FASU	21
3.5	Connections	22
3.6	Computer	22
3.7	Software	23
3.8	Field of view	28
4	The Aurora photometer	30
4.1	Description of the photometer.	30
4.2	Running the photometer	31
5	Observations	33
5.1	Objects	33
5.2	Ready to observe	34
5.2.1	One typical observation night in Skibotn	34
5.2.2	First light at Skibotn Observatory for TCP.	35
5.2.3	Photometry with the TCP.	37
5.3	Testing the TCP in Tromsø	38
5.4	Observations	39
5.4.1	Skibotn 15.-17. February: Observation of AM CVn.	39
5.4.2	Skibotn 22. and 23. February: Observation of GD 358	41
5.4.3	Skibotn 14.-16. March: Observation of LX Serpentis	44

6	Reduction	47
6.1	Real time reduction	47
6.2	Final reduction	48
6.3	Reduction of GD 358	53
6.4	Reduction of AM CVn	55
6.5	Seeing	58
6.6	The aurora photometer	61
7	Results	62
7.1	AM CVn	62
7.1.1	Combining several nights	66
7.1.2	Influence of aurora	73
7.2	GD 358	77
8	Conclusion	84
A	Observation log	87
A.1	17.-20. January 2000	87
A.2	26.-27. January 2000	89
A.3	07.-8. February 2000	89
	Bibliography	90

Preface

I started studying at the University of Tromsø four years ago. After finishing the obligatory courses in Physics, I decided to take a course in general astrophysics as a part of my Cand.Mag degree. This was my first experience with observational astrophysics. I decided to continue with astrophysics for my Cand.Scient degree. Together with Professor Solheim I decided that I in my Cand.Scient.Thesis should use the newly developed CCD Photometer for photometry under auroral conditions.

In January 1999, I started the project. The first semester I followed the two obligatory courses *observational astrophysics*, treating stellar photometry, spectroscopy and imaging, and *Astrophysics I*, treating stellar interiors and stellar modeling. In August the same year I joined a two-week NORFA course in photometry at the Moletai Observatory in Lithuania.

We got our first full night of observation with the Photometer in February 2000. A long dream for the Astrophysics group was fulfilled. After many years of hard work, we could observe faint variable stars in the Auroral zone!

The work with this thesis has been very interesting, and I have had the chance to get many new friends during my time in the Astrophysics group. In July 2000, I went with José to the Nordic Optical Telescope (NOT), at La Palma, Canary Islands. We observed variable Planetary Nebula Nucleus (PNNs) for the Dr.Thesis of Jose. We used the Tromsø CCD Photometer (TCP) software system with the CCD camera at NOT. It was very interesting to see how this 2.5 meter telescope was performing with the same system for photometry that I had been using on our 50 cm telescope at the Skibotn Observatory.

I wish to thank all the people around me that have made it possible to write this thesis. First of all I want to thank my supervisor Professor Jan-Erik Solheim for guiding me through the work. Great thanks to Dr. Roy Østensen

for his job with the whole TCP system, Frank Johannessen for all the help at the Skibotn Observatory, Torfinn Roaldsen and Yngve Eilertsen for assistance with technical problems, Per Ivar Emanuelsen for al problemsolving with Linux, José Miguel Pérez for help with IDL, the observations at the Nordic Optical Telescope, and lots of good advice. Thanks to Anja Strømme for help with L^AT_EX, Synnøve Johansen for the observation of ‘her’ star LX Ser, and Mosab Nasser for the time spent together.

Special thanks are given to my family and to my Maria for all the support during this time.

Robert Kamben
Tromsø, December 2000

Chapter 1

Introduction

The aurora gives a bright and rapidly changing sky in the north, and difficult conditions for stellar observations. For 25 years, the Astrophysics group has built various types of photometers to deal with this problem [Solheim et al. (2000)].

This thesis describes how a newly developed CCD photometer can improve the high speed stellar photometry in the auroral zone.

In this introduction chapter we start with general stellar photometry and explain the concept of continuous photometry . Then we take a look at the work previously done in Tromsø with photometry as a topic, and discuss the problems previous observers faced during observation under auroral condition. After a short introduction on how we can improve the observations, we describe the Skibotn Observatory where the observational part is performed.

Chapter 2 deals with the aurora itself and we discuss, if we can use any filters to avoid some of the light from the aurora.

Chapter 3 is about the Tromsø CCD Photometer (TCP) system. We describe how the different parts work, and then we give a description of the software package developed for the system.

In chapter 4 we describe the one channel photometer used to measure the auroral activity. The photometer was used to get an indication of when we had aurora in the same area of the sky that we were observing with the TCP.

In the beginning of chapter 5, we describe the preparations necessary before we could perform photometry. Then we present the observations that make the basis of this thesis.

During the winter we got three full nights of observation of the cataclysmic variable star AM CVn and two shorter runs of the white dwarf GD 358. In chapter 6 we go through all the reductions for the best extraction of data with the TCP software. Then we use this to reduce the data from AM CVn and GD 358.

The result of the reduction, and a discussion of how the aurora is influencing the observations, comes in chapter 7.

In the final chapter we discuss the results, and how this instrument can be used in the future, continuing the good performance demonstrated in this thesis.

1.1 Photometry

Photometry, in the sense used here, is measuring of the photons from a star. The science of photometry has a long history and started 2000 years ago with classification of stars after their brightness, with the brightest star as class one and the faintest class six. The instrument used was the naked eye. The response of the eye is nearly logarithmic, so the system used in the ancient time was logarithmic in terms of intensity. A class one star is about 2.5 times brighter than a class two star, a class two star is about 2.5 times brighter than a class three star, and so on. This can be expressed in a precise mathematical law:

$$m_1 - m_2 = -2.5 \log(E_1/E_2) \tag{1.1}$$

where m_1 and m_2 are the magnitudes of star 1 and 2, and E_1 and E_2 are the energies per unit area at the surface of the Earth for star 1 and 2. The scale is relative, and the magnitude of one star is expressed in terms of the magnitude of another. To fix the scale it is decided that magnitude 0 is the magnitude of the star Vega [Bohm-Vitense (1989)]. The magnitudes as we see them from the Earth, and just described, are called apparent magnitudes. The apparent brightness is a function of the objects intrinsic brightness and its distance. A second type of magnitude, that is only a function of the intrinsic brightness, is called absolute magnitude, M . It is defined as the apparent

magnitude of the object if it is moved so its distance from the Earth is ten parsec [Kitchin (1991)].

The type of photometry we have used in our observations is called continuous photometry, and is used to measure the variation of flux from the star as a function of time. The objects we are interested in are periodic variable stars, where the maxima and minima of the stars brightness recur at nearly equal intervals. There are many types of variable object, with periods ranging from years down to milliseconds. Of practical reasons, continuous photometry is performed to determine periods less than a few hours. To determine the right periods, it is important to get as long light curve as possible. For one telescope, the length of the night sets a limit for the length of the light curve. To obtain longer light curves, several telescopes, placed around the world, can co-operate in observing the same star, and make a continuous light curve of several days. The integration time and precision of each measurement depends on the brightness of the star, and the type of telescope and detector used.

With the introduction of the photo-multiplier, it was possible to resolve the light curve in shorter time intervals than with photographic plates, and therefore determine the short period variations. During the last ten years, CCD technology has taken over most of the use earlier done with photographic plates and photo-multiplier tubes. The CCDs has higher quantum efficiency, good linearity, simultaneous measurement of the background, and a better possibility of data handling and reduction. But for the case of continuous photometry of rapidly changing objects (high speed photometry), the case is different. The CCD chip has to be read out after each measurement, and this takes typically from 10 seconds or longer [O'Donoghue (1995)]. The read-out time sets a limit how short sampling time we can use. The photo-multipliers dont have this problem.

A technique called windowing, makes it possible to read out the chip in shorter time. In the following chapters we will explain how the Tromsø CCD photometer, with the windowing function, works as a high speed photometer.

1.2 Previous Photometry at Skibotn Observatory

From the beginning photometry has been an important field for the Astrophysics group in Tromsø. In the history of the Skibotn observatory, several

thesis projects has been done with photometry as topic.

Hans Kristian Myrabø did in 1976 a study of stellar photometry in the auroral zone [Myrabø (1976)]. He started with a one channel classical photometer, but had to develop a new system because of the rapidly changing background. To deal with this he made a chopping photometer with one channel and observed target star and background. With this system he could measure star down to magnitude 5 under normal auroral substorms.

In 1978/79 Høydalsvik studied star occultation at the limb of the moon with the use of photometric observations [Høydalsvik (1980)]. He used a two channel photometer built in Austin, Texas, on the same telescope as we use today. He observed 11 of 120 possible occultations. His conclusion from the observations was that both photometer and telescope had to be improved to get good quality data. He expected a improvement of the signal to noise ratio of 8-9 times with an improvement of the instruments.

Egge studied variable binary stars of the W Ursae Majoris type. He used the same telescope as Høydalsvik with a improved version of the chopping photometer [Egge (1982)]. He obtained good results on the type of stars he observed.

In 1996 Tommy Thomassen improved the measurements with his work of UBV photometry. He reached 1 mma on a 6.1 V magnitude star, but had to stop observing under the aurora conditions [Thomassen (1996)]. His conclusion was that the measurements of the sky were to far away from the star, and the correction for sky variation failed under aurora conditions with the technique he used.

Construction of new instruments has been important to improve the quality of observations. Specially a three channel photometer works very well on WET campaigns around the world, but again for observations in Skibotn the aurora disturbs. Another problem with photo-multiplier photometers, and the strong background light in the auroral zone, is that it is difficult to see stars fainter than magnitude 8-9.

To deal with problems like this, CCD-technology is good. Instead of counting the photons from the star with a photomultiplier, a picture is taken and we can measure the amount of light inside a chosen aperture around the star. For photometry with CCDs, we then take a time series of pictures, and get a light curve by measuring the light around the star in each picture. CCD-technology is widely used on the observatories around the world, but it has

some disadvantages when used for high speed photometry, as we discussed previously.

The Astrophysics group in Tromsø has constructed a system for high speed photometry with the use of CCD technology. The Tromsø CCD Photometer (TCP), was a Doctor Thesis project for Roy Østensen, and the first version was finished November 2000. The readout time is around 23 seconds for a full read-out of the 1K*1K chip like the TK 1024 we use. With the windowing used for the TCP, we can read out 5 windows in 2.3 seconds. With a sampling time of 20 seconds, we spend 90 % of the time observing the target, background and the reference stars, and the last 10 % for readout time.

My thesis project has been to test out the system in Skibotn for high speed photometry under the influence of the aurora.

1.3 Skibotn Observatory

The Skibotn Observatory was built in the years 1977-1978. The position is E 20 21.9 N +69 20.9. The observatory is placed in a valley surrounded by high mountains. Wind turbulence can be high, and the mountains prevent from observing below 10°. The season for observing is from October to March. It's about 80 clear nights in this period, but only 15-20 of these can be considered to be of photometric quality. Due to aurora and night sky emissions, the sky is quite bright (15mag/Arcmin² while "normal" dark observatories with 5 mags fainter sky) and is rapidly changing due to auroral substorms (Information from the Skibotn Observatory homepage).

At the observatory we have bedrooms, kitchen and a computer room with Internet connection.

1.3.1 The Telescope

The main telescope at the observatory is of type Cassegrain reflector. The primary mirror has diameter $D= 50$ cm, and the focal ratio is $f/10$. This gives focal length $f/10 = 50 \rightarrow f = 500$ cm, and focal plane scale $\theta = d/f = (1 \text{ mm}/5000 \text{ mm})\text{rad} = 41.25$ arcseconds per mm when $d=1$ mm.

Attached to the main telescope we have one refractor for finding, one small view-finder and one Schmidt-Cassegrain Celestron reflector for auto guiding.

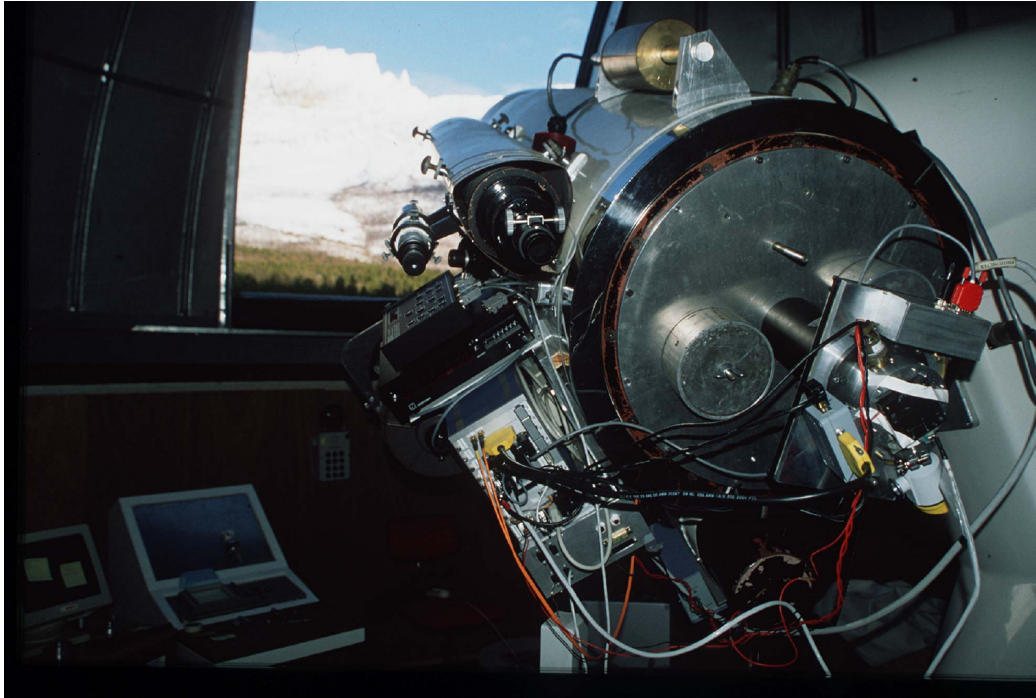


Figure 1.1: The Skibotn telescope with the Tromsø CCD photometer.

The Celestron primary mirror is $D=20$ cm, and the focal length is 160 cm. ($f/8$). The focal plane for this main guider, valid for the whole field of view is:

$$\theta = d/f = 1/1600 \text{ rad} = 128.915 \text{ arcseconds per mm.}$$

1.3.2 Auto guiding

For auto guiding we use a Sbig4 auto guiding CCD-camera attached to the Celestron. The camera is operated from an old Intel 386 computer running on Windows 3.11 with SBig CCD-track software.

The system is easy to use, but we experienced some problems with it. The mirror cell of the main mirror in the Celestron is worn, and the mirror can move a little bit from side to side. During observations the position of the guiding star moves because of this. A new system is under development with the auto guiding integrated in the main telescope. This will be ready in 2001.

To start auto guiding, we run the CCD-track program which works as follows: We choose guiding in the menu and take an exposure. An image of the field

will appear on the screen, and we point out the star we want to use for auto guiding and start the tracking. If there are no stars in the field, we have to move the Celestron manually with three bolts to find a star, which can be very difficult. The guiding camera has a flip mirror and an ocular, so we can find a star visually. The CCD-chip is small, and the field in the ocular is much larger than we get on the chip, so it is important to center the star.

1.3.3 Telescope control

The position of the telescope is controlled by a DOS computer in the control room. With the program **deskview** (dv) we can set the position (Ra, D, Alt, Az) and the time. It is important to start the **dv** program before turning on the telescope to keep the right position in the computer from the last time we used it. We can move the telescope from the dome with a hand controller or a fixed control box. In the control room we have a hand controller which is very helpful in keeping the star in the right position when we see it on the screen of the TCP computer. Because of the movement of the mirror in the Celestron the auto guiding was not working properly, and we often had to correct manually.

Chapter 2

Aurora

Aurora Borealis means the northern dawn. When the aurora is observed from lower latitudes it appears red, and from this it got its name. In these places the aurora is a rare and exotic phenomena, and not a problem for observers. In the auroral zone, the background sky varies more and is brighter than outside, and this gives special demands to the equipment used for observing. In this thesis we investigate how photometry with the TCP, and high speed photometry in general, can be performed under the influence of the aurora.

We start this chapter with the frequency and appearance of the aurora. Then we make an overview of the energy distribution and intensity. At the end of the chapter we look at the possibility to avoid some of the aurora with the use of filters.

2.1 Frequency and appearance of the aurora.

After the discovery of the solar cycle in 1844, it was realized that the auroral occurrence is strongly related to this cycle. The cycle has an period of around 11 years in average. The time between each maxima varies from 7.3 to 17 year and between the minima from 8.5 to 14 years [Brekke (1998)]. The total numbers of sunspots varies from cycle to cycle. When the number of sunspots is low, we also have a low magnetic activity in the upper atmosphere and visa versa. However, the strongest magnetic distortion is not following the maximum number of sunspots in one cycle. From a study of the relation between the maximum number of sunspots and the magnetic activity in

Tromsø, the maximum activity occurs three to four years before the next minimum [Brekke (1998)]. This is because the maximum distortion comes from the sunspots at high latitude, where the sunspots are created. This can give an indication of when the next maximum of the cycle will be. During one year it seems that we have more aurora at equinoxes than solstices, even when corrected for clouds and number of dark hours per night [Brekke (1997)]. This mean that we expect high activity around March and October, and a minimum in June. The sun has a rotation period seen from Earth close to 27 days and the aurora frequently show a 27-day periodicity. In the time scale of a day, the auroral activity often starts in the afternoon and can last until about 2 o'clock in the morning.

The maximum appearance of the aurora follows approximately the geomagnetic latitudes close to 67° N and S. The aurora form a belt around the geomagnetic poles, and this is what we call the aurora ovals. The oval has a fixed position with respect to the sun while the sun is rotating under it. In the north of Norway we enter the oval in the afternoon and pass through it during the night. In the night aurora the particles comes from the antisunward side of the magnetosphere and often makes a strong and active aurora. On the day side of the Earth the particles comes more directly from the sun and makes a more quiet day aurora. This can be seen on Svalbard in wintertime where it is dark 24 hours a day. The ovals are not static, but changes in size and position because of changes in the activity of the sun. It is compressed on the sunward side and stretched out toward the antisunward side. When the activity is low, the oval is smaller and we see the aurora north of us and it is usually weak. With high activity we can see it south of us, and it can be seen from south of Norway and even more south. In figure 2.1 we see a drawing of the Northern aurora oval. The geomagnetic pole is marked in the center of the oval. The area on Earth where the oval appears most of the time is called the auroral zone. The height of the aurora is most often from 90 to 130 km with the base of the auroral layer at 100 km [Bone (1991)], but some stretch up to hundreds of km above the Earth.

2.1.1 Auroral prediction and space weather forecast

With the modern satellites and constant observation of the sun and magnetic activity in the atmosphere it is possible to make predictions of auroral occurrence and report the coming space weather. On the Internet it there are several sites with information of the magnetic and auroral activity. NASA has

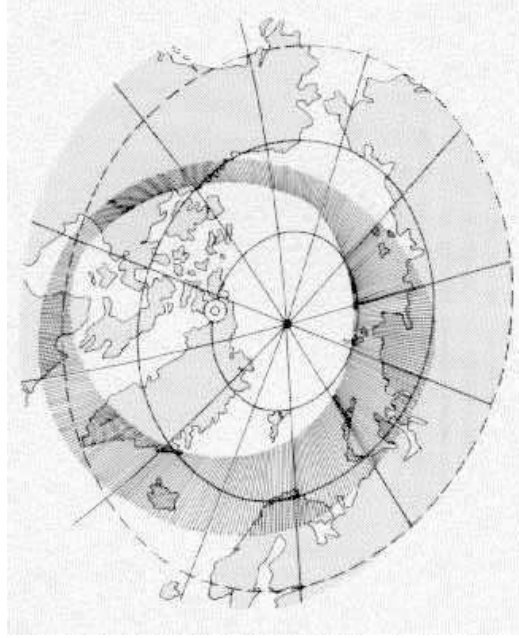


Figure 2.1: Drawing of the auroral oval over the northern hemisphere.

a space weather page [www.sunspotcycle.com] and daily information of geomagnetic activity at [www.spaceweather.com]. The National Oceanographic and Atmospheric Administration (NOAA) uses current satellite passes and statistical data to estimate the position and intensity of the auroral oval at [www.sel.noaa.gov/pmap]. Geomagnetic data from Tromsø Geophysical Observatory is found at [www.tgo.uit.no/geomag.html].

2.2 Emission lines

Auroral spectroscopy was introduced by Ångström in 1866, when he observed the yellow-green emission, and determined the wavelength to 5577 units. The unit would later be known as Ångström. 60 years later the reason for this emission was found: the transition in atomic oxygen from the metastable excited state 1S to the lower 1D . The line is centered around 100 km (Brekke (1997)). The different emissions are due to transition between energy states in neutral or ionized N_2 , O, O_2 and N. The wavelength of the light emission due to transition between two energy layers, E_1 and E_2 where $E_2 > E_1$, can be expressed as:

Emission(\AA)	Upper state	Lifetime	Particle
$\lambda 5577$	OI^1S	0.7 s	O_2
$\lambda 2972$			O
$\lambda\lambda 6300 - 64$	OI^1D	110 s	N_2
$\lambda\lambda 7319 - 30$	OII^2P	5 s	N_2
$\lambda\lambda 3727 - 9$	OII^2D	2.9 h	N_2
$\lambda\lambda 10395 - 404$	NI^2P	12 s	N_2
$\lambda 3466$			O_2
$\lambda\lambda 5199-201$	NI^2D	26 h	O_2, O, NO
$\lambda 5755$	N_{II}^1S	0.9 s	O_2, O
$\lambda 6584$	N_{II}^1D	246 s	O_2, O
$N_2(LBH)$	$^1\pi_g$	0.14 ms	
$2(VK)$	$A^3\Sigma_u^+$	$2s^n$	O
$O_2(Atm.)$	$b^1\Sigma_g^+$	12 s	N_2
$O_2(IRAtm.)$	$a^1\Delta_g$	60 min	O_2
$N_2^+(1N)$	$B^2\Sigma$	70 ns	$N_2 + O_2$
$N_2^+(M)$	$A^2\pi$	$14\mu s$	N_2
$N_2(1P)$	$B^3\Sigma$	$6\mu s$	N_2
$N_2(2P)$	$C^3\pi$	50 ns	O_2
$O_2^+(1N)$	$b^4\Sigma$	$1.2\mu s$	N_2

Table 2.1: Auroral emission lines and their emission source (upper state). Lifetime and dominant particle is also given. Table from Brekke (1997)

$$\lambda = \frac{hc}{E_2 - E_1} \quad (2.1)$$

where $c(=3 \cdot 10^8 \text{ m/s})$ is the speed of light and $h(06.63 \cdot 10^{-34} \text{ J/s})$ is Plank's constant. The ionization potential is of the order $E_I = 15 \text{ eV}$ and $E_2 > E_1$ [Brekke (1998)]. This gives that the different emissions in the aurora has wavelengths larger than the one corresponding to this energy.

$$\lambda_I = \frac{E_I}{hc} = 824 = 82.4 \text{ nm} \quad (2.2)$$

In table 2.1, we see the different auroral emissions and their upper state emission source, lifetime and dominant particle. The emissions in the table without a indicated wavelength are bands with more than one wavelength. The $N_2^+(1N)$ has a maximum at 4278 \AA .

In the figures 2.2 to 2.5 we see the aurora specter from 3100 \AA to 9000 \AA . The particles that gives the different emissions, are marked in the figures.

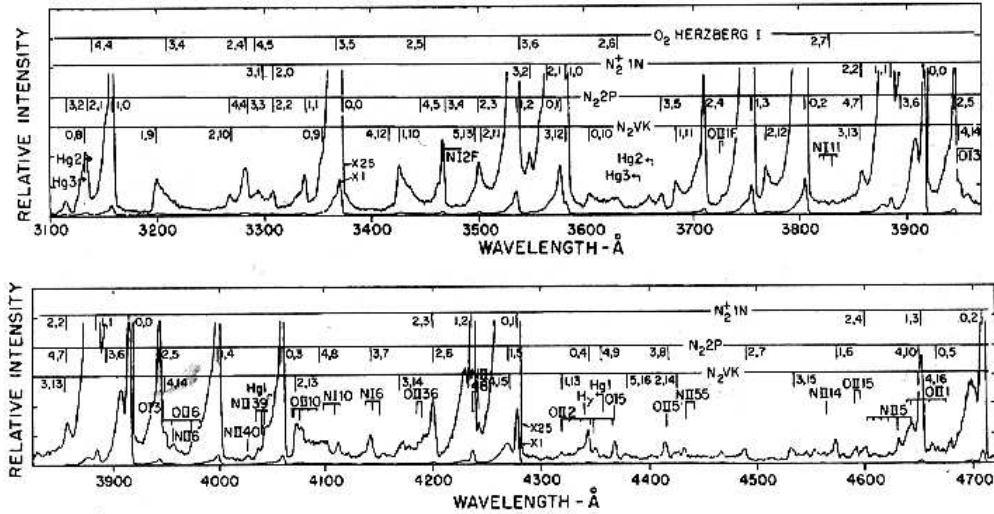


Figure 2.2: Auroral spectrum between 3100 and 4700 Å. The upper curve is the same as the lower one x25. (From Jones (1974))

The intensity of the emissions are not constant, and the figures shows mean values relative to each other..

2.3 Intensity

The intensity (I) of the aurora is often given in Rayleigh, (R). One R is 10^6 photons \cdot cm^{-2} (col) $^{-1}s^{-1}$, (col because we have volume emission). $4 \cdot \pi \cdot I$ represent the total emission of photons $cm^{-2}s^{-1}$.

To classify the aurora we use the strong green line from oxygen at λ 557.7 nm. A logarithmic classification system called 'International Brightness Coefficient' is defined the way that aurora with coefficient I, II, III and IV emits the green oxygen line $4 \cdot \pi \cdot I$ equals 1, 10, 100 and 1000 kR.

The aurora have many forms and structures. We can divide the forms in arcs, bands, patches, veils and rays. The structure can be homogeneous, striated or rayed. The temporal behavior can be described as quiet, pulsating, flickering or flaming [Eather (2000)].

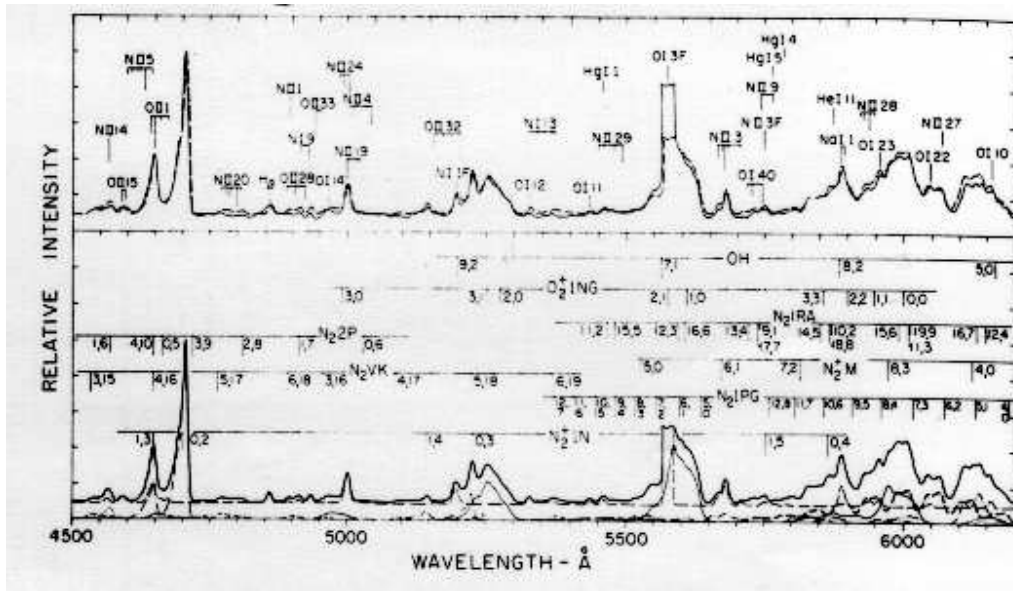


Figure 2.3: Auroral spectrum between 4500 and 6200 Å. Upper panel: solid line is the observed average spectrum of aurora with I(5577) in the range 20-60 kR ; dashed line is total synthetic spectrum. (From [Jones (1974)])

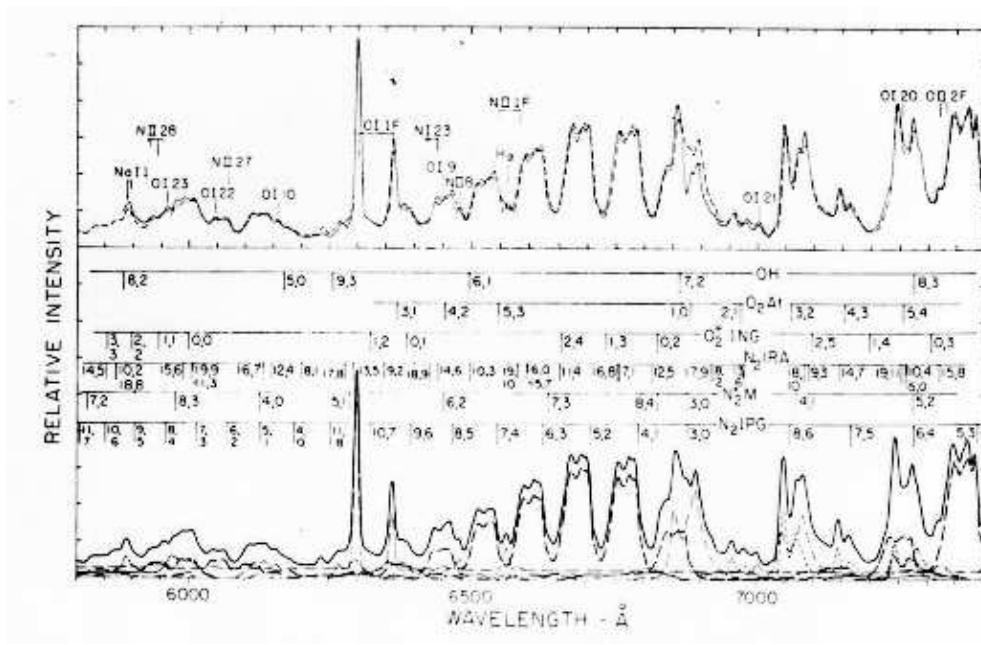


Figure 2.4: Auroral spectrum between 5800 and 7400 Å (continuing of the previous figure).

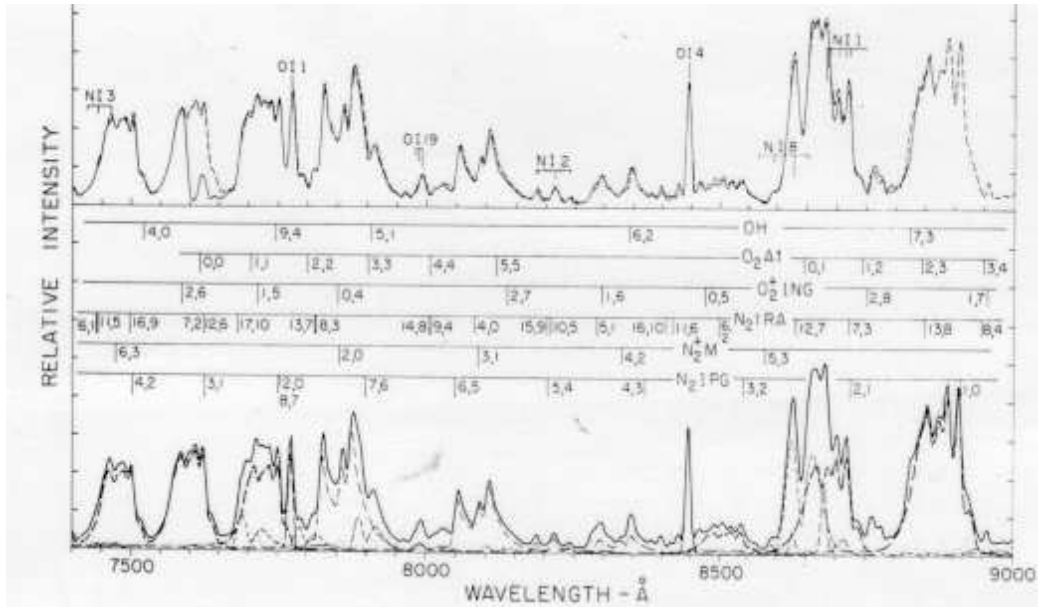


Figure 2.5: Auroral spectrum between 7200 to 9000 Å (continuing of the previous figure).

2.3.1 The auroral substorm.

An aurora event can be divided into four phases, the quiet phase, growth phase, expansion phase and recovery phase. Together these phases form the auroral substorm. The highest intensity is observed during the expansion phase, A full description of the different phases is found in (Brekke, 1997, page 477-480)

2.4 Filters for observing through the aurora

To avoid some of the background noise, we planned to make a filter that removes most of the strong green line at 5577 Å in the aurora. The line is the dominant background emission in the visual part of the spectrum. Observing faint stars, we wish to receive as much light from the objects as possible. A filter that blocks part of the spectrum will give us less signal, but hopefully also less noise. What we wish to achieve is a better signal to noise ratio than without blocking the green line. Before ordering such a filter, we have to calculate what effect we can expect from it.

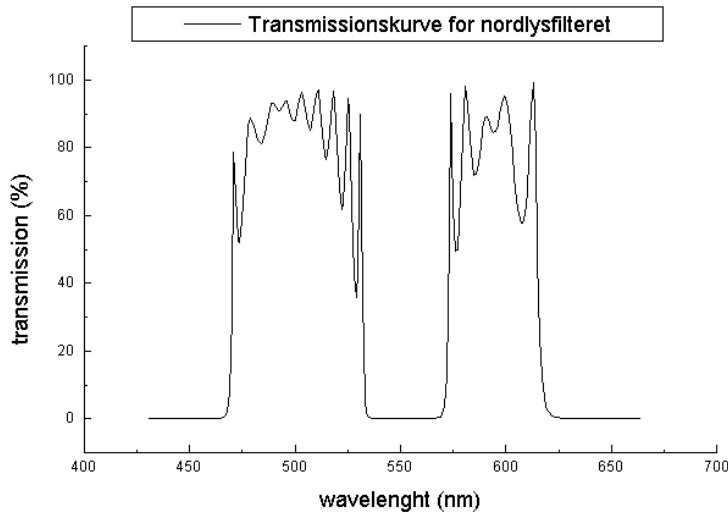


Figure 2.6: Filter profile for the proposed aurora filter. The filter transmits 430-630 nm, and blocks the 55.7 nm line.

We got an offer for such a filter from Custom Scientific. The filter profile is seen in fig. 2.6. The filter in the profile has transmission from 470 to 610 nm. With a different design they could make a filter with transmission from 430 to 630 nm.

The filter blocks much of the light from the star, and this can be a problem because we observe faint object, and want to receive as much light as possible. To calculate the signal to noise ratio with and without the filter we need a lot of information of the conditions in the auroral zone. First of all we need to know the intensity of the aurora in the 557.7 nm line. Then we need the average background light we observe. It is also important to have in mind how much of the observing time we have aurora compared to the stable conditions. We also don't know how the TCP system can correct for the aurora.

No conclusion was made before the start of observation in January 2000. We decided not to order the filter, but use the B-filter we already had.

The chip itself set a limit for in what wavelength we receive light. In figure 3.3 we see the quantum efficiency of the chip as a function of wavelength,

One of the conclusions of the work of Thomassen in Skibotn, was that to avoid aurora, one should use the filter b [(Thomassen, 1996, page 116)] from

λ (3160-3330)Å
 λ (3385-3510)Å
 λ (3590-3690)Å
 λ (4090-4190)Å
 λ (4290-4620)Å
 λ (4730-5185)Å
 λ (5310-5510)Å
 λ (5700-5800)Å

Table 2.2: Pass bands wider than 100 Å with little aurora [From (Myrabø, 1976, page 71)]

the Crawford photometric system, with the central wavelength at 4700 Å, and fwhm of 300 Å. Myrabø found in his work 8 areas with band width more than 100 Å with no significant auroral emissions [(Myrabø, 1976, page 71)]. The areas are put in table 2.2.

In the B filter used in the TCP we have the N_2^+ (1 neg) 3914, 4278 and 4709 emissions. Figure 3.3 in chapter 3 we show the filter profile of it. The filter was used for all the observation this winter. As we will describe later, we used a one channel photometer with a small band filter at 4278 Å to measure the aurora activity during observation with the TCP. Comparing the measurements from the aurora photometer and the TCP, we see they are quite similar. That may indicate that the λ 4278 Å emission is dominating in the background (see figure 5.4.1 for comparison of raw light curves of the two instruments).

Chapter 3

Tromsø CCD photometer

The Tromsø CCD photometer, TCP, is a newly developed system for high speed photometry. It uses the Copenhagen University Observatory (Brorfelde) CCD controller system, and a software package developed by Roy Østensen. A full description is found in the Dr. Thesis of Østensen [Østensen (2000)], and a shorter description is found in Østensen and Solheim (2000).

The system is fully portable, and has already been used on travels to Moletai Observatory in Lithuania, and the Nordic Optical Telescope (NOT), at the Canary islands. The TCP consists of a camera head, a filter end shutter unit (FASU), a controller for the camera, a controller for the FASU, and a portable computer.

3.1 Camera head

The camera head is of aluminum, and is made to hold vacuum. To obtain vacuum, we had to pump the camera head before we went to the Observatory. Figure 3.1 shows the parts and connections to the unit. The chip is placed in the center of the vacuum chamber. A window of 40 mm diameter lets the light come to the chip. The chip is cooled by a thermic peltier element, and the heat is removed with an electric fan on the back side of the camera head. For use in warmer areas than Skibotn, we have prepared it for water-cooling.

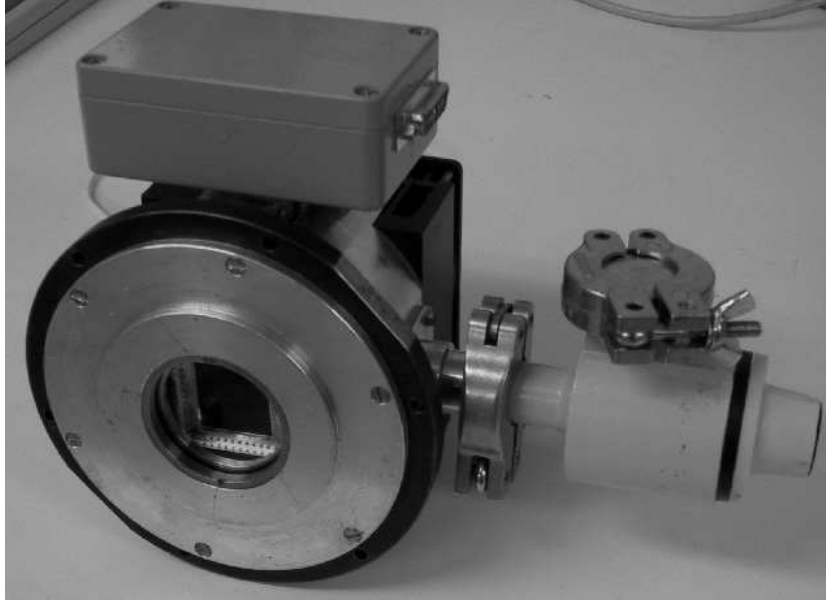


Figure 3.1: Picture of the camera head. The chip is seen behind the window, down to the left.

3.2 Filter and shutter unit.

The FASU is made of aluminum, and is attached to the camera head in one end, and to the back plate of the telescope in the other. It contains a filter wheel with place for 6 filters, and the shutter. In the filter wheel we have one hole completely covered, one open, and in the other holes the filters red, yellow, blue and violet. The size of the filters are 40 mm. A sensor registers when the filter wheel is in the position for the blue filter. The other positions are found by stepping from this position.

The shutter was original designed with two openings in the circular shutter plate, and the plate turned 180 degrees for each measurement. During the testing period, we found that this gave a teeth like pattern in the light curve. The reason was that the shutter did not stop in exactly the same position after a half turn. To solve this we covered one of the openings, and turned the shutter wheel 360 degrees between the measurements.

In figure 3.2 we see a picture of the FASU from the inside. We have covered some of the areas with light absorbing ‘flock’ paper to reduce reflections. In the picture the original shutter plate that we used is replaced with a new one.

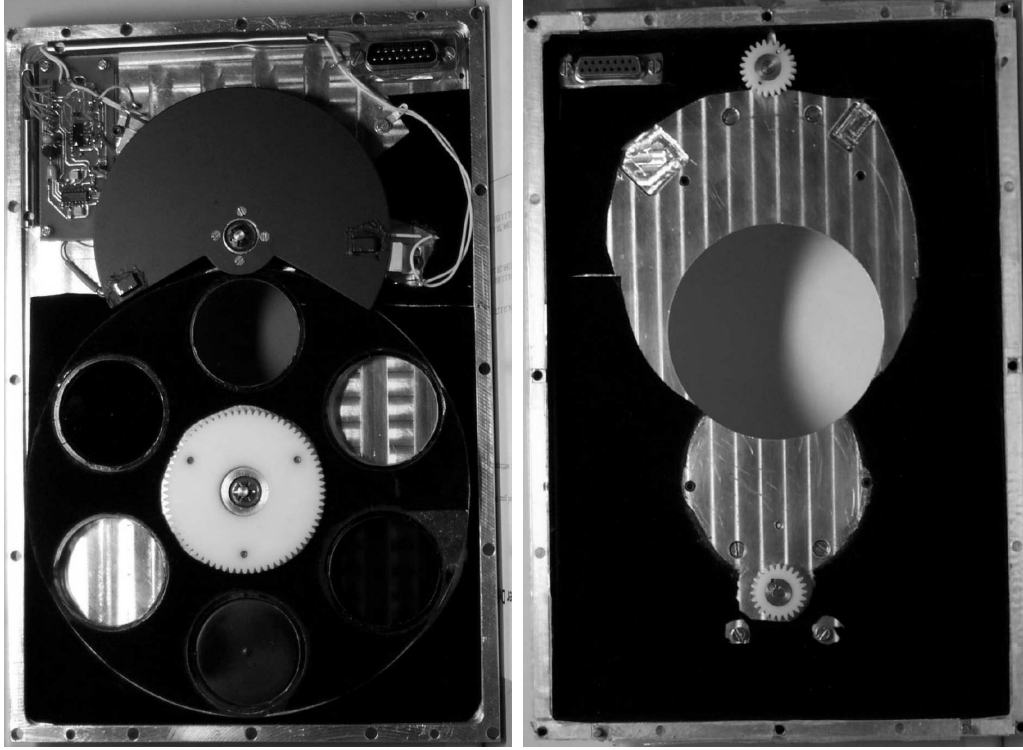


Figure 3.2: The filter and shutter unit seen from the inside. The inside is partly covered with light absorbing ‘flock’ paper. The shutter wheel seen here is not the same as the one we used in our observations. In this version the opening angle is wider and it is only one opening.

We only used the blue filter for photometric observation. Figure 3.3 shows a filter profile of this filter. The filter has center wavelength (cwl) around $430 (\pm 5)$ nm and has 100 nm full width and transmission approximately 70 percent. For comparison the B-filter at the Nordic optical telescope has cwl 432.4 nm, fwhm 106.6 nm and transmission. 53 percent (from NOT homepage). The Johnson B is centered around 440 nm with fwhm of 98 nm. The V and R filter both have cut off towards blue. To the right in figure 3.3 we see the filter profile for the R filter. The visual filter has a cut off around 475 nm and the red around 600 nm. The I-filter has cwl of 894 nm and fwhm of 337 nm [from Custom Scientific]. The quantum efficiency of the chip (seen down to the right in figure 3.3), sets a limit in the red end of the spectrum.

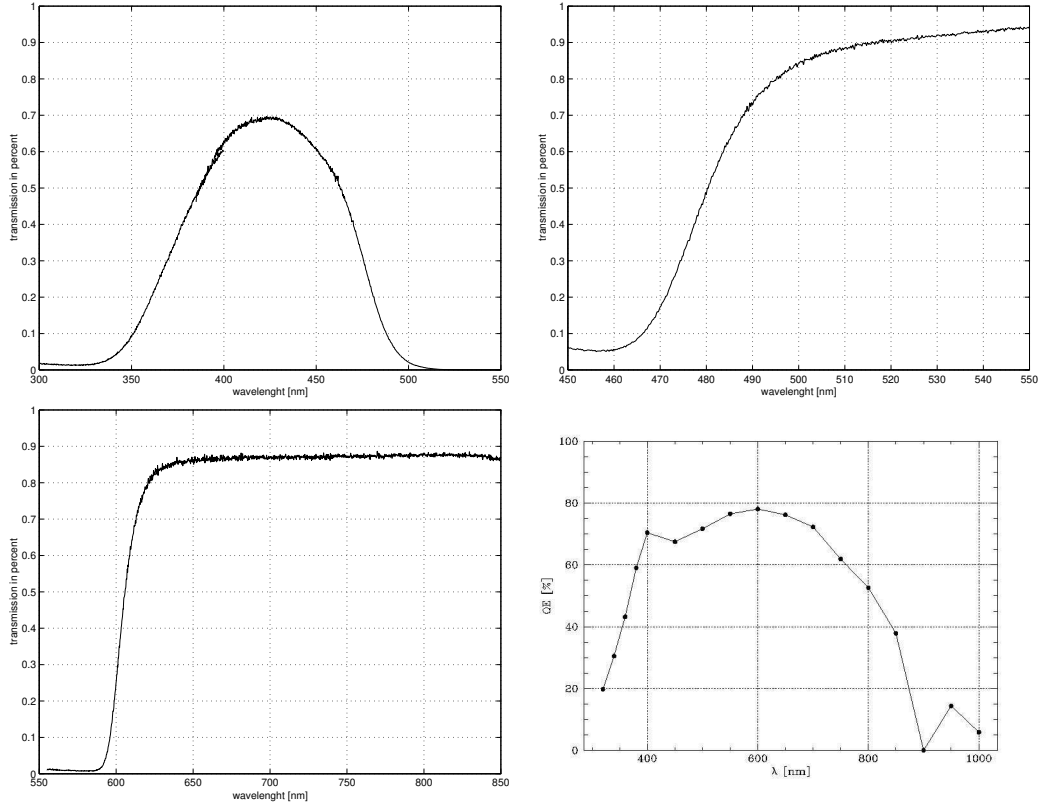


Figure 3.3: Filter profile of the filters in the tcp and the Quantum efficiency for the TK1024 chip. Up to the left is the profile for the B filter and up to the right the profile for the V filter. Down to the left is the profile of the R filter and down to the right is the QE for the chip. The profiles are measured with the Spex spectrograph we have at the University, and the QE for the chip is from the web site of the fabric that make the chip.

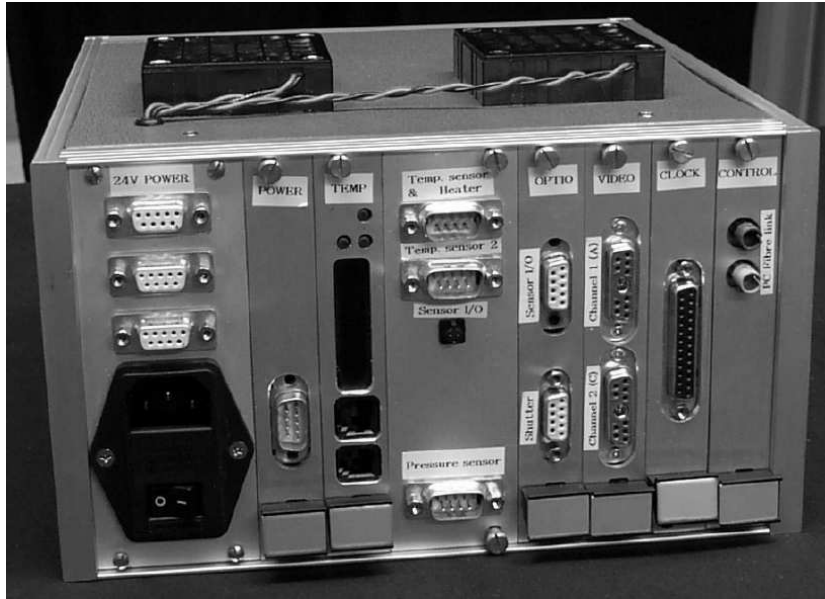


Figure 3.4: Picture of the CCD-controller.

3.3 Controller for the camera (Copenhagen controller)

The CCD-controller is a compact aluminum box with the electronics needed to operate the CCD-chip. Figure 3.4 shows a picture of the CCD-controller. It contains a power supply, six cards labeled CONTROL, CLOCK, VIDEO, OPTIO, TEMP and POWER, and a panel with temperature and pressure sensors. The controller is produced by the Copenhagen University Observatory and described fully by Østensen (2000).

3.4 Controller for the FASU

The FASU controller box, fig.3.5, contains controllers for the filter wheel and for the shutter. In addition it gives power to the peltier cooling. The shutter and filter wheel is operated from the computer through a RS-232 cable. The FASU is produced at the University of Tromsø, department of Physics.

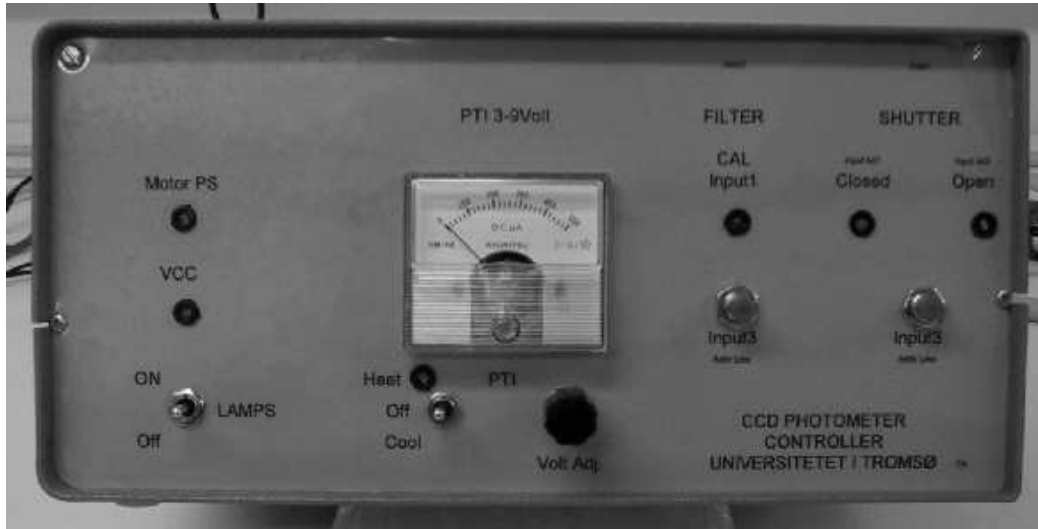


Figure 3.5: Picture of the fasu-controller.

3.5 Connections

There are many cables between the different components in the system. From the computer there is an optical fiber to the CCD-controller and a RS-232 cable to the FASU-controller. The FASU-controller communicate with the FASU through a thick 25 pin cable, and gives power to the peltier element in the camera head. From the CCD-controller to the FASU we have a 9 pin cable for the shutter. Between CCD-controller and the camera head there are two cables for the readout of the chip, one cable from the clock card, and a cable for the temperature sensor and heating of the peltier element. In addition the electrical fan on top of the camera head gets 24 V power from the CCD-controller box. Figure 3.6 shows all the connections except the the two to the filter wheel. As seen i figure 3.4 there are three connections internally on the CCD-controller box: 24 V power to the power card, 24 V power to the temperature card and a cable from the temperature regulation board to the OPTIO board.

3.6 Computer

The computer is a 'lunchbox' type and runs on Linux. It contains an optical fiber I/O card for communication with the CCD-controller and a serial port

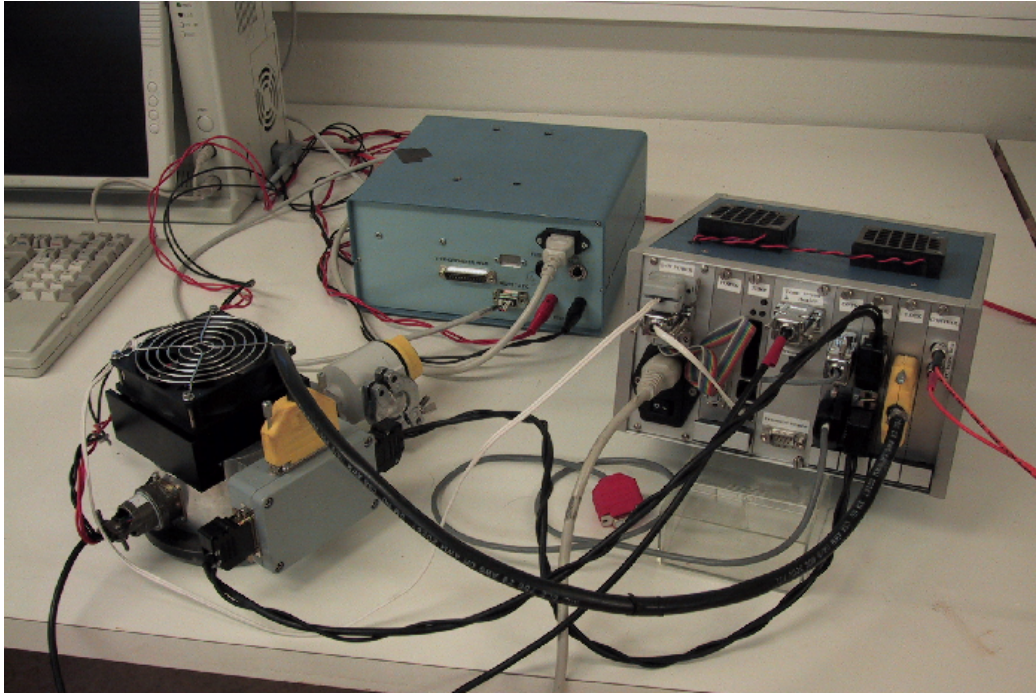


Figure 3.6: Picture of cable connections.

for communication with the FASU. For connection to network we have a 3com 10 MBit combo network card. The hard drive of 4 GB gives enough space for the data storage. In Skibotn we have permanent cables from the telescope to the computer. For use in Tromsø we have a 3 meter optical fiber and a 4 meter RS-232 cable. Figure 3.7 shows the computer from the side where the connections are.

3.7 Software

The software used with the system is written by Roy Østensen, and a full description can be found in his doctor thesis [Østensen (2000)]. We will here give a short description of each program. A description of how we used the programs are found in the observation chapter and in the reduction chapter.

The plan is to make a user interface that combine all these programs to make it easier to use the system, but for the moment we operate each program separately.



Figure 3.7: The tcp computer. Input for the connections to the left.

```

tccd <31>download im.srec
PC-card RAM size: 16 Mb
delay = 4374
0D (0) 0D (1) 0A (1) 42 (1) 52 (1) 4F (1) 43 (1) 41 (1) 4D (1) 20 (1) 36 (1) 38
(1) 30 (1) 32 (1) 30 (1) 23 (1)
Response: [BROCAM 68020#]
Downloading to camera
*****
Download complete.
tccd <32>

```

Figure 3.8: Message in the terminal when textbf download program runs.

download

After turning on the CCD-controller, the program `im.srec` must be downloaded to the RAM of the computer in the controller. This is done by the program **download** with `im.srec` as input. `Im.srec` contains code for the window readout of the chip in addition to the normal readout. In the final version of TCP the program will be burned in the EP-ROM of the small Motorola computer and in normal operation **download** will not be necessary.

tcpcom

tcpcom is a two way communication program that let the user give commands to the camera, and receive information back. The program is not very user friendly, but works good. The **im.srec** file has to be downloaded before **tcpcom** can be run.

The picture taken will be stored in the same directory as **tcpcom** is started in.

tcpcom initializes the camera, shutter and filter wheel, and if it runs the tcpcom-screen appears in the terminal window. If not, you get the message *Camera::getHeader(): Lost connection - giving up..* If this happens, check if the file im.srec is downloaded. The **tcpcom** screen is divided in two parts where the upper part shows basic information about camera status. In the lower part we can change between different type of information with the number keys '0' to '4' and help page with '9' or '?'. Figure 3.9 shows the tcpcom-screen with the help menu. In the help menu we find the most of the commands used to operate the camera.

When a picture is taken the default filename will be *tcp0001.fits* in full frame mode and *w00001.fits* in windowing frame mode and successive pictures will be counted up. The file name base (here tcp and w) can be changed with 'N' in full frame mode and 'W' in windowing frame mode.

phot

For the photometry we use **phot** to pick the areas or 'windows' on the chip we will use. Normally we choose four windows: target star, two comparison stars and one background. To run **phot** write 'phot' with the frame we want to pick out windows as input. SAOimage will then open with the specified file. We pick out the areas we want with 's' (A square will appear in the image). The information are saved with 'W'. This makes a file called photwccd.dat which contains information of the size and positions of the windows.

rtp

rtp is a program for real time photometry. It allows us to look at the light curve and make sky subtracted and differential photometry as the pictures come from the chip.

```

roy@tccd:~/temp
ID: BROR  CCD: TK1024  VERSION: Roy v0,9  UT: Sat Nov 4 10:21:11 2000

MODE: IDLE          DATA: HEADER          TRANSFER MODE: FULL FRAME
totx      1124      toty      1024      ccd_temp   -0.33 C
beginx    1         beginy    1         ln2_temp   204.62 C
imx       1124      imy       1024      ref_temp   -100.00 C
binx      1         biny      1         pressure   N/A
exptime   0,00 s   expleft   0,00 s   seqtime    0,00 s
frame_left 0         frame_total 0         readdr     A

TCPCom Kestroke commands:
e: start Exposure           E: set exptime and start Exposure
d: start Dark exposure      D: set exptime and start Dark exp
s: start exposure Sequence  S: set Sequence time interval
a: Abort exposure or sequence  b: start bias exposure
w: read Windows definition file  W: set Window filename base
f: set filter               F: next filter position
A: re-init filterwheel and shutter  H: toggle safe/fast Header read mode
l: start temperature Logging mode  R: toggle safe/fast data Read mode
t: toggle Transfer mode         1: display Timing specifics
N: set Filename base           2: display Voltages setup
?: display this help page       3: display tcpcom internal System variables
#: toggle Debug option          4: display filter and shutter info
@: send raw commands to camera  0: set Normal display mode
T: set Exposure time

```

Figure 3.9: TCPCOM screen with the help menu in the lower part.

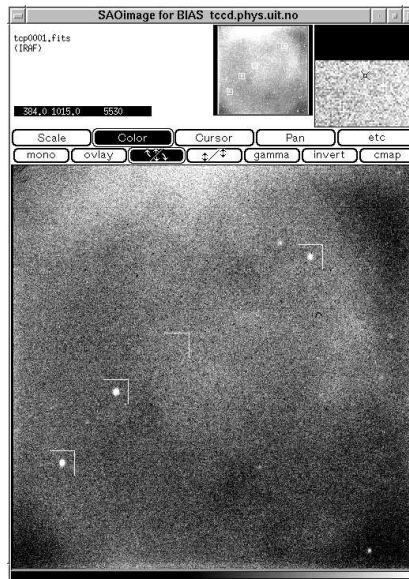


Figure 3.10: Picture of four marked areas in the field of LX Ser with phot.

```

SYNTAX: rtft -[options] [range] infile
OPTIONS:                                DEFAULTS:
-a      Output an Amplitude spectrum    Is default
-P      Output a Power spectrum         Amplitude spectrum
-n #    Output # data points in the transform
        Compute # with 10x sampling
-o name Use 'name' as output file basename
        Derive from infile name
-p      Output a separate peakfile      No peakfile
-w      Output a window, based on largest peak
        No window
-C #    Read specific column from INFILE
        Column 1 (ignoring time col.)

RANGE:  [Freq1 Freq2] Range in Hz or MicroHz    100 - 5000 MicroHz
INFILE: Data file from Qmrg or rtp              none - gotta have one

```

Figure 3.11: Options for the **rtft** program.

rtp is also used for sky subtraction and differential photometry in the final reduction.

rtcnv:

The files from the windowing readout is not standard fits images, and has to be converted to if we want to work with them visually. This is done with a program called **rtcnv**. Calling **rtcnv -h** gives a help file with the commands used in **rtcnv**.

rtft: Fourier Transform

To make a Fourier transform of the light curve we use **rtft**. **Rtft** is short for real time Fourier transform. Figure 3.11 shows the input commands for **rtft**. Writing just 'rtft' in the terminal window gives the same screen as in the figure.

rtcorr: Extinction correction

The program **rtcorr** correct the sky subtracted light curve for extinction. The extinction is corrected with use of the Airmass $A(t)$ and the extinction coefficient k_f for the filter used.

$$C = 10^{0.4k_f A(t)} \quad (3.1)$$

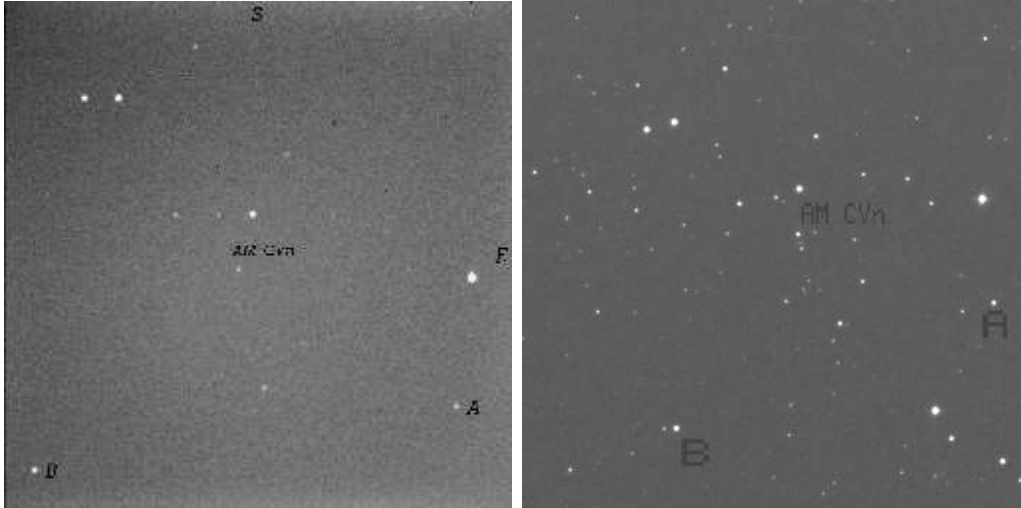


Figure 3.12: Field from the TCP (left), and the same field from ESO Sky survey (right). South is up and East is to the right in the Sky survey.

The output of **rtcorr** is the sky subtracted data file corrected for extinction with the new extension `‘.ext’`. We also get the differential photometry of the extinction corrected data. This file has the extension `‘.edf’`. The differential photometry is normalized by fitting a straight line to the light curve with the least squares algorithm and divide by the line. Now we have the final differential photometry in normalized modulation magnitudes, with the extension `‘.nma’`.

3.8 Field of view

The TCP has a 1024x1024 pixels large chip. To find the field of view we used the frame from the TCP of the star AM CVn, and the same field from the ESO sky survey using the Unix program XEphem.

With XEphem we can find the distance between two stars in arcseconds, marked in figure 3.12 as A and B. With SAOimage we find the same distance in pixels on the TCP frame, and can then calculate number of pixels per arcseconds. The distance between A and B in the TCP field is 860 pixels, and the same distance in the sky survey field is 808 arcseconds. This gives 1.06 pixels per arcsecond. The chip is 1024 by 1024 pixels, which gives a field of view $16' 6''$. One pixel is $24 \mu\text{m}$ which gives 1 mm on the chip equals 39.3

arcsec. From the focal length and focal ratio we got $\theta=41.25$ arcsec/mm. Why do we get this difference? Because the TCP has its focus point behind the back plate of the telescope, we have a higher f value than 5000 mm, and hence a smaller field of view.

Chapter 4

The Aurora photometer

To measure the aurora activity during observations we use a one channel classical photometer with a narrow band filter. A classical photometer is a photometer with no moving parts. The filter is centered at λ 4278 Å, and has half width of 10 Å. A filter profile of the filter is found in figure 4.2 The system is set up with help from Professor Ove Harang and is the same that Myrabø used for his aurora measurements in 1978. The data is not used to improve the measurements from the CCD photometer because we get a much more accurate correction by the CCD system itself. The use of the aurora photometer has been to monitor the short time variation of the aurora to compare this with the background measurements from the TCP. It has also been useful to learn about classical photometry and programming to operate instruments and do reduction. The software is written in QBASIC by Professor Harang.

4.1 Description of the photometer.

The photometer consists of a tube with a glass window in front, a filter, an aperture, a photo multiplier and a pre- amplifier. The aperture $d = 0.5$ mm and focal length $f = 50$ mm. This gives field of view :
 $\theta = d/f = 0.5 \text{ mm}/50 \text{ mm rad} = 2062 \text{ arcsec} = 0.57^\circ$. Figure 4.1 shows the different parts of the photometer. The aurora photometer is attached in front and under the main telescope, and the optical axes are the same for both.

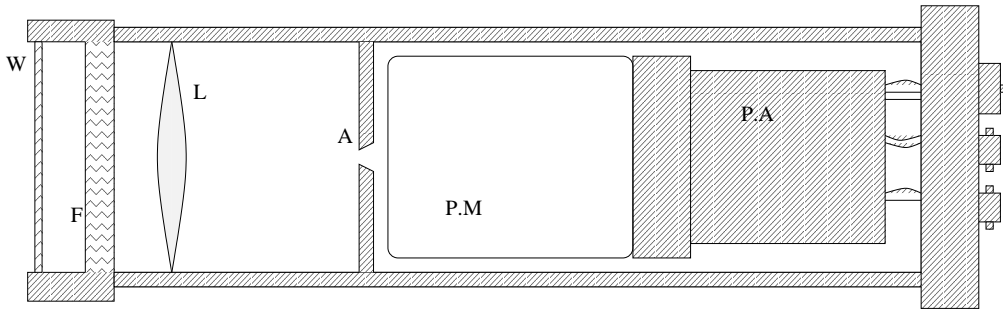


Figure 4.1: Drawing of the aurora photometer with the window (w), lens (L), aperture (A), photo multiplier (P.M) and pre- amplifier (P.A).

4.2 Running the photometer

The photometer is operated from a DOS computer in the control room with some QBASIC programs. Before observation we turn on the ratemeter and high voltage. The high voltage should be positive 1300V. Power to the pre amplifier is in the dome, and is connected to the main power of the dome. This is turned on with the same power switch as the dome power (Green button at the power box in the dome).

In the computer: Go to C:_NLTELSC, start QBASIC, load the program SKAB24.BAS and start observation with shift+f5.

We now get the light curve on the screen. Every ten minutes the data are stored on the hard drive. To stop observation press <ctrl> + <break>.

To see the stored data we go to the NLDATA directory. Here we run SKI-DAT22 in QBASIC. This program reads the files from the catalog A.DAT. From this program we can save the files in ASCII code for easy plotting in other programs.

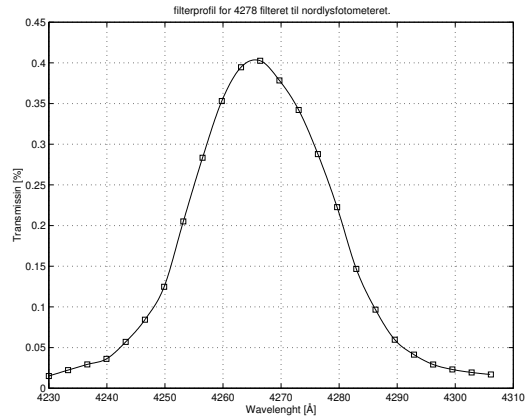


Figure 4.2: Filter profile for the $\lambda 4278$ filter. The profile is made with the use of the Spex spectrometer that we have at the university.

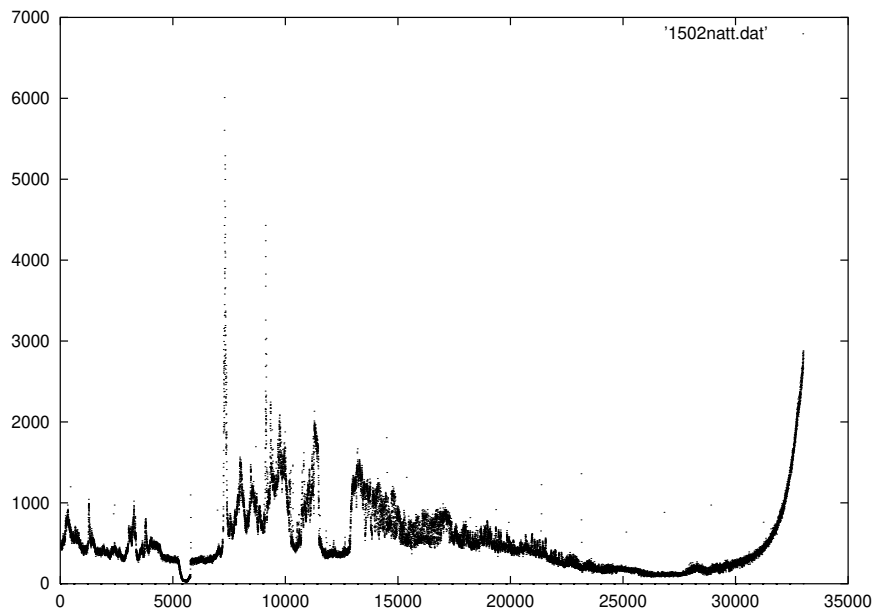


Figure 4.3: Example of aurora measurements from the night of 15. February. The start time is 19:56 UT and end time 05:11 UT. The y axes shows the raw counts from the photometer and the x axes time in seconds.

Chapter 5

Observations

Observing with the TCP is different from observing with the previous photometers we have used at the Skibotn Observatory. Earlier, we had to run up and down between the dome and the computer room to check the centering, but now this is done very easily because the stars appear on the computer screen, and we can simply center it with the hand paddle. But still it is a lot of work. The tracking of the telescope is not very good, and the auto guiding do not work properly, and the dome must be moved manually.

5.1 Objects

To get the positions and field images of our target stars, I have used these sites on the Internet:

The white dwarf database: <http://procyon.lpl.arizona.edu/WD/>

The STScI Digitized Sky Survey: http://stdatu.stsci.edu/dss/dss_form.html

The SIMBAD astronomical database: <http://cdsweb.u-strasbg.fr/Simbad.html>

The Linux program **XEphem** is also useful to locate stars. It uses the ESO sky survey combined with the Hubble guide star catalogue (gsc) and gives a very good image of the field with all the stars in the gsc marked with it's catalogue number.

Information of some of the stars we have observed:

AM CVn (HZ 29)[(Solheim, 1998)], α 12 34 54, δ 37 38 28, V-mag:14.18,

P(sec)=350, 525 [(Bradley, 1998)]

LX Serpentis (Stephanian star), $\alpha(1950)=15\ 35\ 44$, $\delta(1950)=19\ 01\ 30$, $P=3^h\ 48^m$

GD 358, $\alpha(2000)=16\ 47\ 19$, $\delta(2000)=32^\circ\ 28'\ 30''$, v mag 13.65, B-mag 13.54,

Amp 0.10 mag, $P=700$ s [Bradley (1998)]

GD 358 is a variable DB white dwarfs [Hoffmeister et al. (1985)] *HS 2201+2610*, $\alpha(2000)=22\ 04\ 10.7$, $\delta(2000)=26^\circ\ 25'\ 14''$ [(Bradley, 1998)]

5.2 Ready to observe

5.2.1 One typical observation night in Skibotn

The following describes the preparation and accomplishment of an observing night at the Observatory

Turn on the power on the TCP one hour before the observations to cool down the chip.

Open the dome manually.

Set the computer time.

Take flats of the sky before it gets dark.

Point the telescope to a known star to set the right coordinates.

Point to your star.

Take a picture to see if you are in the right place.

Move telescope with hand controller to your desired field.

Start the auto guiding.

Start the aurora photometer.

Choose filter and exposure time.

Take a new picture.

Do windowing with *phot*.

Start the run.

Write down the starting time.

Start **rtp** to see the light curve on the screen.

Check the centering (make fits image with W in *textbfrtp*, called *testview.fits*).

If the centering is bad, stop the auto guiding and move the telescope manually until the target star is in the center.

Then start auto guiding again.

Remember to write a log! (Weather conditions, wind, temperature, problems, bad files ..)

At the end of run: Check the time and write it down, and compare with the computer clock in the TCP computer (The computer clock is not very good!).

5.2.2 First light at Skibotn Observatory for TCP.

Thursday 08.12.99, Frank Johannessen and I, went to Skibotn to mount the system. This was the first test of the TCP on the Skibotn telescope. The plan was to figure out how to put the control boxes on the telescope, stretch out the cables, and take some test pictures to see how good the chip was. The weather was clear and the temperature -14 C. The temperature of the chip fell down to -50 C, which is good with the cooling system we had (peltier cooling, and electric fan with cooling ribs). At this time we didn't know how to use the TCP for photometry, so we only did some imaging. After focusing and finding the right position on the sky we started with imaging of the Messier object M74. We got problems: The filter wheel would not calibrate on the B-filter, as it should. After some rounds, the filter wheel calibrated, and we took pictures in all filters. We continued with SAO 52680 and HS 2333+3927.

In figure 5.2 we see HS 2333+3927, a B-magnitude 14.5 subdwarf. The last object this night was M42. The filter wheel had big problems to stop on filter B, the calibration position. The first picture was good (fig 5.1). On the next picture some strange marks appeared. We tried the other filters with the same result. Then we close the system.

The results were stored locally on the TCPs computer and transferred to Tromsø over the net in the morning. Before transferring, all the files we did not need was deleted. The files were put together in a zipped 'tar' file. 'Tar' makes one file of all the files we want to transfer, and it keeps the directory structure. The command in Linux to make a tar file is:

```
'tar cvfz directory-name.tar.gz directory-name'
```

To pack out the files again use:

```
'tar zxvf directory-name.tar.gz'
```

In the morning the next day, we took new sky flats. The same marks appeared. Figure 5.5 shows a sky flat taken in the morning. The pixel level is about 17000 ADU. The flat is not good. We have a strong light from the

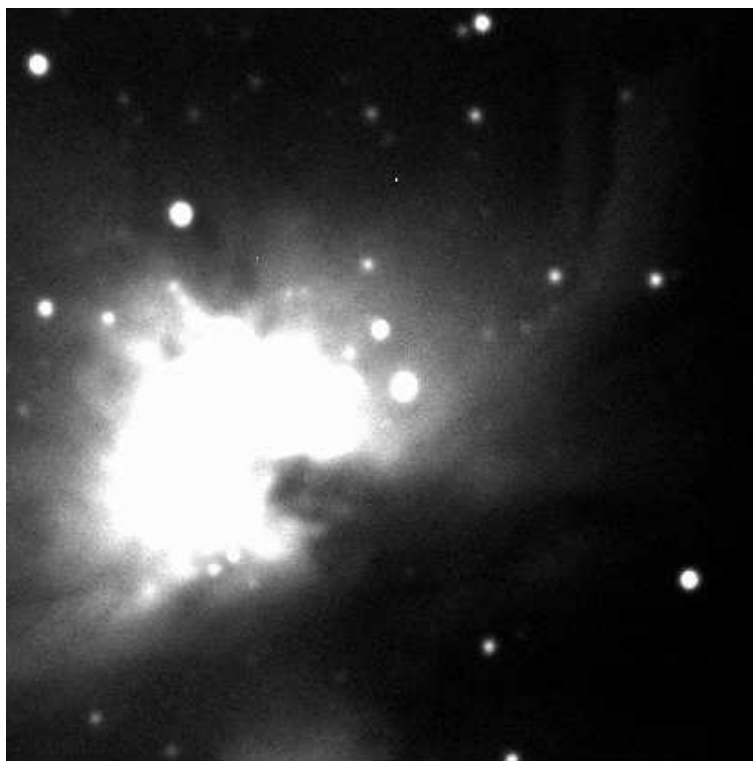


Figure 5.1: The Orion nebula, M42, a 2 sec exposure without filter.

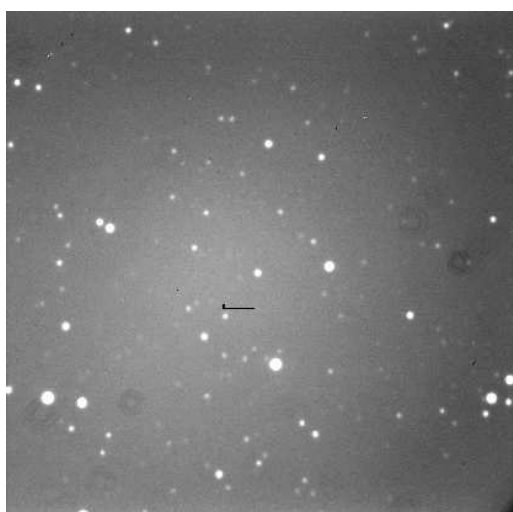


Figure 5.2: HS2333+3927 field, 40 sec exposure with V-filter.



Figure 5.3: m74, a spiral galaxy in Pisces, 60 sec exposure with V-filter.

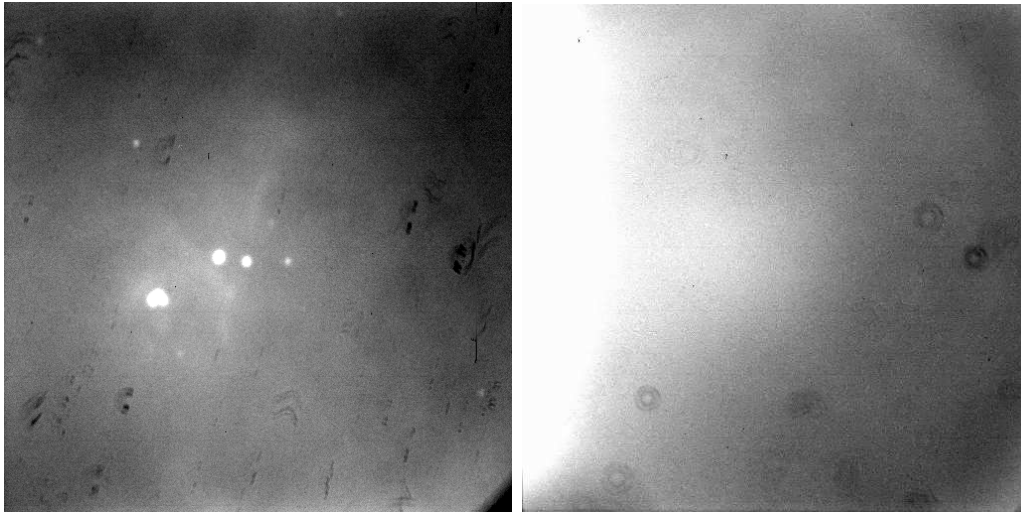


Figure 5.4: M42 with strange marks. Figure 5.5: Sky flat with V-filter.

left, and some marks because of dirt on the window in front of the chip. The reason we did not see the marks on the previous pictures, is that the background was darker and the marks were hidden in the dark background. When we took flat field all the chip was illuminated with the same amount of light and then we clearly saw the marks.

After the first test we had several problems to solve:

- How to mount the two boxes to the telescope
- Calibration of the filter wheel.
- Dirt on the window in front of the chip.

5.2.3 Photometry with the TCP.

Tuesday 14.12.99 Roy Østensen went with me on a day trip to the Skibotn telescope. Our program was to find out how to make high speed photometry.

We solved the problem with the filter-wheel by putting on a small voltage on the motor to keep the wheel in place. We did not see any bad effects in the data because of this.

For the first time in Skibotn, we tried the TCP for what it is made for: High speed photometry. We started to investigate **tcpcom**: how to give raw commands, the different menus and so on. Then we used **phot** to pick out stars and background on the chip, we linked the **data** and **dev** directory and started. Everything was written down, and I felt ready to begin my observations next time.

5.3 Testing the TCP in Tromsø

The two first weeks of January was used for testing the TCP in Tromsø. The purpose was to learn more about the system and do the modifications needed. In Skibotn, we had seen a teeth-like pattern in the light curve, something that indicated a problem with the shutter.

To find out more about this, we put up the TCP in a box to have stable light conditions, and used a argon lamp as light source. Then we took one hour time series with the shutter open all the time, closed all the time and the normal auto shutter that open/close between each exposure. In the shutter plate we have two openings opposite of each other, and each of them is used every other time. From the series with normal auto shutter, it was clear that we received unequal amounts of light from the two openings. We decided to cover one of the openings, and turn the shutter wheel 360° between each exposure. We repeated the same test, and now the teeth-like pattern had disappeared.

The reason for the teeth-like pattern, might be that when we used two openings, the opening did not stop exactly in the same position after a 180° turn with the filter wheel. Under perfect conditions this should not be a problem, because the opening is bigger than the chip that is receiving the light. But because of light reflecting from parts in the TCP and the telescope, light that don't fall directly on the chip can hit it after reflection.

To have the opening at the same place every exposure helped a lot, but we still had problems with the reflected light. The telescope is not pointing in the same direction all the time, and the scattered light changes from frame to frame illuminating the chip different places.

To avoid some of the light reflected from the inside of the telescope, we tried to put a plastic tube, painted black, in the opening of the FASU, that

made the hole smaller. When designing the FASU, the critical size of the filter opening was 36 mm (from private discussion with Solheim), and filters diameter were made 40 mm. Decreasing the hole in from of the filters effected the light from the mirror falling on the chip by vignetting. This effect could be seen in the picture as darker areas in the outer part of the chip. Because of this we decided not to use this tube. A better solution would be to make the inside of the FASU black to avoid reflections. This will be done in the new planned version of the FASU.

We have two different amplifiers that we can read out the chip through, marked A and C on the camera head unit and on the control box. By default we were using channel A. We discovered that by using readout channel C we got a more stable light curve, and this was put as default in the `tcpcom` program. We then used readout channel C for all the observations.

5.4 Observations

In this section we present the observation logs for the observations of good quality that we have used for reduction in the next chapter. The other observation logs, that we will not show reduction of in these thesis, are put in Appendix A. A table of all nights of observation is also put in the appendix.

5.4.1 Skibotn 15.-17. February: Observation of AM CVn.

We started the evening 15.02. taking sky-flats. The sky was clear and we were ready to observe AM CVn. We started 19:56 UT. The sky were still clear, and no aurora. The SBig4 auto guiding camera had developed ice on the window in front of the CCD chip, and could not be used. We used manual auto guiding the whole night. The moon was 3/4 full and gave a bright sky. After two hours of observation the aurora started in the North-east. For two hours we had strong aurora. In the end of the night the moon set down, and the sky was very dark before sunrise. At the end of the night we took more sky flats.

In figure 5.6 we see the field of AM CVn used for the observations. South is up and East is to the right. The first night we used two comparison stars

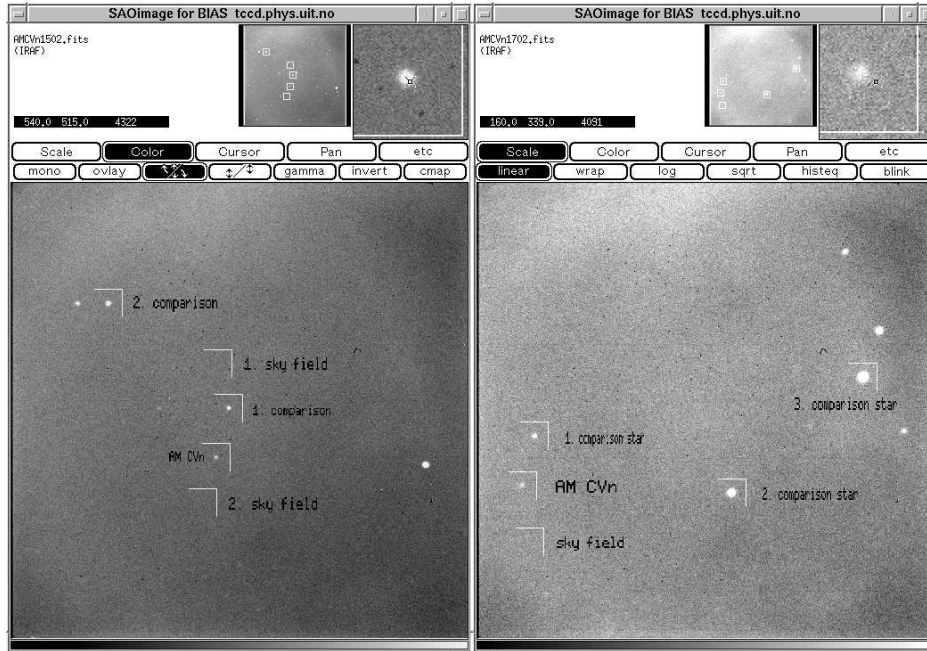


Figure 5.6: Areas on the chip used in the observation of AM CVn. The windows in the figure to the right were used the first night, and the windows in the figure to the left in the second and third nights.

and two sky field. After the first night we saw that we didn't need two sky fields, because we used the sky annulus subtraction, and decided to use three comparison stars instead. This was done the two following nights. When we pick out the stars we want to observe, we have to look for bad pixels inside the window. If a bad pixel is placed behind the star, this can affect the observations. If we saw any bad pixels, we had to move the stars a little bit in the field, to avoid this. The chip is good, with very few bad pixels, so this was not a big problem.

Target:	AM CVn
File:	tue1502/run1
Start observation:	19:56:02 UT
End observation:	05:11:43 UT
Temperature:	at start: -8.8° C, at 0400 UT: 10.2° C
Temperature chip:	-42.6° C
Sky:	clear, some strong aurora, 3/4 moon

The second night we continued observing AM CVn. At the start of observations we had some thin clouds. After two hours the sky was completely

clear. Like the day before, we had aurora for two hours between 22 and 24 UT . We got a gap in the light curve for 10 frames between frame number 83 to 93. We lost these points because I pressed w in textbfrtp, and textbfrtp, while waiting for a new file base name, did not save the new data coming from the camera. The auto guiding is working, but not good, so we all the time we had to correct the centering of the star. At the end of the night the moon set.

Target:	AM CVn
File:	wed1602/run1
Start observation:	19:09:49 UT
End observation:	05:10:30 UT
Temperature:	at start:−11.6° C, at 0100 UT:10.5° C
Temperature chip:	−45.8°
Sky:	clear, some strong aurora, 3/4 moon

The third and last night of AM CVn everything ran perfect. After six hours we had some thin clouds, but they disappeared quickly. The moon was strong. It was only 2 days before full moon. We had some strong aurora in the beginning of the night, but the rest of the night was stable, except from some aurora after 6 and 8 hours.

Target:	AM CVn
File:	thu1702/run1
Start observation:	18:31:20 UT
End observation:	05:12:31 UT
Temperature:	at start −6.7° C
Temperature chip:	−44.5°
Sky:	clear, some strong aurora, 4/5 moon

The observation of AM CVn was the first full night observation this winter. The sequence time was 45 s in all three nights.

5.4.2 Skibotn 22. and 23. February: Observation of GD 358

The sky was clear, and we began to observe AM CVn. The temperature was -8, and there was no aurora. After two hours, clouds came in front of the star, and we have to stop the observation. At 0300 UT it clears up again, and we start to observe the white dwarf GD 358. We can observe this for 1.5 hours until sunrise. In figure 5.11 we see the raw light curve of this run.

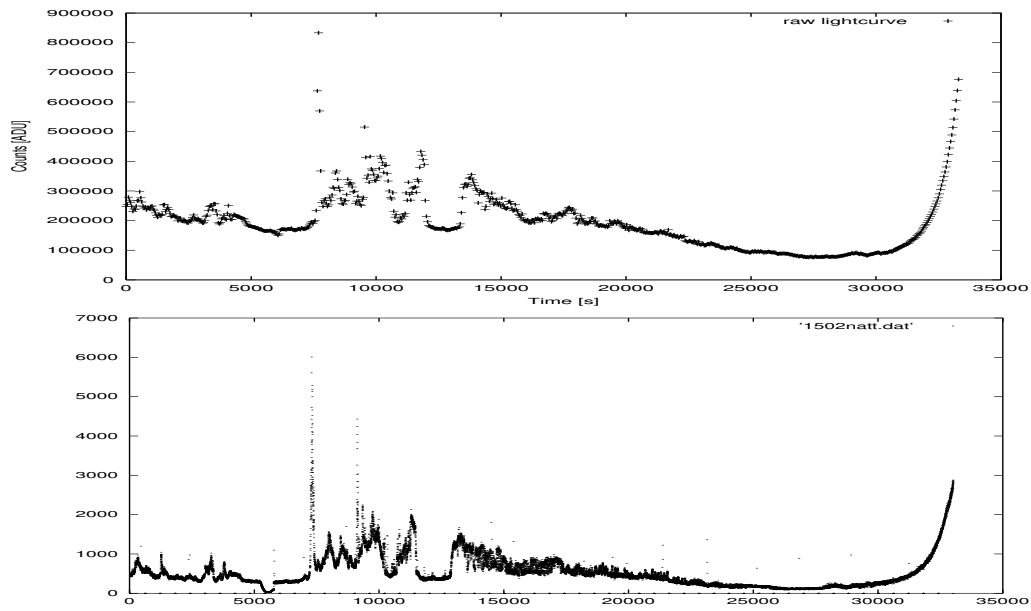


Figure 5.7: AM CVn Skibotn 15.02.00, start 19:56:02 UT, end 05:11:43 UT. The first window is the raw light curve from the TCP, second light curve from the aurora photometer.

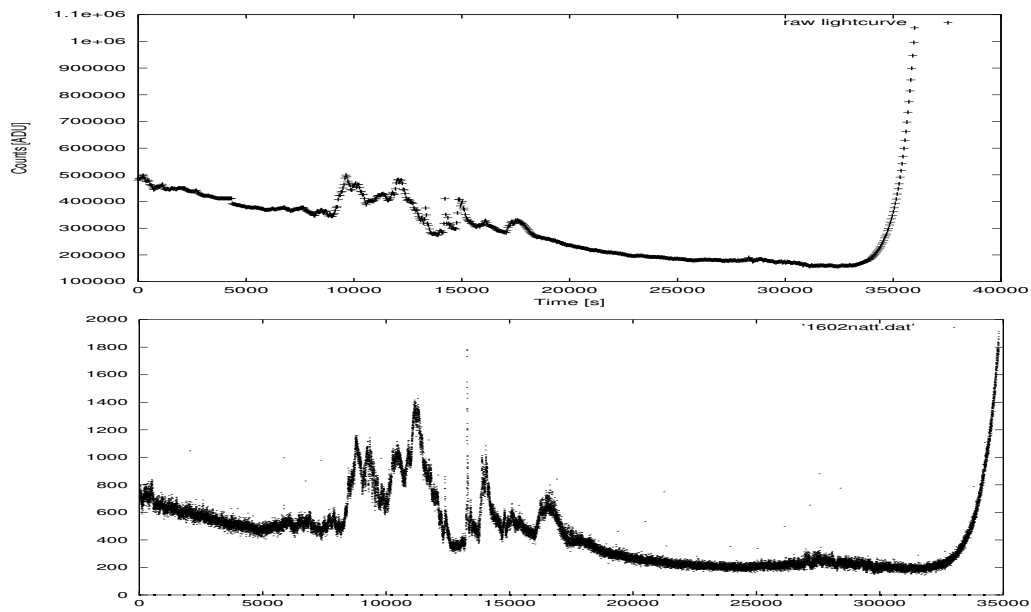


Figure 5.8: AM CVn Skibotn 16.02.00, start 19:09:49 UT, end 05:10:30 UT. The first window is the raw light curve from the TCP, second light curve from the aurora photometer.

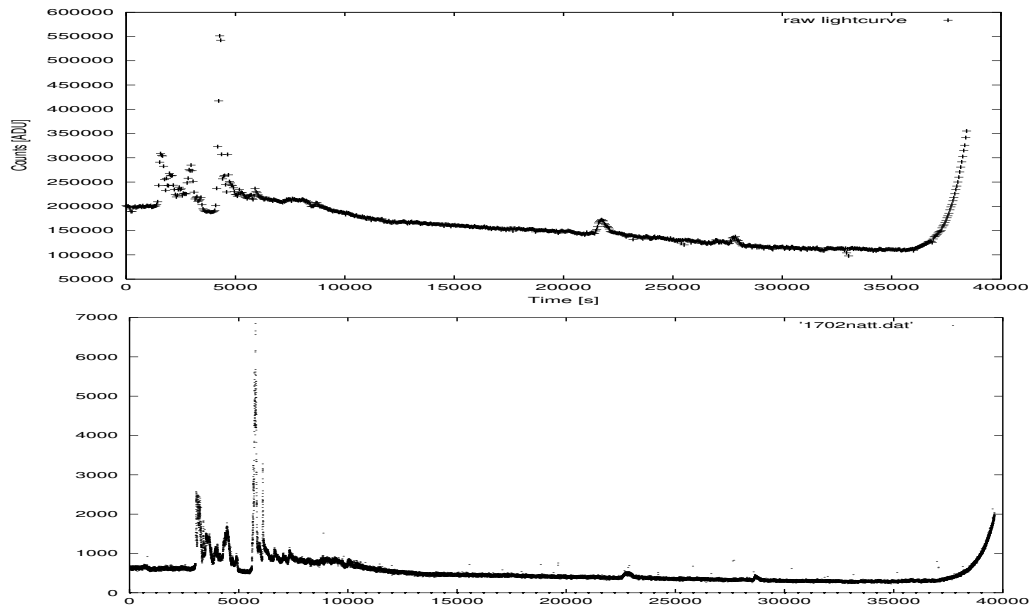


Figure 5.9: AM CVn Skibotn 17.02.00, start 18:31:20 UT, end 05:12:31 UT
 The first window is the raw light curve from the TCP, second light curve from the aurora photometer.

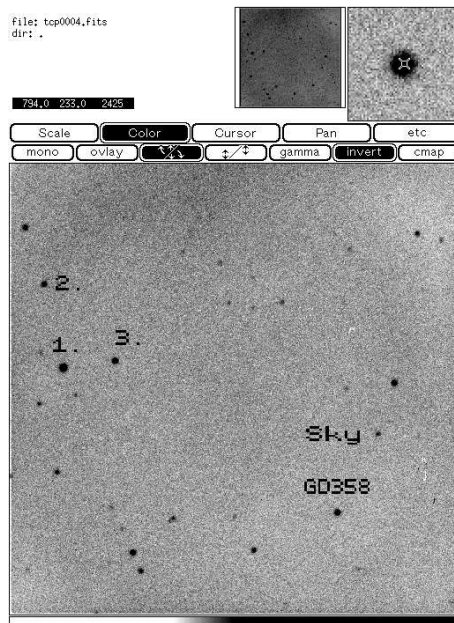


Figure 5.10: Field of GD 358 used for both observations. South is up and East is to the right.

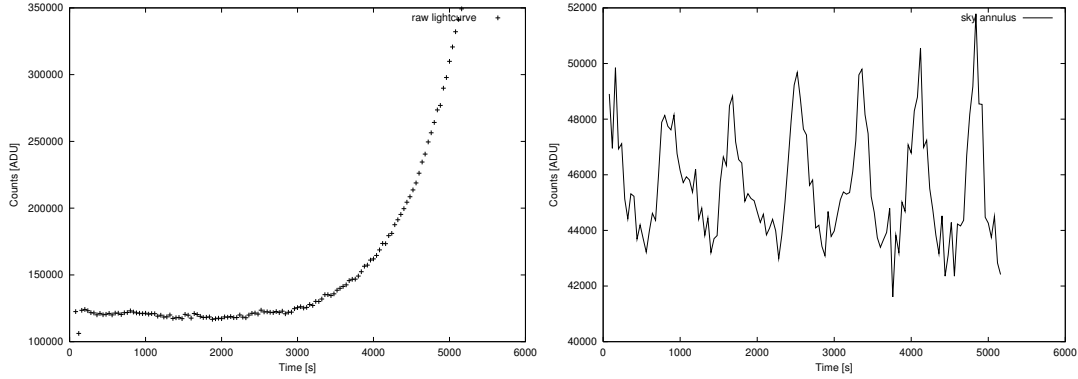


Figure 5.11: GD 358 Skibotn 22.02.00, start 03:08:02 UT, end 04:35:00 UT. The first plot shows the raw data, and the second plot shows differential photometry between target star and the comparison star.

Target: GD358
 File: tue2202/run2
 Start observation: 03:08 UT
 End observation: 03:35 UT
 Temperature: -8
 Temperature chip: -46°
 Sky: clear, 3/4 moon

The second day of this round, we have clouds in the beginning of the night. At 23 UT we have clear sky, and at 00 UT we start observing GD 358. The moon is low and 3/4 full. Strong wind around 5-10 m/s. The star is often at the edge of the window. In figure 5.12 we see the raw light curve of this run.

Target: GD358
 File: wed2302/run1
 Start observation: 00:00 UT
 End observation: 03:36 UT
 Temperature: at start: -12.4° C
 Temperature chip: -47°
 Sky: clear, 3/4 moon

5.4.3 Skibotn 14.-16. March: Observation of LX Serpentis

These three days I went with Synnøve Johansen to observe LX Serpentis. This is a star in an eclipsing binary system. It's period is around 3 hours

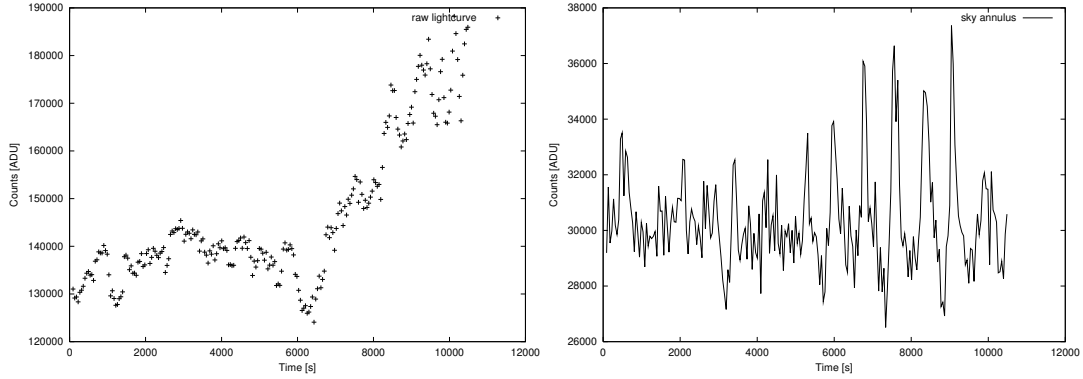


Figure 5.12: GD 358, Skibotn 23.02.00, start 23:06:05 UT, end 02:01:32 UT. The first plot shows the raw data, and the second plot shows differential photometry between target star and the comparison star.

and 48 minutes.

The star was not above the mountains before approximately 21 UT, so we had lot of time to do some imaging. Image of M1, M3, M92 and the moon were taken.

The first night we observed the star from 01:21 UT until sunrise. The 15. March we had clouds and could not observe. The third night we observed from 21 UT until sunrise. The conditions were good both observing nights and we did not have any problems with the system.

Target:	LX Ser	Target:	LX Ser
File:	tue1403/run1	File:	thu1603/run1
Start observation:	01:21 UT	Start observation:	21:11 UT
End observation:	03:32 UT	End observation:	03:38 UT
Temperature:	-10.4	Temperature:	-9
Temperature chip:	-38.8° C	Temperature chip:	-39.6° C
Sky:	clear, 1/2 moon	Sky:	clear

In figure 5.13 and 5.14 we shows the raw light curve and differential photometry of LX Ser the two nights. As we see from the differential photometry we get one eclipse each night. The length of the night was not long enough to observe two eclipses in the same night.

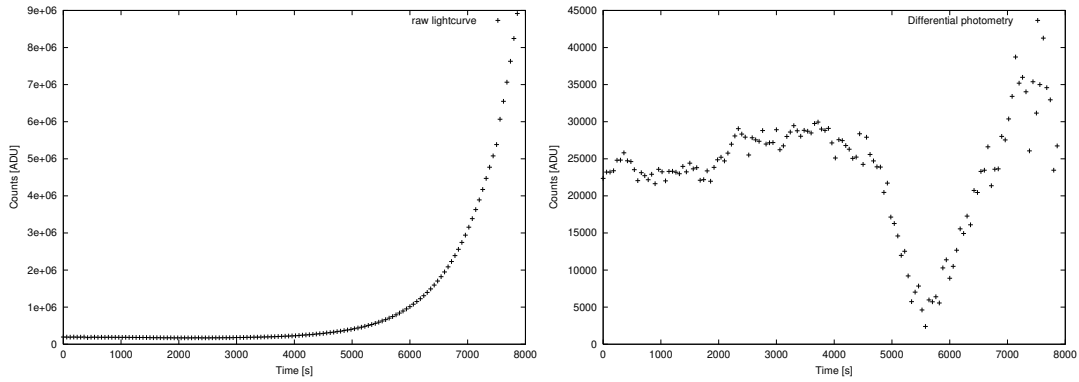


Figure 5.13: LX Ser tue 1403, Start 01:21, stop 03:32 UT. The first plot shows the raw data, and the second plot shows differential photometry between target star and the comparison star.

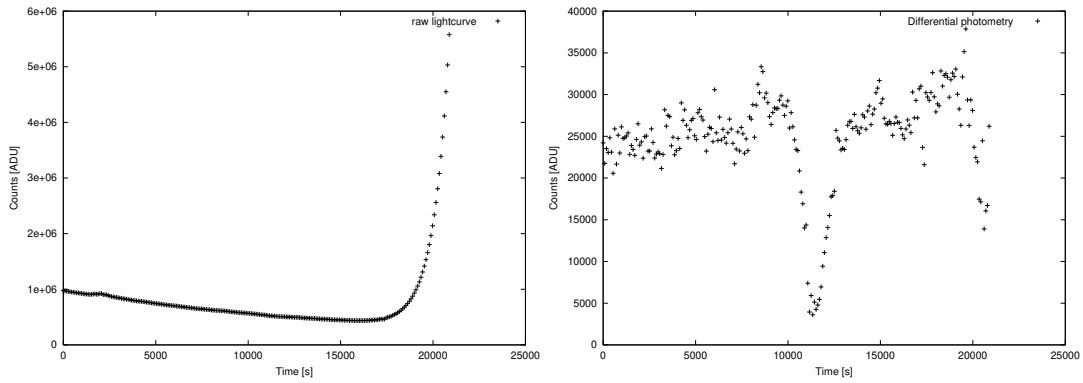


Figure 5.14: LX Ser thu 1603, start 21:21, stop 03:11. The first plot shows the raw data, and the second plot shows differential photometry between target star and the comparison star.

Chapter 6

Reduction

In this chapter I will describe how we did the data reduction of the observed data from the TCP.

6.1 Real time reduction

One of the main advantages of the TCP system is the possibility of real time reduction. As we observe we immediately get the raw light curve, sky subtracted data and differential photometry on the screen. We can also take a Fourier Transform (FT) to check for periods and see the noise level. This has been very useful when looking for new variable stars [Østensen (2000)].

The default window (the area around the star) is 64 times 64 pixels. For observing bigger objects the window can be made bigger, but in my observations I always used 64x64 pixels. With the program **rtp** (Real Time Photometry) we see every new point, for each star and background, during the observation. We can switch between light curves of raw data, sky subtracted data, and differential photometry data. We also can choose which star we want to have on the screen. With **rtft** (Real Time Fourier Transform) we get the FT of the data.

6.2 Final reduction

When we have finished the observation, we have to do more accurate reduction than we do in real time. All the programs needed for reduction of the observed data with the TCP, except SAOimage and GNUplot, are inside the software package developed for the system. SAOimage is a image viewer program for pictures in Fits format, which is the format used by astronomers. GNUplot is a program for making plots. GNUplot is installed in most UNIX/Linux systems.

We have transferred all the observed data to a different PC with one directory for each target, and can now work independently of the TCP computer. The reduction programs: **rtp**, **rtcnv**, **rtft** and **rtcorr** are stored in a **bin** directory to be accessible from everywhere. To be sure not to destroy any of the observations, we create a new directory for the reduction of each target. To get access to the data in the reduction directory we create a symbolic link to the directory where the data is stored. This is done with:

```
ln -s <directory where the data is stored> data
```

The data can be flat fielded, and you have to link to the directory where the flat-fields are with:

```
ln -s <directory where the flat-fields are> flats.
```

Now you can run **rtp** with the options we want.

Command	Description
-f <name>	Name of flat field images. Default is flat*.fits
-n <num>	Start processing at number <num>. Default is 0.
-M	Moving aperture.
-O	Compute individual centering offsets for each star.
-c <num>	Center on star number <num>. Default is 1.
-r <rad>	Aperture radius.
-s <size>	Size of sky annulus. Default is 4.
-i <num>	Number of iterations for the centering.
-B	Non interactive processing; gnuplot will not be opened.
-z <num>	Number of sky fields. Default is 1.

There are two ways of subtracting the sky. One way is to use what we call sky field subtraction where the sky level is calculated from the sky window. All the pixels in the sky window are used except the first four columns. To avoid cosmic rays and dead pixels in the sum, a median filter is used. The number of sigmas, N, in the median filter is by default set to 3, but can be changed with the **-m <nsig>** option in **rtp**. The other method is called

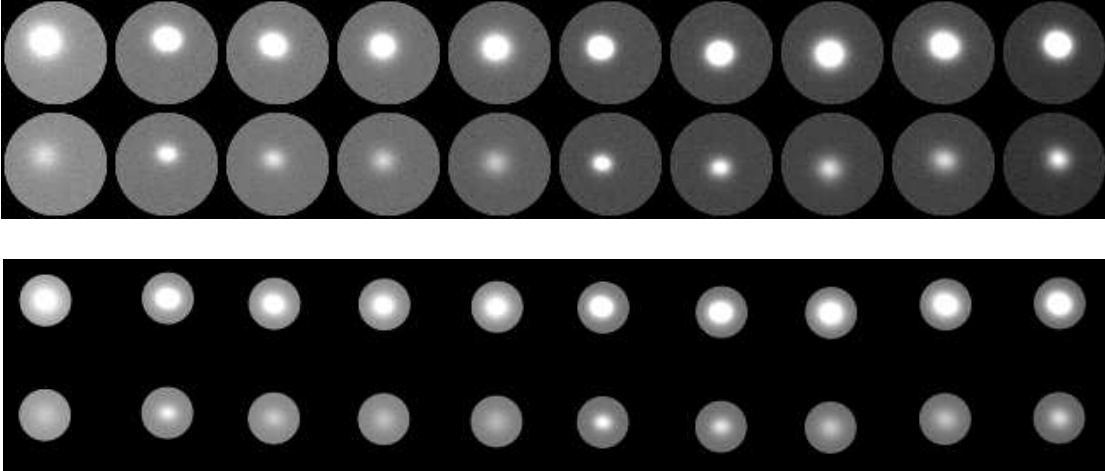


Figure 6.1: Example of the use of moving aperture. In the upper part the star is not centered in the aperture. This can be corrected for by using moving aperture as shown in the lower part.

sky annulus, where we use the outer area around the star in each channel as sky. The median filter works the same way as for the sky field subtraction.

By default **rtp** use the sky field subtraction. To use sky annulus, run **rtp** with **-s <rad>**, where **<rad>** is the number of pixels from each edge to be used. Both methods have advantages and disadvantages. First of all, the sky field method always have more pixels to average over. Second, when using differential photometry, the same sky level is subtracted from both the target star and the comparison star.

The differential photometry for the target d_t for each observation i is by

$$d_t(i) = n_t(i) - \frac{\bar{n}_t}{\bar{n}_r} n_r(i) + \bar{n}_t \quad (6.1)$$

where $n_t(i)$ and $n_r(i)$ are the counts of target and reference star for each frame (i), \bar{n}_t and \bar{n}_r are the mean of target and reference star.

With the program **rtcnv** we can convert the window files to standard fits files that we can inspect using SAOimage. For the picture in figure 6.1, we have used **rtcnv** we to convert our window files to pictures. **Rtcnv** can use the same options as **rtp**, plus some additional options for choosing which window we want to convert. The **rtcnv** commands are listed in table 6.1

Figure 6.1 shows the use of moving aperture. The aperture is the area (circular) in the window from which we count the light. In the upper panel in the

rtcnv - convert photometry data files to FITS images

SYNTAX: rtcnv [options] out file

OPTIONS:		DEFAULTS:
-a name	Format name string of data files	"data/w%05d"
-c #	Center follows star #	No centering
-f name	Flat field names	Flat.fits
-m #	Median filter sigma clipping factor	3
-n #	Number of sequence frame to convert	One frame
-s #	Start frame	Zero = first frame
-t #	Compute sky from sky field number	First sky field
-w #	Number of windows to use	All minus bias window
-x #	Aperture x center	Center of win avoiding bad cols
-y #	Aperture y center	Center of win
-z #	Number of sky fields	1
-B	Don't remove bias level	On
-M	Aperture mask follows centroid star	Off
-O	Use individual aperture offsets	No offsets
-R	Raw sequence (no conversion)	Convert from ccd to user order
-S	Don't subtract sky values	Subtract sky
-X	Don't use the aperture mask	Use mask if mask.fits exists
-h,-H	Print this help page and exit	

Table 6.1: Command used with **rtcnv**. This table is the same as we get in the terminal when we use the -h option.

figure, we see that the stars are not centered in the window. With moving aperture (lower panel), the program **rtp** calculates the center of the star in each frame, and the aperture can follow the star. Using this, we can use a smaller aperture, and reduce the amount of light from the background.

A normal run of **rtp** can look like this:

```
rtp -f "flatBA*.fits" -M -O -c 2 -i 5 -r 10 -s 10
```

Here the flats we want to use from the **flats** directory are called **flatBA1.fits**, **flatBA2.fits** and so on. Running **rtp** with the **-f** option, a superflat called **Flats.fits** is from all the **flatBA*** flat-fields. We use **-c 2** because the target star is weak, and we want to center with the brighter comparison star. The radius of the aperture is here 10 pixels, and we use sky annulus subtraction with 10 pixels from the edge and in.

The files we get from **rtp** is raw data (**phot.raw**), sky subtracted data (**phot.dat**) and the differential photometry data (**phot.dif**).

With **rtcorr** we correct for the extinction to get the right level of counts. To do this we need the location of the telescope, the position of the target and the time. The information is put in to a file called **TELESCOPE** looking like this:

```
Observatory:    "Skibotn Telescope"  
Longitude:     "+20d21m54s"  # Negative for West / Positive for East  
Latitude:     "+69d20m54s"  
Altitude:     "157m"  
Instrument:    "tcp"  
Filters:      "BVRIXN"
```

and **TARGET** looking like this:

```
# Target information:  
TARGET:       "LX Ser"  
RA(J2000):    "15h35m44s"  
DEC(J2000):   "+19d01m30s"  
# Observation run information:  
DATE:         "2000-03-15"  
TIME(UT):     "01:20:59"  
# Extinction coefficients  
K_B:          "0.38"
```

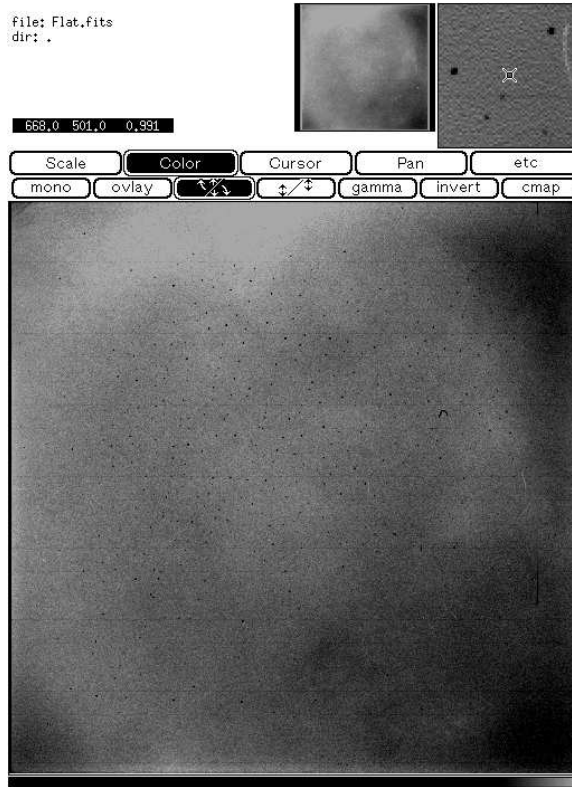


Figure 6.2: The flat field image used to correct for variations in the chip itself. The image is a combination of 35 flat fields taken during the observation of AM CVn. The flat-field is normalized to one. The difference between the darkest and brightest areas is around 5 percent.

K_V: "0.22"
 K_R: "0.09"
 K_I: "0.05"

The extinction coefficients in the **TARGET** file is typical extinction coefficients for observatories at the same altitude as Skibotn [Thomassen (1996)]. We have only observed with the B filter, so this is the only coefficient we have to worry about.

The sky subtracted data, 'phot.dat' is the input file for **rtcorr**. To run the program, write **rtcorr phot.dat**

The output is the same file corrected for extinction. From this 'phot.edf' (differential photometry), 'phot.nma' (differential photometry centered around

0) and ‘phot.win’ (centered around 0 and beginning and end put down to 0, called tapering), are made.

To make FT of the data we use **rtft**. The input is one of the three files above. I used phot.nma because it gave the best result.

With rtp we can choose the aperture we want (circular), within the 64x64 pixels squared window that we observed. We want to have the aperture that gives the best signal to noise ratio. To find this aperture we have a Perl-script that automatically run **rtp** for different apertures. Then, with a IDL script, we check which FT that gives the best signal to noise. The signal is the value of the largest peak, and the noise the average FT in areas where we don’t expect large peaks. If we plot the signal to noise ratio as a function of radius, we find the best aperture radius for each observation. To be sure we have the right main peak, we plot the the frequency of the largest peak as a function of radius. In figure 6.3 we see an example of these two plots for the nights we observed GD 358. Typically, with to small aperture radius, we do not get all the light from the star in the aperture, and the signal is low and noise high. With to big radius we get to much disturbing light from the background, and the noise level is high. Somewhere between we find the best signal to noise ratio.

6.3 Reduction of GD 358

We have two nights of observations of the white dwarf GD 358. From figure 6.3 we have that the first night sky field subtraction and differential photometry of target star minus the first comparison star with radius 8 pixels give the best signal to noise. The FT give the primary pulsation period of $1269 \mu Hz = 788$ s.

The second nighti, sky field and sky annulus subtraction give the same result of the signal to noise. Both are calculated with aperture radius 10 and differential photometry of target star minus first comparison star. The primary pulsation period is 788 s. The sky annulus is preferred in this case because it has less noise in the area 0 to 1000 μHz . In the test for the signal to noise as a function of radius we see that with radius >10 the S/N falls dramatically. This is because the star is not always centered in the 64x64 pixels aperture we use for observing, and in this case the stars are to far to one edge (see figure 6.3).

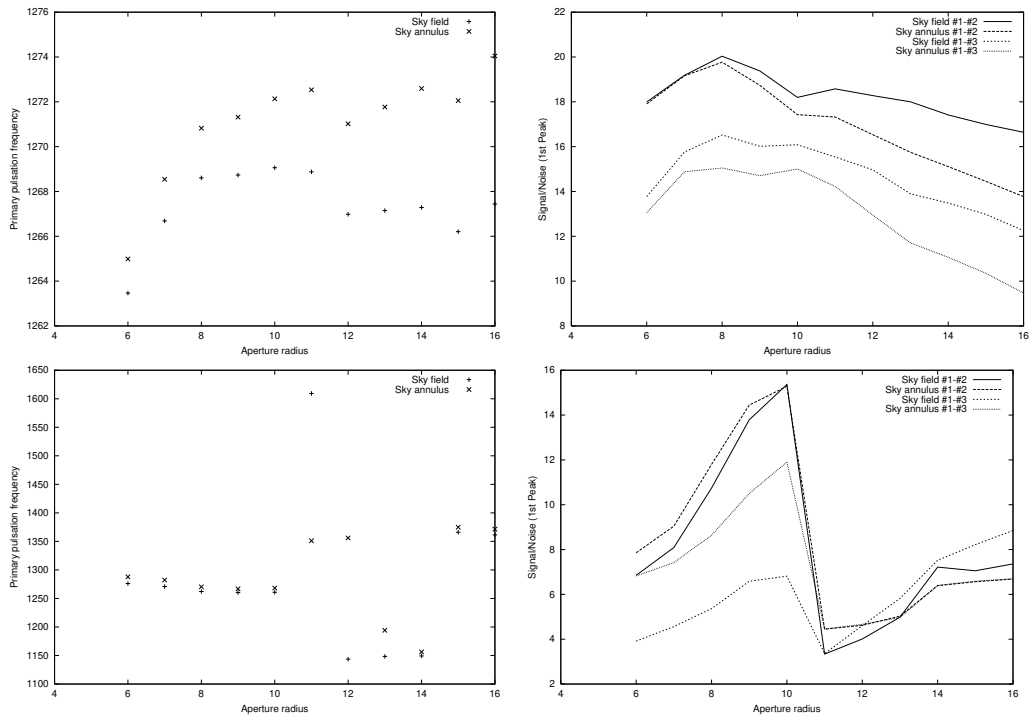


Figure 6.3: The figures on the left side show the frequencies for the largest peak in the FT as a function of aperture radius. The figures on the right side shows the signal/noise ratio as a function of aperture radius. The upper graphs is for GD 358 2202 and the lower the same star 2302.

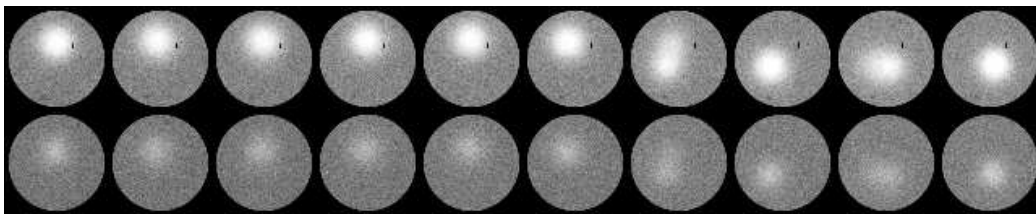


Figure 6.4: Example of stars not centered in the aperture.

6.4 Reduction of AM CVn

We were lucky to get three nights in a row with perfect conditions and the system fully operating. The target chosen was AM CVn, a 14.2 V-magnitude star. A description of AM CVn is found in Solheim (1998)

In figure 6.5 we see the main frequency and the signal to noise ratio plotted against the aperture radius for each night. For all the nights, sky annulus was the best to use for background correction. This is because of the rapidly changing background, and different background for each star. To correct for this we need the sky as close as possible to the star.

From figure 6.5 we have, that the first night, the best result was with differential photometry of target star and comparison star 1 and radius 7 pixels, second night comparison star 2 and radius 7 pixels and the third night, comparison star 1 and 5 pixels. All with sky annulus.

As we discussed in chapter 3 when using sky annulus it can be an advantage to have as much pixels for the background as possible, but if we use too much of the window for background area, light from the star can come into the background and give a wrong estimate for this. To check if the number of pixels used for background changed the noise level in the Fourier Transform we run `rtp` with `-s` equal 5, 10 and 15. The value shows the number of pixels from the edge of the window and in towards the aperture, used for sky. The result with radius 5, 6, 7, 8 and 9 pixel aperture radius for AM CVn is given in figure 6.6. We see from the figure that 10 instead of 5 pixels gives better signal to noise in some cases. For all the plots represented in the result chapter 10 pixels is used for sky annulus.

To improve the results, we have combined the sky field background and sky annulus the way that we use sky annulus on the aurora part of the light curve, and sky field subtraction on the rest. Because more noise is introduced when we use sky annulus subtraction, we thought this would decrease the noise level, but this gave no improvement in the FT of AM CVn 1702. The reason for this can be that we have strong moon light this night that gives a changing gradient in the field during the whole night. To correct for this it is important to have the area for background as close as possible to the star. In the observations done by Østensen with TCP at the Nordic Optical Telescope, he got a better result with sky field subtraction [Østensen (2000)]. If we can decrease the reflection in our system, a combination of sky field and sky annulus can improve the result in some cases, when we have aurora

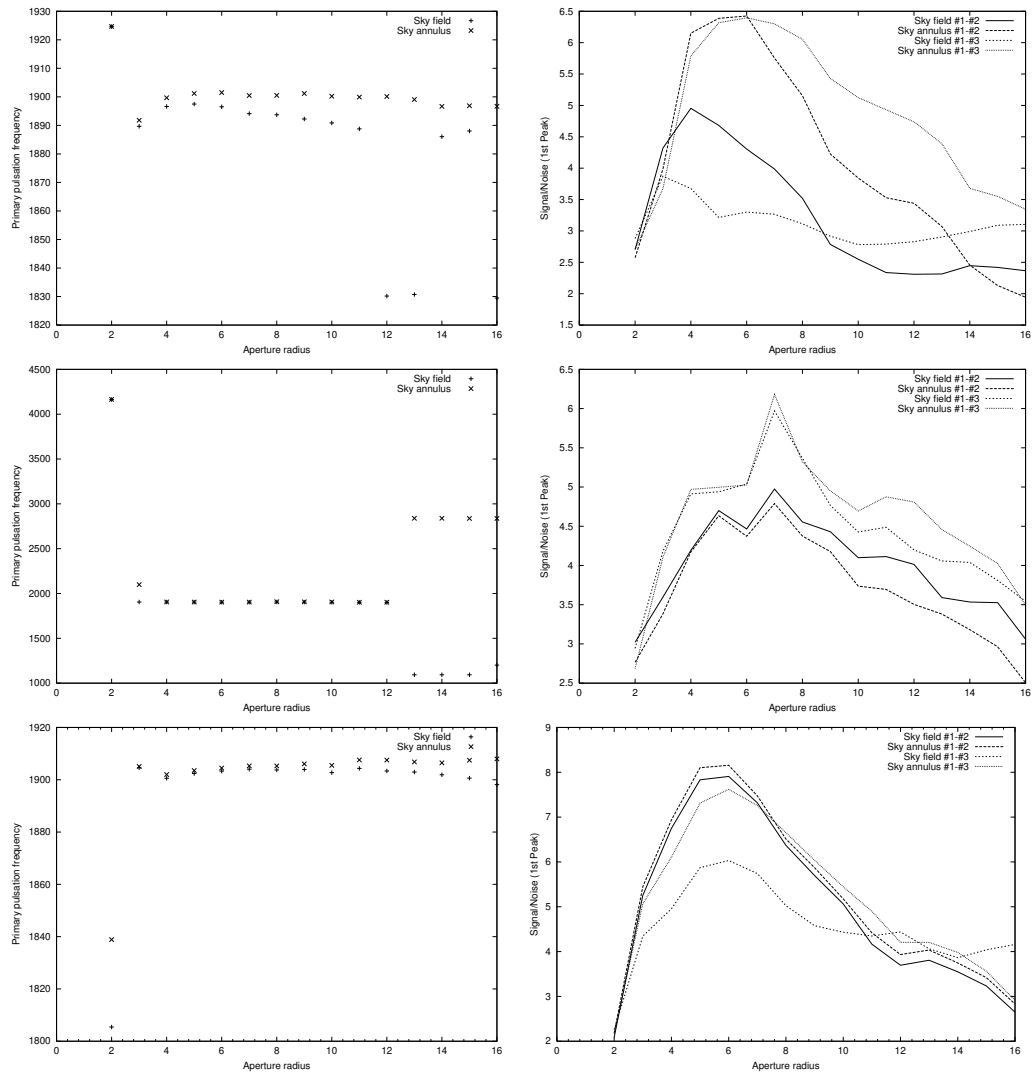


Figure 6.5: The figure to the left shows the frequencies with largest amplitude in the FT as a function of aperture radius. The figure to the right shows signal/noise as a function of aperture radius. All curves are of AM CVn. From the top: 15., 16. and 17. of February.

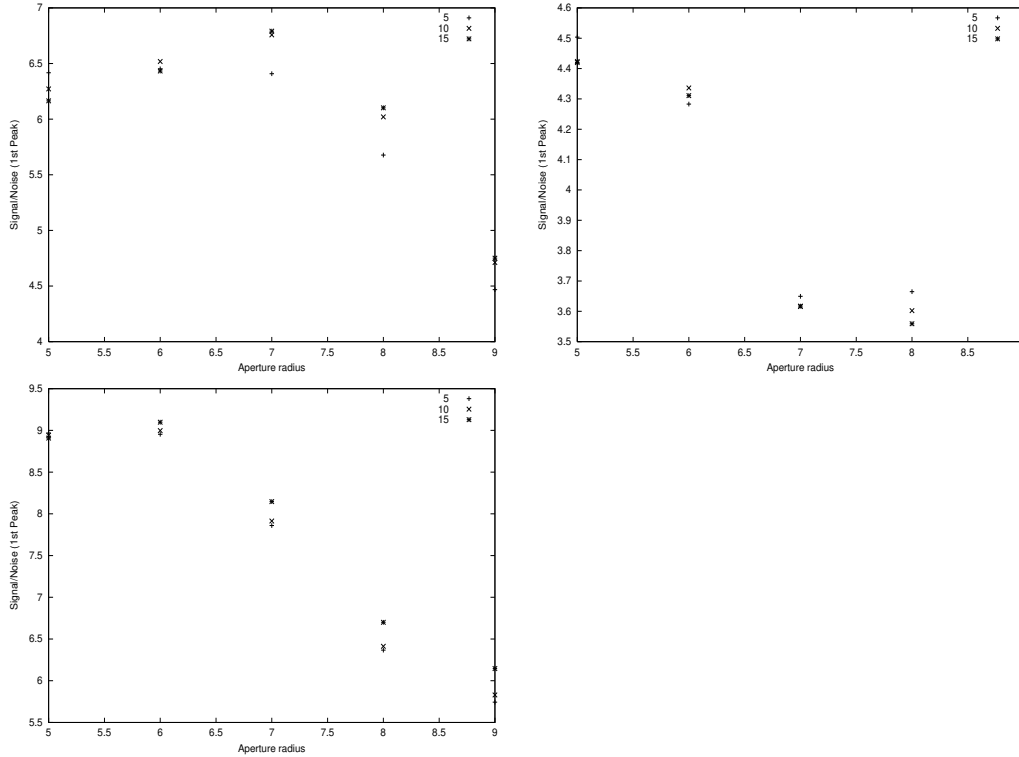


Figure 6.6: Different number of pixels used for sky in sky annulus subtraction, plotted with signal to noise ratio as a function of pixel radius in the aperture. The night of AM CVn 15.02 in the left graph and 1602 in the middle and 1702 to the right.

in some parts of the night, and stable background in other parts. This can also be valid if we have moonlight. This should be tested in the future.

From the WET campaign in 1990 of AM CVn the frequencies μHZ (amp(mma)):
 972(1.2), 988(1.2), 1902(10.4), 1923(4.4), 1944(1.2), 2853(2.9), 2874(1.8),
 2895(1.2), 3805(1.0), 3825(0.9), 4756(1.25), 4777(0.6) and 5707(0.9) were determined [Solheim (1998)].

Figure 6.4 shows the normalized light curve from all the observations in the WET campaign in 1990. The Fourier Transform of this gave the Frequencies given above. In this type of observation it is important not to have gaps in the light curve. The gaps will introduce small side bands in the FT due to periodic gaps in the data samples. The WET (Whole Earth Telescope) organization uses many telescopes around the world to cover the star during all the WET run. As we see in figure 6.4 there are several gaps in the curve. This can be because the telescope covering this part of the night have clouds.

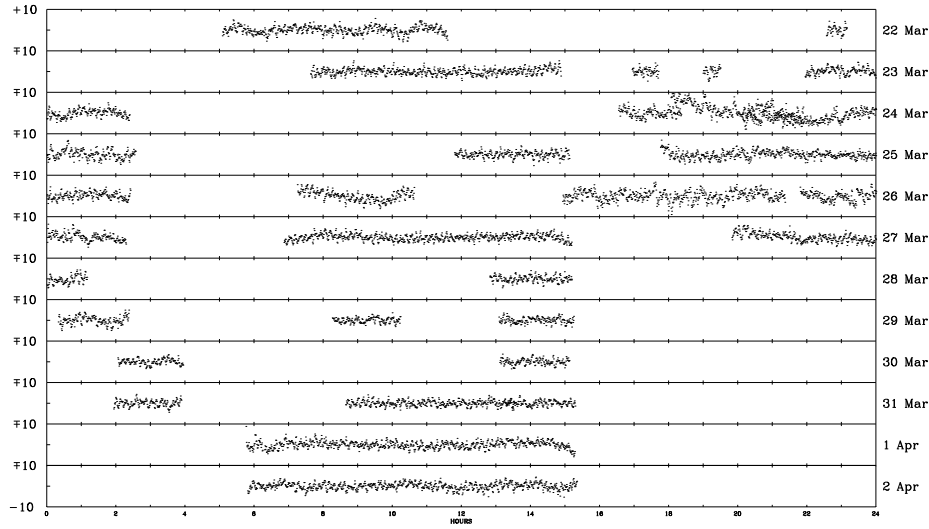


Figure 6.7: The normalized light curve from the WET run of AM CVn in 1990. Each panel shows one day of data [Solheim (1998)].

With `rtfft` it is possible to combine the Fourier Transform for several nights. This is done with the nights of AM CVn and represented in the result chapter.

6.5 Seeing

Due to the turbulence in the atmosphere, the resolution of the image has a limit. The full width half maximum (fwhm) of how the energy is distributed in the image, gives the seeing. The seeing is measured in arcseconds, and tells directly how much an image can be resolved. To get as low seeing as possible, the telescopes are placed at high altitudes, and in areas with steady wind. The best earth based telescopes has a seeing of 0.5 arcseconds (Bohm-Vitense, 1989, page 49). With adaptive optics, that correct some of the disturbance from the atmosphere, the seeing can be as low as 0.2-0.3 arcsec [from discussion with Solhem].

The Skibotn observatory is placed at low altitude, and the shape of the valley gives much turbulence. From previous work, we expect a seeing between 5-10 arcseconds.

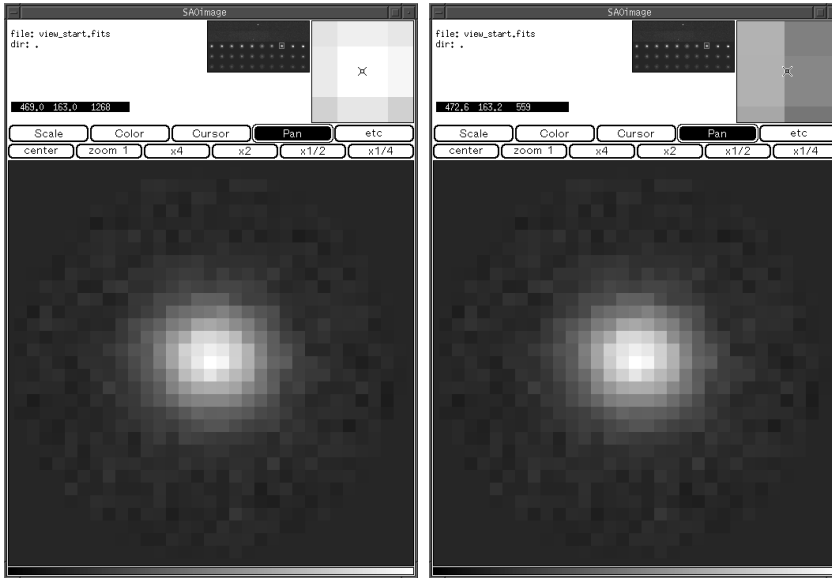


Figure 6.8: Example of method 1. The first picture shows the value of the pixel in the center. In picture two, we have moved out to we get half of that pixel value. Two times the distance we have moved, gives the fwhm in pixels.

To calculate the seeing we use two methods. Method 1: In **saimage** we visually inspect the image of the star, and find the number of pixels for the full width half maximum. We know how many arcseconds we have per pixel and 'fwhm' in arcseconds gives the seeing. This method is easy to use, and we don't need any other programs than **saimage**. We used the method during the observations to check the atmospheric conditions. Figure 6.8 shows an example of this method. In the first frame, the pixel value is 1268 ADU in the center. The pixel number on the x-axes was 469.0. In frame two we have moved from the center towards the right, to a position where the pixel value is half of the value in the first frame. The pixel number in the x-axes is now 472.6. We have moved 3 pixels to the right which gives a fwhm 6 pixels.

Method 2: We have an IDL-routine that fit a point spread function (psf) for the star, and from this find the fwhm. In figure 6.9 we see the distribution of photons from three stars. In figure 6.10 we see how the seeing is changing with time from the night of 17. February. The seeing varies between 4 and 10 arcseconds, with an average of around 6. We can also use a program called **imexam** in **iraf** (a software package for reduction of astronomical data), to find the fwhm. The best seeing found in the data gave with method 2 3.4 arcseconds.

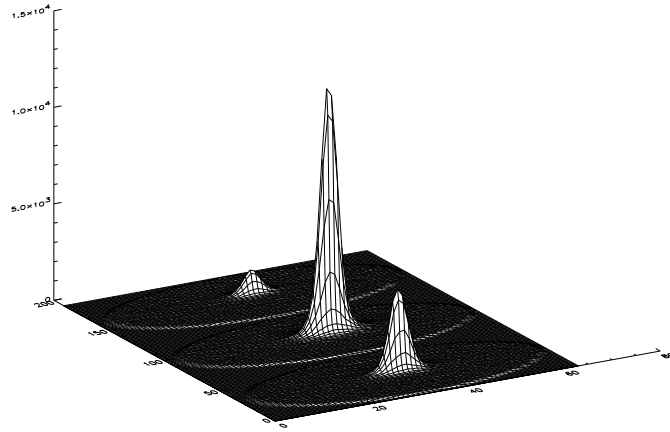


Figure 6.9: Example of how the photons from the star is distributed in the aperture.

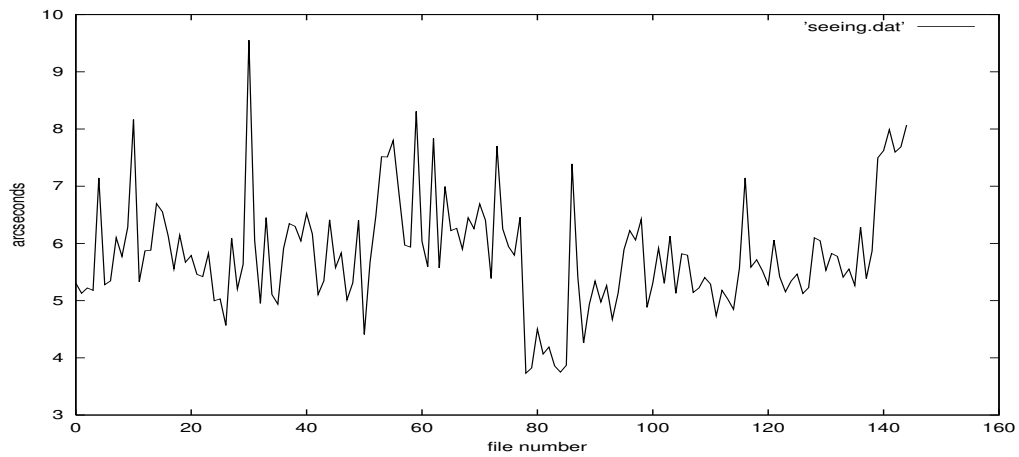


Figure 6.10: Example of how the seeing is changing with time. This is from the night 17. February observing AM CVn

6.6 The aurora photometer

The data from the one channel aurora photometer is reduced with the QBasic program described in chapter 4. The output is a data file with one column containing the counts from the photometer and a header each 600 point. The header is market with a #, and contains information of date, time and sampling time. We used 1 second sampling time for all the aurora measurements. After each header 15 points are missing, because every 600 points, when the data are read to the hard drive, the new data from the photometer is not stored. This is a software problem, and was not discovered until after the observations.

To check for auroral pulsations that could influence the observations from the tcp, we edited the data file to be the same way as the .dat file from the TCP. Then we can use **rtft** to make an Fourier Transform. We ran **rtft** in areas where we could have pulsating aurora, without detecting any periods.

Chapter 7

Results

In this chapter we will present the results of the reduction of AM CVn and GD 358, and discuss what these results means for the possibility of observing variable stars in the auroral zone.

7.1 AM CVn

The raw light curve of the observation of AM CVn is completely dominated by the background light. The signal for the target star is 10 percent over the background signal with 6 pixel radius aperture. Using **rtcorr** and a extinction correction of 0.5 in the blue, we get a flat curve of the differential photometry. Figure 7.1, 7.2 and 7.3 show the three nights of AM CVn. The upper part of the figures show from top: (1). The raw light curve of the target star, (2.)differential photometry of target star and (3.) differential photometry of the two comparison stars. The lower part show: Amplitude spectrum of target star (1.) and the comparison stars (2.) from the Fourier Transform (FT) of these. The differential photometry for the target star has more amplitude variation than the constant stars. This indicates that the star is variable, and was in fact the way this star was discovered as a short period pulsator. [private discussion with Solheim]. In the amplitude spectra in the lower part, we clearly see a period of around 1900 μHz . The amplitude is around 10 mma, and is 5 times over the noise. The amplitude spectra for the constant stars shows no peaks. The noise is between 1 and 2 mma which is good for the conditions we have in Skibotn and for such a small telescope.

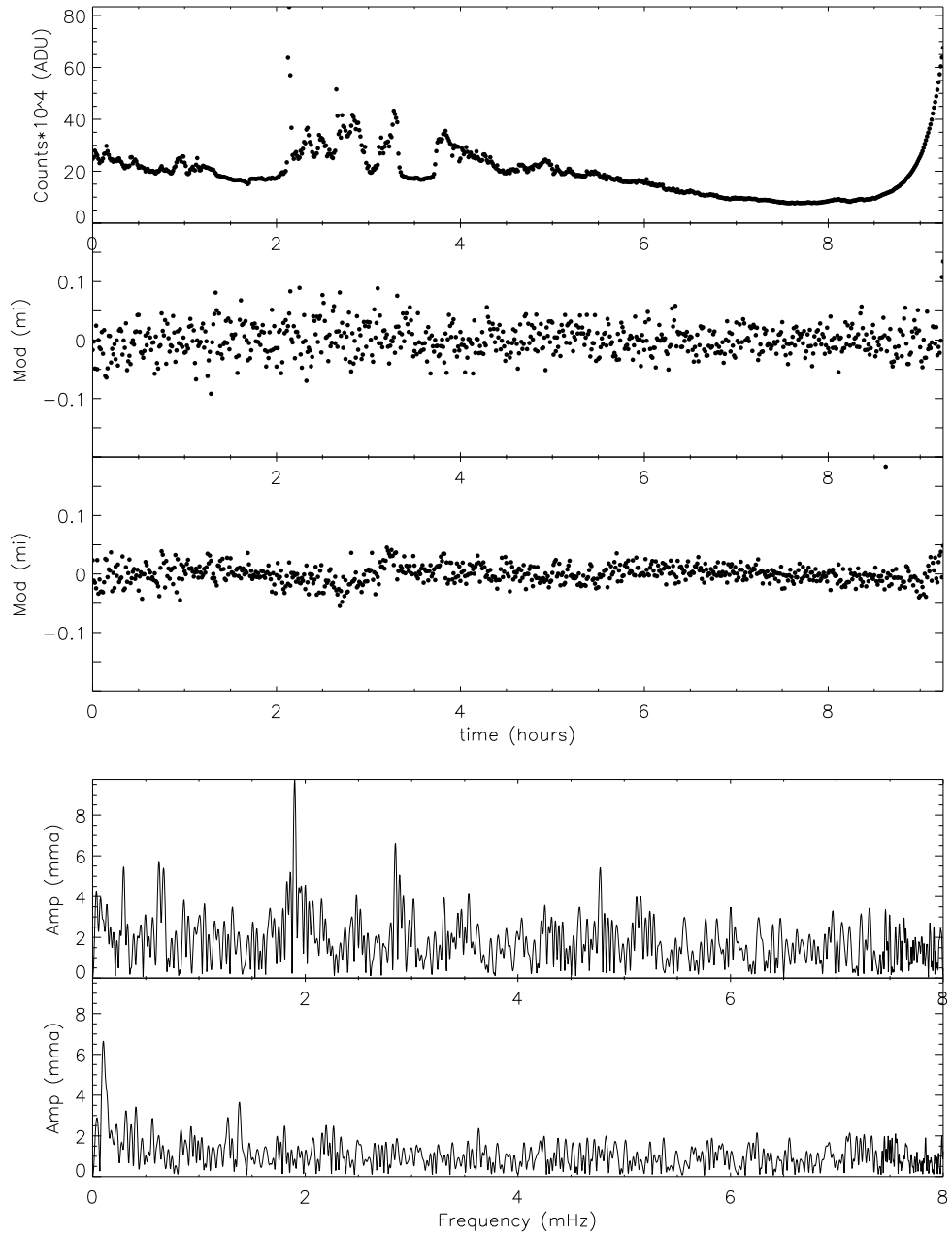


Figure 7.1: AM CVn 1502. From the top: Raw light curve, differential photometry of the target star, differential photometry of the constant star and amplitude spectrum of the target star and the constant star.

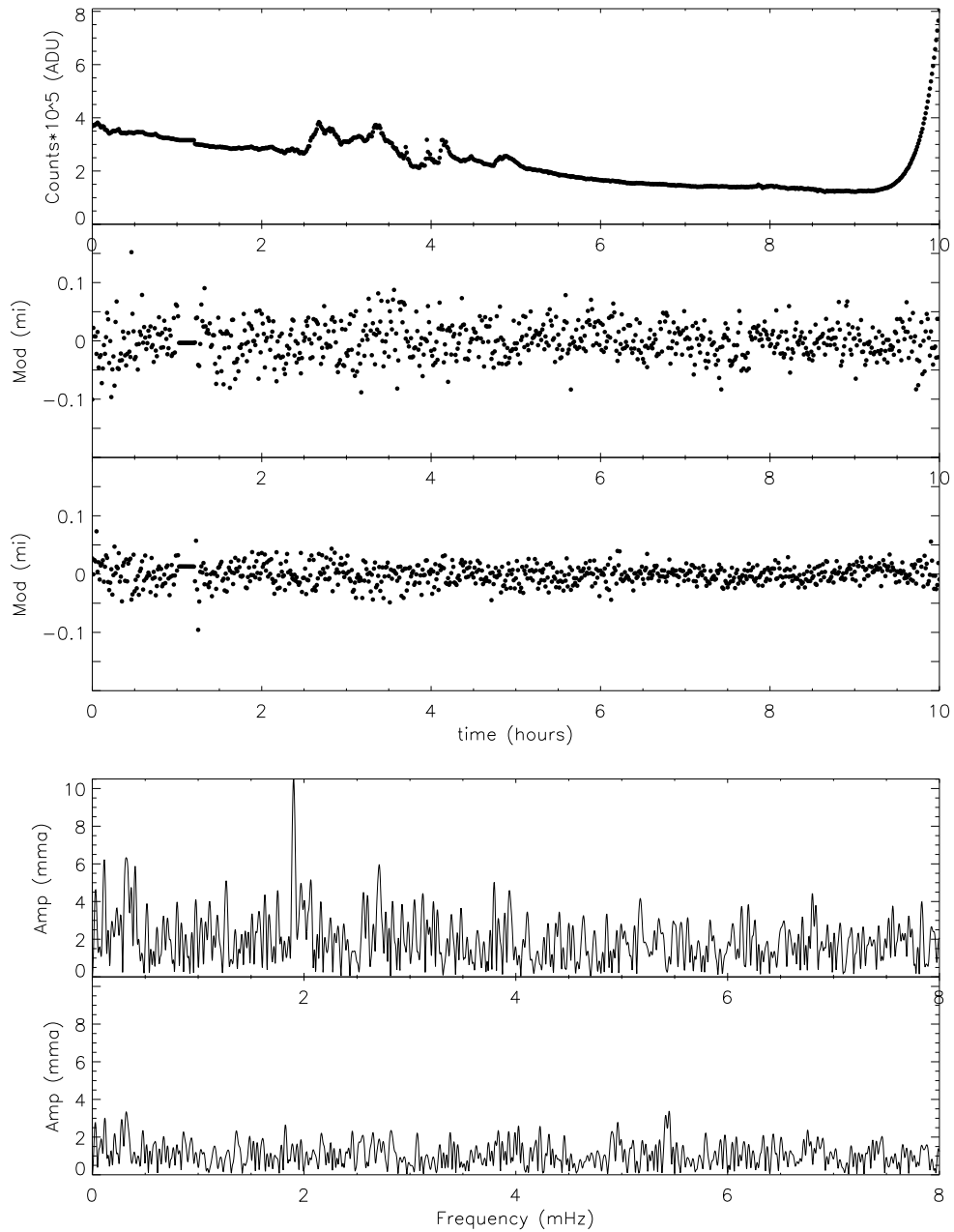


Figure 7.2: AM CVn 1602. From the top: Raw light curve, differential photometry of the target star, differential photometry of the constant star and amplitude spectrum of the target star and the constant star.

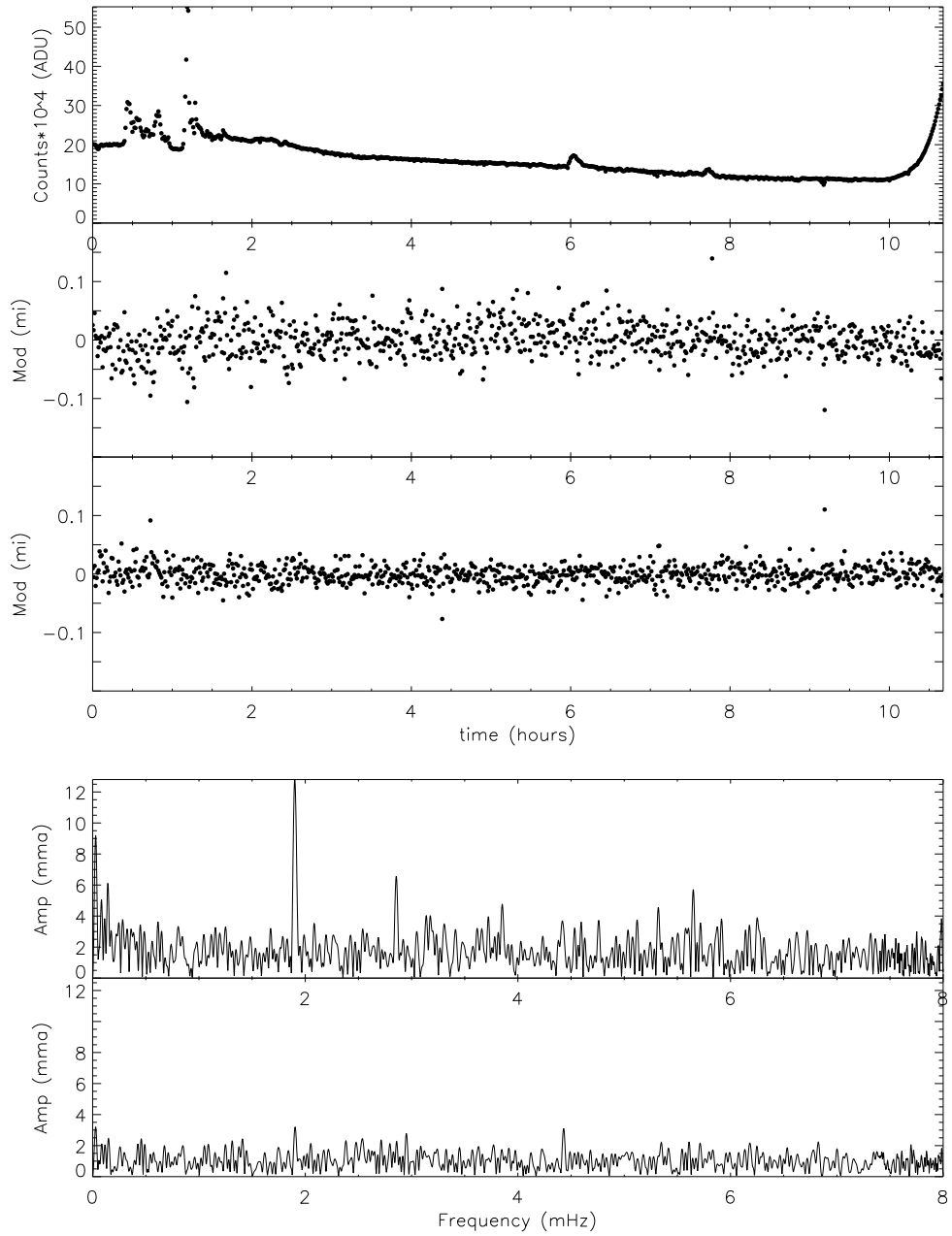


Figure 7.3: AM CVn 1702. From the top: Raw light curve, differential photometry of the target star, differential photometry of the constant star and amplitude spectrum of the target star and the constant star.

To be considered as real, it should be 3 time over the noise for a single night run [private discussion with S.O Kepler].

From the peak file generated when running **rtft**, we get information of amplitude, period, T-Max, phase and width for all the frequencies found from the FT. Knowing the amplitude, period and phase we can fit a synthetic spectra to the observed data. Equation 7.1 gives the formula for the synthetic spectra. The amplitude is in amplitude, the period in seconds, the phase in radians and t the time in seconds.

$$Y = amp_1 \cdot \cos\left(\frac{2 \cdot \pi}{period_1} \cdot t + phase_1\right) + amp_2 \cdot \cos\left(\frac{2 \cdot \pi}{period_2} \cdot t + phase_2\right) + \dots \quad (7.1)$$

We have used the information from table 7.1 of the peaks in the FT of AM CVn to make a synthetic spectrum for each of the nights. The spectra are seen in figure 7.4, 7.5 and 7.6. As seen in the figures, the synthetic spectra follows the observations quite well, but it is not a perfect fit. First of all the modulation amplitude is lower in the synthetic spectra. AM CVn is a faint star at the limit of what can be observed in Skibotn. We see by comparing the observed and the synthetic spectrum, that many of the observed points fall far from our theoretical line. When we made the synthetic spectra, we used the amplitudes found from the FT of differential photometry. AM CVn can have nonlinear modulation that sets a limit for the FT [Solheim (1998)]. The FT only detect periods that is consistent through the whole observation. If the pulsation changes we will get a smaller amplitude in the FT than what we can see in light curve.

7.1.1 Combining several nights

With **rtft** we can combine the FT from several nights. In figure 7.7 we see the combination of the three nights of AM CVn. In the middle panel we show the FT from the area around the largest peak. Combining observations with time gaps between the observations, will create side bands in the FT. The lower panel shows the window function. The spacing between the largest peaks in the window function is $11.5 \mu\text{Hz} = 24.2$ hours. This is the time between the start of each observation. Between these peaks we have a side band of $5.73 \mu\text{Hz} = 48.5$ hours which comes from the starting time between the first and the last observation. The same spacing will appear in all the real peaks in the FT. When combining several nights of observation it is important to have

AMCVn 1502

Average noise in the FT: 1.5

#	FREQ	AMPLITUDE	PERIOD	T_MAX	PHASE	WIDTH
---	------	-----------	--------	-------	-------	-------

AMCVn 1602

Average noise in the FT: 1.7

1900.247	9.7446	526.25	141.28	-1.68682	14.3238
2847.837	6.6218	351.14	304.07	0.84226	13.8195
2887.585	5.0692	346.31	3.57	-0.06472	12.3886
4774.629	5.4277	209.44	175.55	1.01673	15.3974
7909.456	4.7784	126.43	28.83	-1.43287	15.5570

#	FREQ	AMPLITUDE	PERIOD	T_MAX	PHASE	WIDTH
---	------	-----------	--------	-------	-------	-------

1901.294	10.5185	525.96	77.53	-0.92619	17.1493
2709.595	5.9452	369.06	247.96	2.06167	20.7481
3795.223	5.0211	263.49	145.12	2.82274	13.0750

AMCVn 1702

Average noise in the FT: 1.5

#	FREQ	AMPLITUDE	PERIOD	T_MAX	PHASE	WIDTH
---	------	-----------	--------	-------	-------	-------

1901.068	12.8241	526.02	116.05	-1.38619	17.1249
2855.912	6.5760	350.15	345.07	0.09108	15.1783
3852.594	4.7582	259.57	3.88	-0.09398	14.6768
5320.710	4.5590	187.94	66.02	-2.20725	13.8628
5649.582	5.7107	177.00	42.45	-1.50679	13.9296
7784.554	4.4685	128.46	120.85	0.37230	12.9097

Table 7.1: Frequency, amplitude, period, T-max, phase and width of all the peaks with amplitude more than three times the noise level.

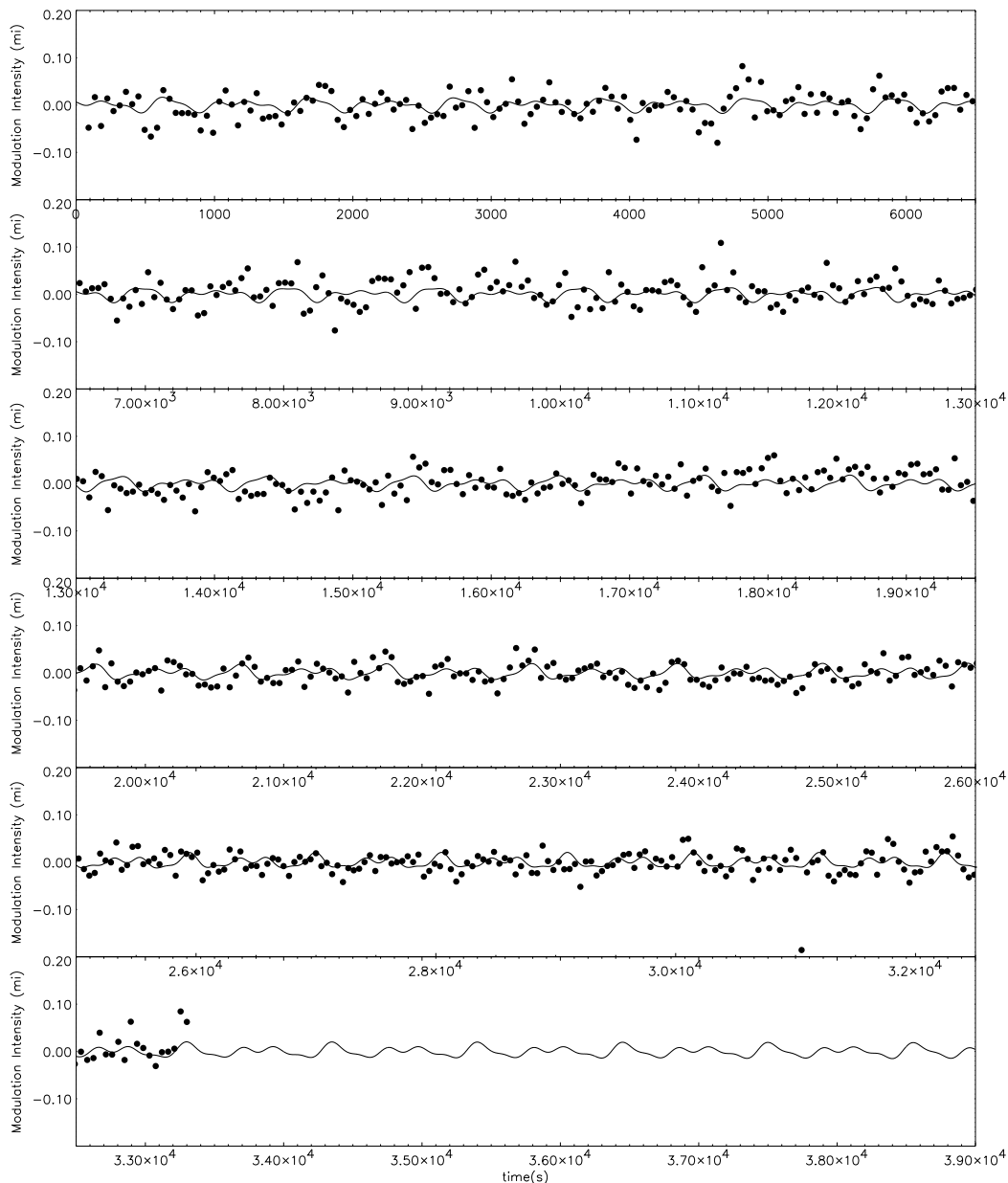


Figure 7.4: Differential photometry of AM CVn 15.02. shown as dots with the synthetic spectra as a solid line.

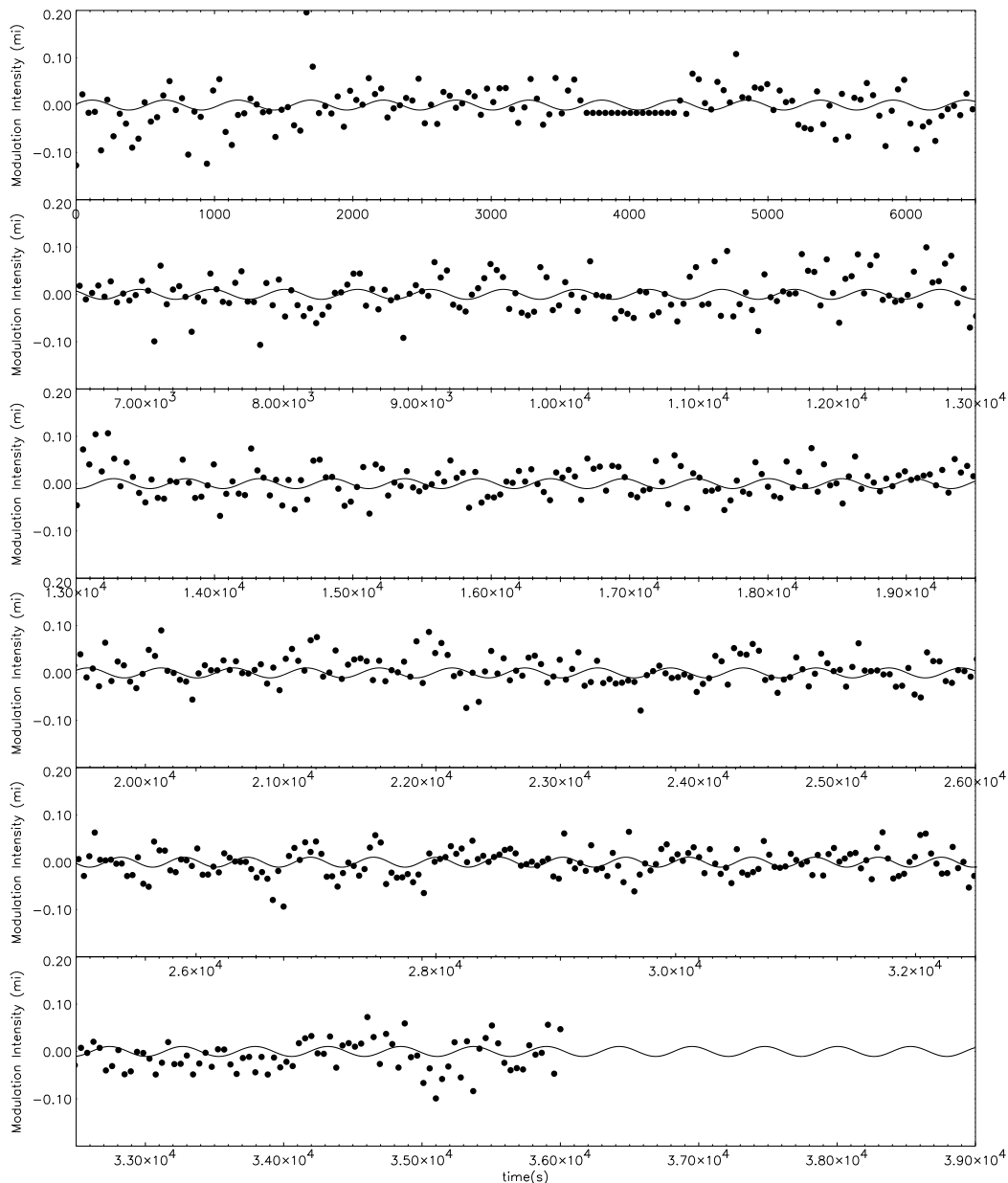


Figure 7.5: Differential photometry of AM CVn 16.02 shown as dots with the synthetic spectra as a solid line.

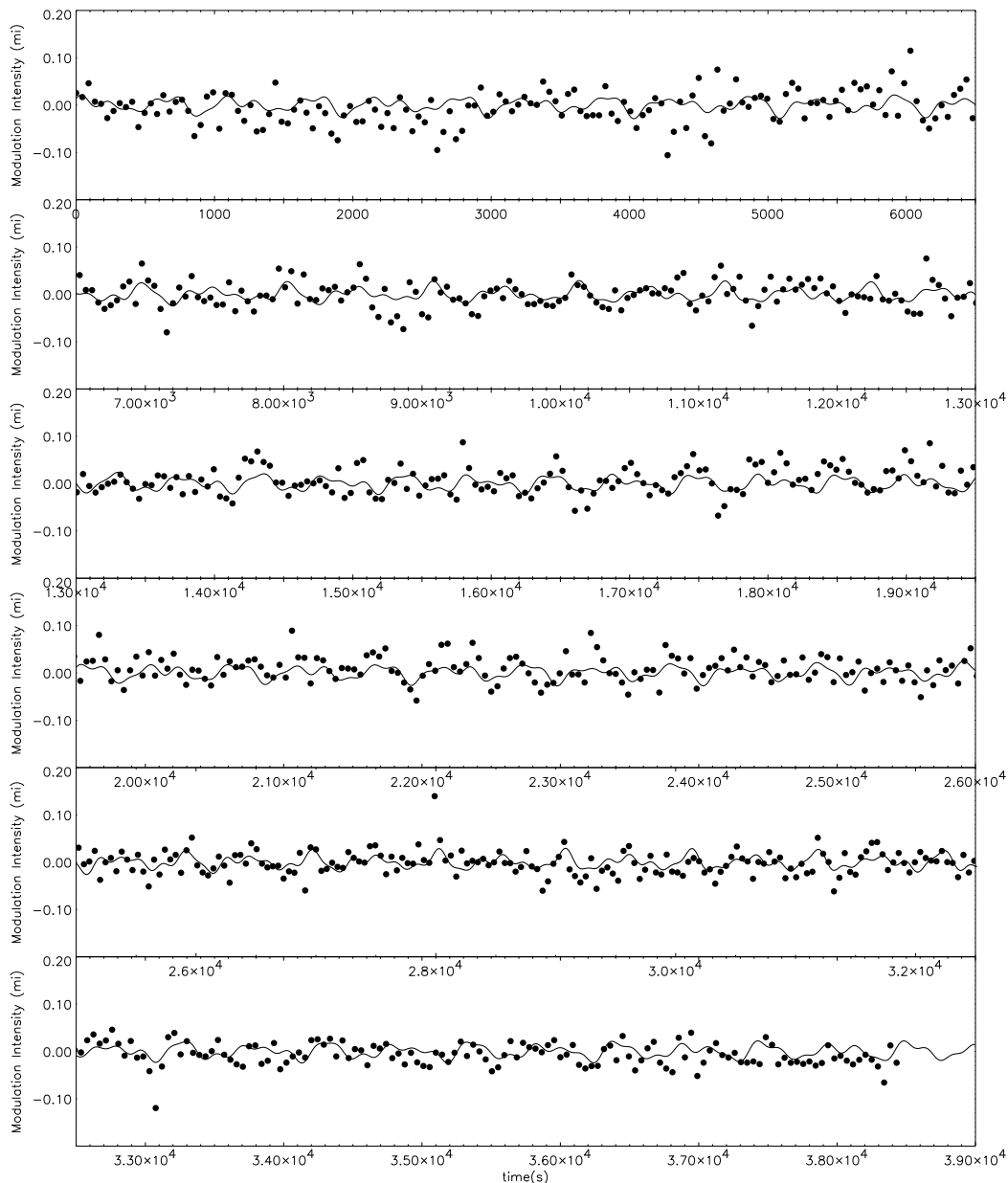


Figure 7.6: Differential photometry of AM CVn 17.02 shown as dots with the synthetic spectra as a solid line.

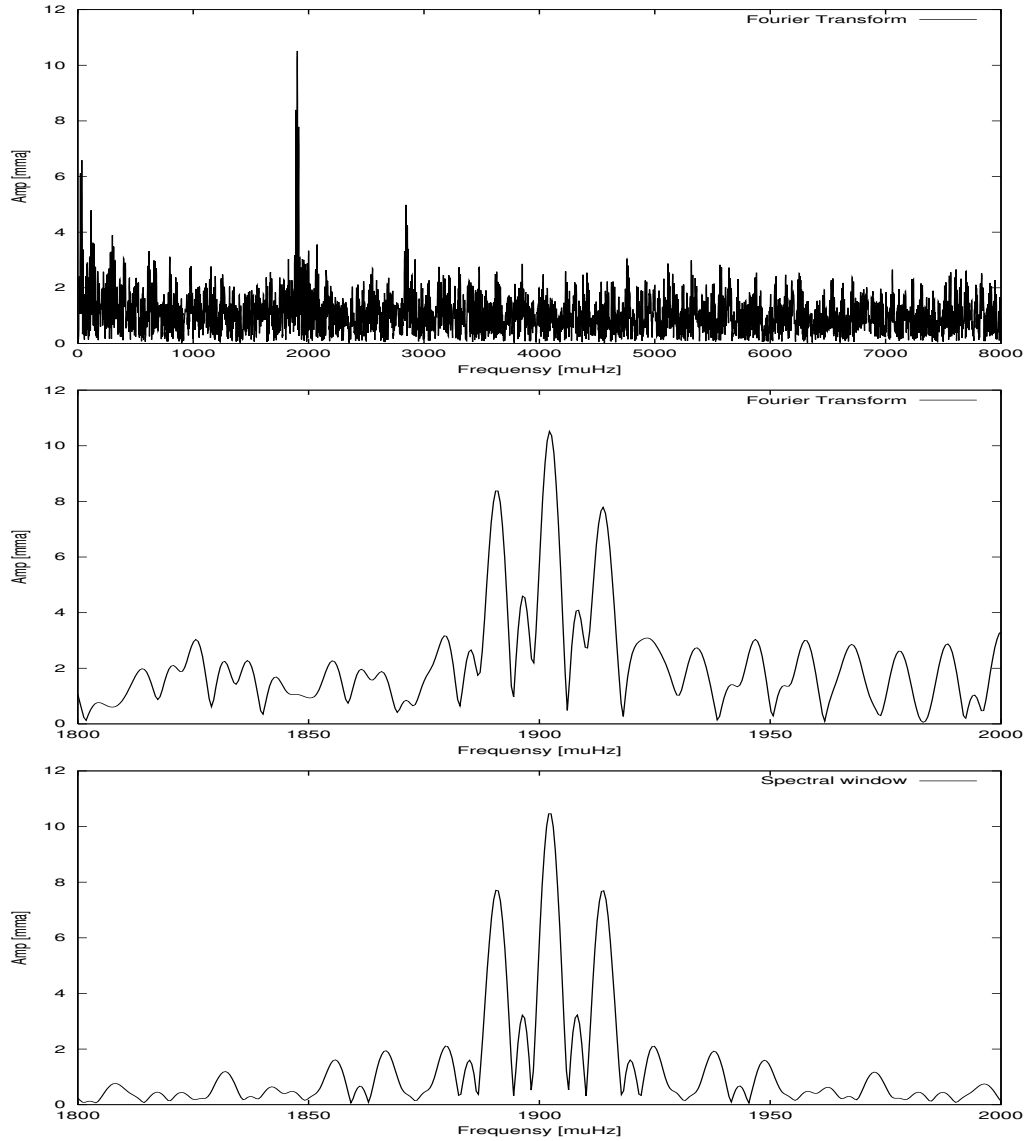


Figure 7.7: Combined spectra from the three nights of AM CVn. From the top: Amplitude spectrum, amplitude spectrum from 1800-2000 μHz and the spectral window in the same range.

#	FREQ	AMPLITUDE	PERIOD	T_MAX	PHASE	WIDTH
	972.444	2.8151	1028.34	846.28	1.11239	2.4355
	982.832	2.9063	1017.47	861.32	0.96426	2.4310
	1902.272	10.5255	525.69	151.00	-1.80481	2.2152
	1924.709	3.3772	519.56	259.24	3.14810	2.9537 *
	1946.748	3.0207	513.68	200.79	-2.45602	2.2705
	2844.045	5.0784	351.61	288.71	1.12411	2.2669
	2850.121	3.4779	350.86	313.55	0.66820	1.7145
	2855.886	4.2296	350.15	5.28	-0.09468	1.9606
	2861.909	3.4800	349.42	40.29	-0.72444	2.0629
	2895.920	2.5389	345.31	38.15	-0.69422	2.1227
	3851.478	2.7772	259.64	256.95	0.06516	2.4987 **
	4757.221	2.9349	210.21	86.73	-2.59255	2.2799

* From the data before correcting for time error.

** side bands with spacing 23.8 hours

Table 7.2: Frequency, Amplitude, Period, T-max, Phase and width found from the FT of the combination of the three nights of AM CVn.

the correct time for the observations. If we use the wrong starting time, the periods found in one night will be out of phase with the one from the next night. After correcting for barycentric error we looked at the phases found for the largest peak for the three nights to see if the phases had changed between the nights. We found an error of 4 seconds between the first and the second night, and 6 seconds between the second and third. This could be because of time error in the computer clock. We made an FT with this new time, but could not see any improvements. In figure 7.7 we only have done the barycentric correction. AM CVn is in a binary system and the pulsations are not very stable [Solheim (1998)]. Because of this we will not rely on the small changes we found in the phase. The peaks with amplitude more than 3 sigma found are put in table 7.2.

The result is very close to the result from the WET campaign of AM CVn given in chapter 6. The average level in the FT is 1.14 when the peaks are included. The noise from 3000 μHz to 8000 μHz is 1.0. We find the same peaks using comparison star two, and the combination of them. When the two comparison stars are combined, the noise level is lower, 0.9 in the range 3000 μHz to 8000 μHz , but the peak amplitude is also lower. The average noise level for the Fourier Transform of the differential photometry of the

two constant stars, is 0.8 mma in the interval 0 to 8000 μHz , and 0.56 in the interval 3000 μHz to 8000 μHz .

The precision in the periods found, can tell about the precision in the timing of the TCP. The 1902 μHz peak (525.69 seconds) differ from the WET observation with 0.07 seconds. This can be the time error in the 45 second sampling time we use for the observation. We did not find the same for the other peaks, so this has to be investigated more carefully later.

7.1.2 Influence of aurora

The aurora makes it difficult to get good observations from the Skibotn Observatory. We have seen in this chapter that we have good results from the observation of AM CVn. In all the night we had parts with strong aurora and parts with little or no activity. In this section we will look at how the aurora is influencing the observations. To do this we have divided the night in parts of 10000 s = 2.8 hours, and made an FT of each part to locate periods and determine the noise level.

In figure 7.8,7.9 and 7.10 we see Fourier Transforms of different parts of the light curve of AM CVn the three nights in February. The first graph is the raw light curve, the second a part of 10000 s with aurora , the third the same length without aurora.

The first night we don't get any peaks from the part with strong aurora, but from the part without aurora we clearly see both the peak at 525 s and 350 s. The noise level is 3 mma and 2.7 mma, respectively. The noise level in the amplitude spectrum from the FT of the two constant stars is 1.7 mma in both cases. The noise level of the amplitude spectrum from the whole 11 hour run is 1.6 mma. The other two nights we can detect the period of 525 s in both the part with aurora and the part without. The second night we see both the 525 s and the 350 s periods but in the part with aurora we only see the 525 s period. The third night is opposite, we better FT from the part with no aurora. The noise level is 4.3 mma and 3.1 mma respectively. The noise from the whole night for the same part of the FT is 1.6 mma.

To explain why we don't see any peaks in the aurora part of the first night, we have two possibilities. The first possibility is that because of beating there should not be any peaks from this part of the night. The other explanation is that the noise is to high to detect any periods. The aurora is stronger this

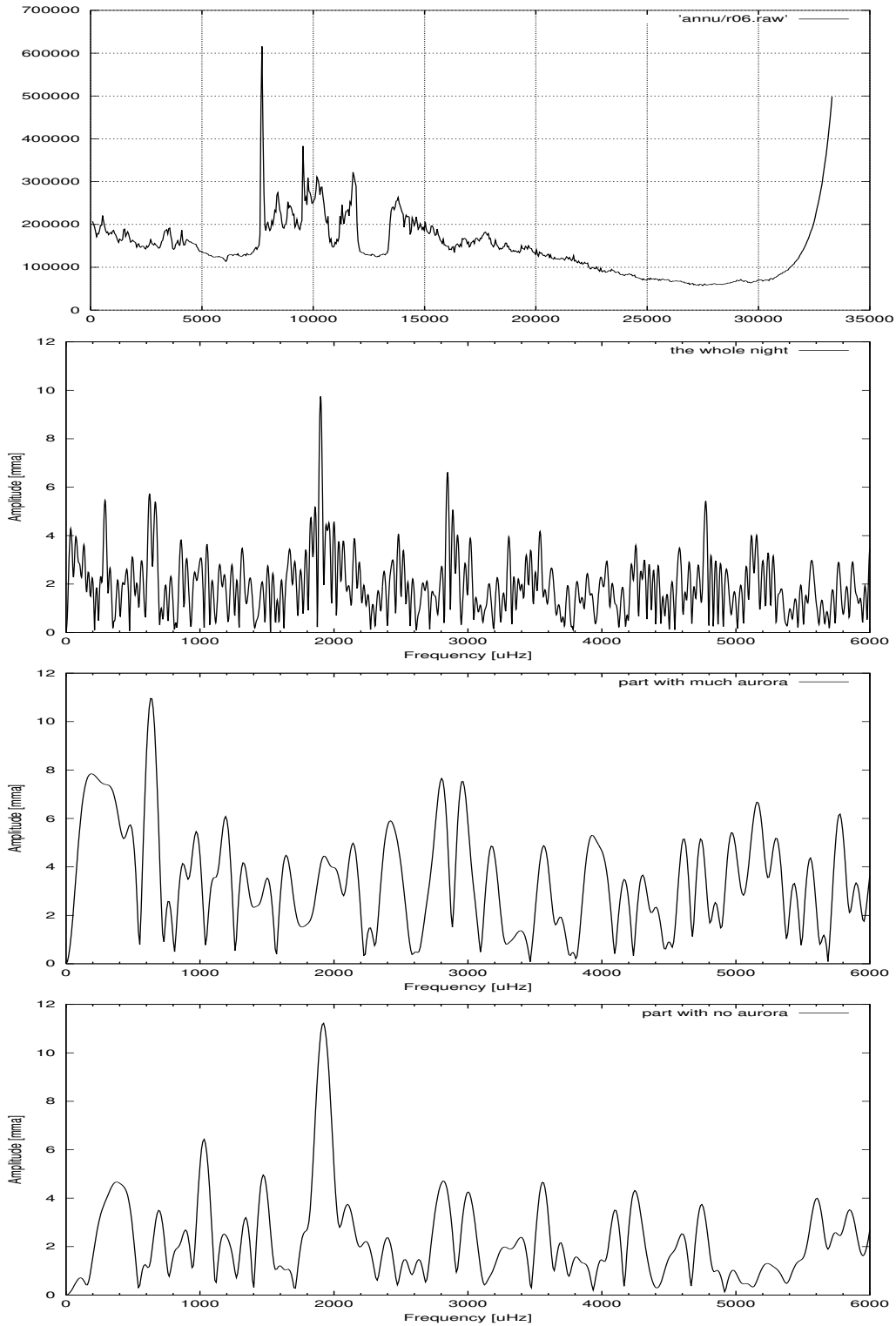


Figure 7.8: Fourier Transform of different parts of the light curve of AM CVn 15.02. From the top: Spectra of the whole night, spectra from 8000-18000 s dominated by aurora, spectra from 29-30000 s with little aurora

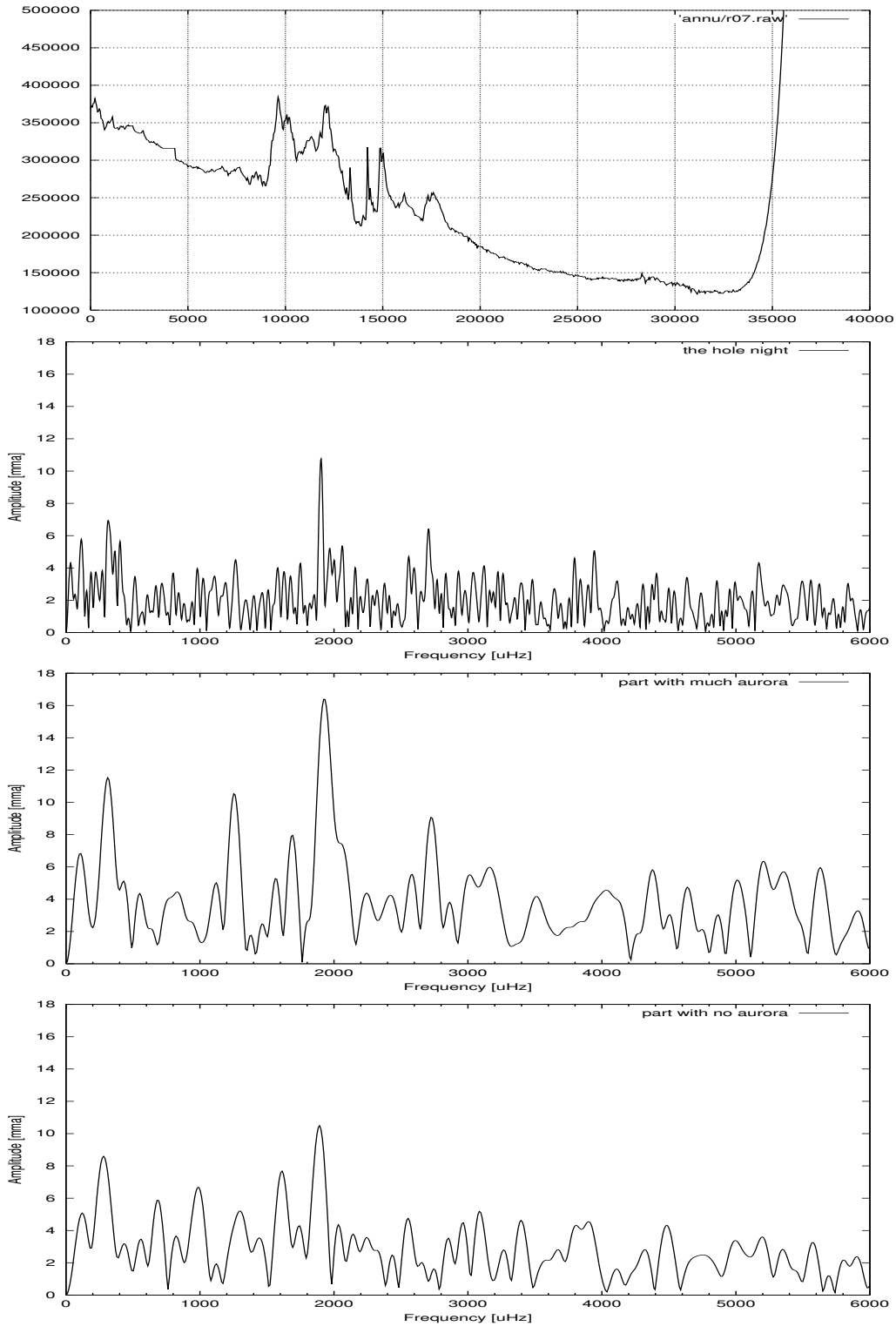


Figure 7.9: Fourier Transform of different parts of the light curve of AM CVn 16.02.00. From the top: Spectra of the whole night, spectra from 8000-18000 s dominated by aurora, spectra from 20-30000 s with little aurora

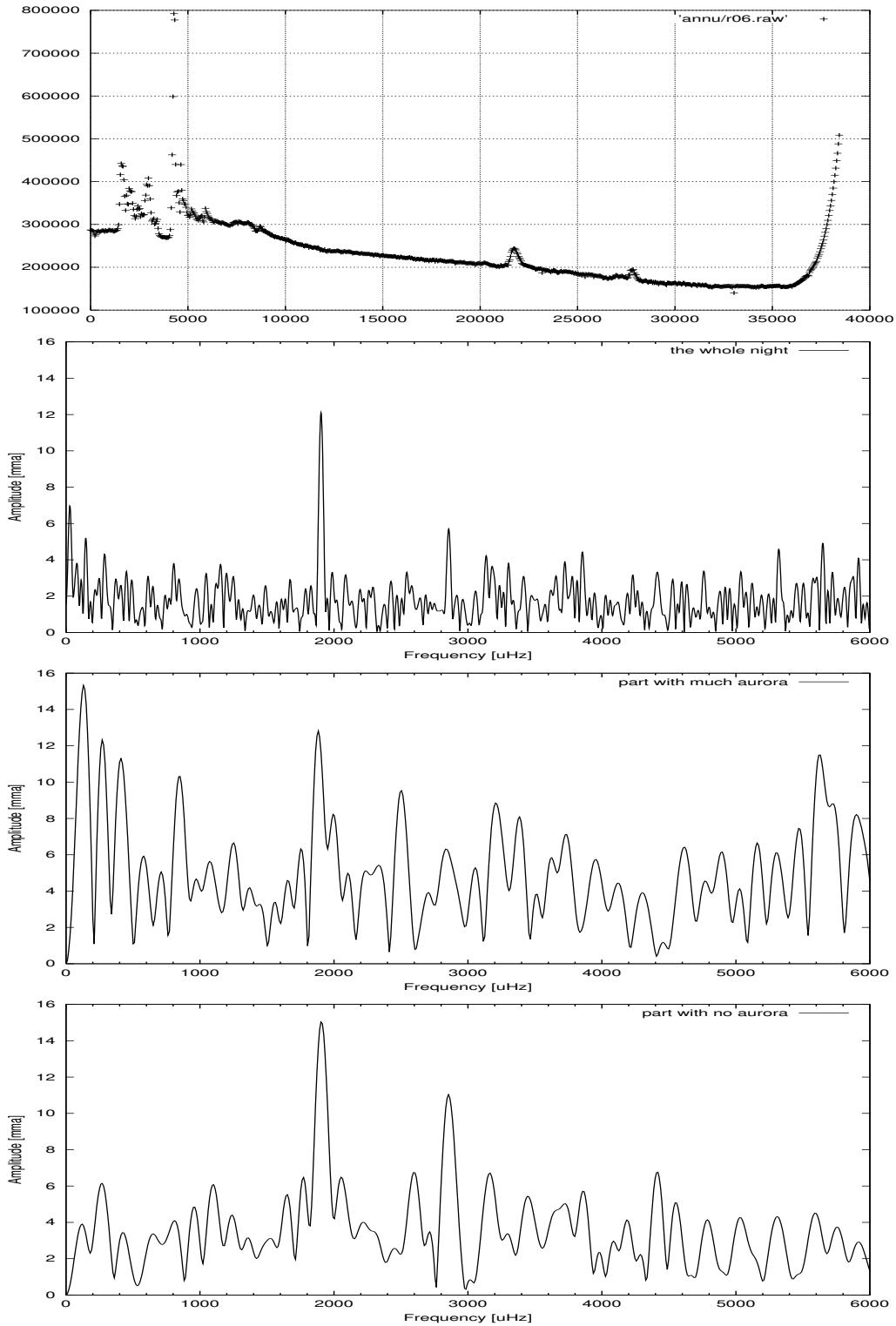


Figure 7.10: Fourier transform of different parts of the light curve of AM CVn 1702.00. From the top: Spectra of the whole night, spectra from 0-10000 s dominated by aurora, spectra from 17620000 s with little aurora

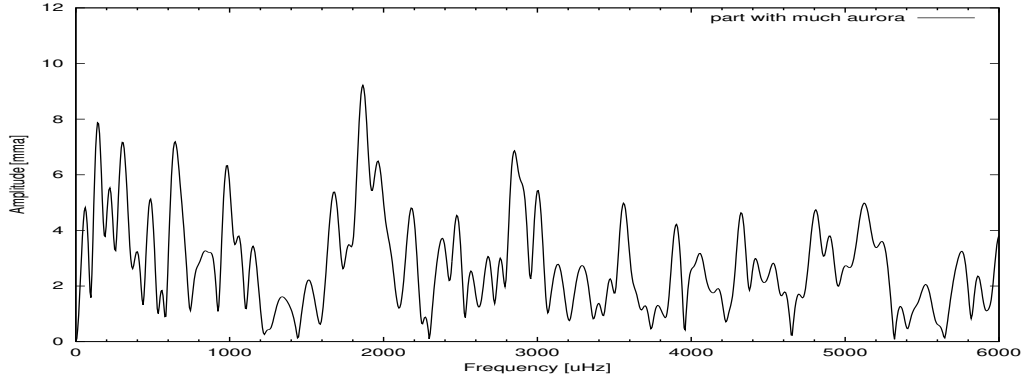


Figure 7.11: Amplitude spectrum of the first part of the night, from 0 to 15000 s, of AM CVn 15.02. The average noise here is 2.6 mma.

night than the other two nights, and the star is moving more in the aperture because of lack of experience this first full night of observation. To check if the first part of the first night really missed the peak at 1902 μHz we make an FT of the part from 0 to 15000 seconds, as seen in figure 7.11. In this figure we clearly have the peak at 1902 μHz .

It is difficult to make a clear conclusion from this because we have only three nights of observation in this test and it is not only the aurora that can disturb the observations. In all of the nights we have strong moon light that is decreasing during the night. We can say that the aurora is disturbing, but not as much as we could have expected from previous observations in Skibotn.

7.2 GD 358

GD 358 is a 13.5 B-magnitude white dwarf. It has a known 700 s period with 0.1 modulation amplitude [Bradley (1998)].

The first night we had stable conditions with no aurora. The second was not as stable as the first but the observation is almost twice as long. In figure 7.13 and 7.14 we see from the top the raw light curve, differential photometry of target star and differential photometry between the two comparison stars and the amplitude spectrum of target and comparison stars.

It is easy to see the pulsation in the differential photometry. The main period in both nights is 787 s with amplitude 50 mma the first night and 45 mma the

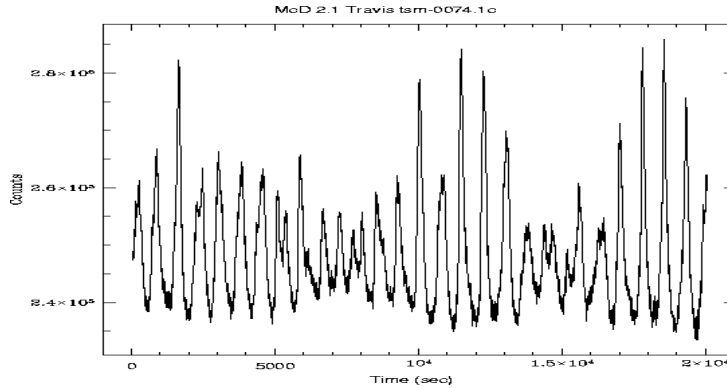


Figure 7.12: Light curve of GD 358 from the Mc. Donald 2.1 meter telescope in the WET campaign 2000 (From the WET Xcov 19 homepage).

second. In addition we see a second period of 657 s with amplitude 20 mma the first night and 710 s with amplitude 25 mma the second. The noise level for the constant stars is around 0.5 mma the first night and 1 the second.

GD 358 is a good object to observe for my project. The pulsation is easy to detect and we also have a lot of observed data from this star to compare our observation. In March 2000, only a month after the observation presented here, this star was target for a WET campaign. The result from this campaign is not published yet, but on the homepage for the campaign [<http://bullwinkle.as.utexas.edu/xcov19/>] they have given the light curves and Fourier Transform for all the observed data.

GD 358 has been observed with WET twice before. In May 1990 and May 1994 the star was the main target for the WET [Nather (1995)]. The basic temporal spectral pattern did not change during those four years, but large changes in relative amplitude were observed for the high power oscillations and noticeable changes occurred on a time scale of few days [Nather (1995)]. Vuille (2000) suggests that the amplitude variation in the temporal spectrum comes from long period beating between eigenmodes and third order cross frequencies.

Compared with the data from this campaign we find six real peaks over the noise level the first night and seven peaks the second night. In table 7.3 we have listed the Frequency, Amplitude. Period, T_{max} , Phase and Width found for the two nights.

From the period, amplitude and phase we can make a synthetic light curve. In figure 7.15 and 7.16 we have plotted a synthetic light curve on top of the

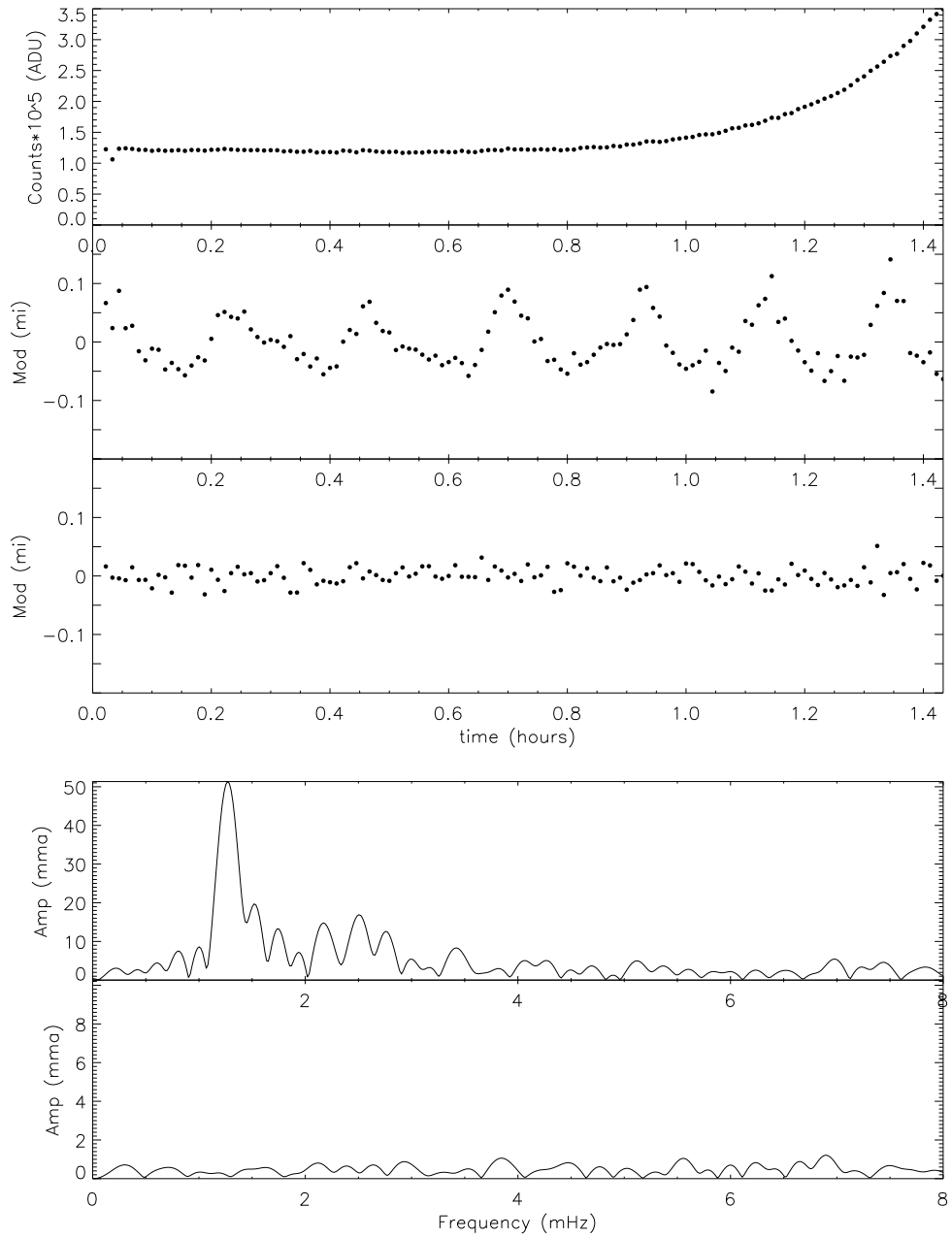


Figure 7.13: GD 358, 2202. From the top: Raw light curve, differential photometry of the target star, differential photometry of the constant star and amplitude spectrum of the target star and the constant star.

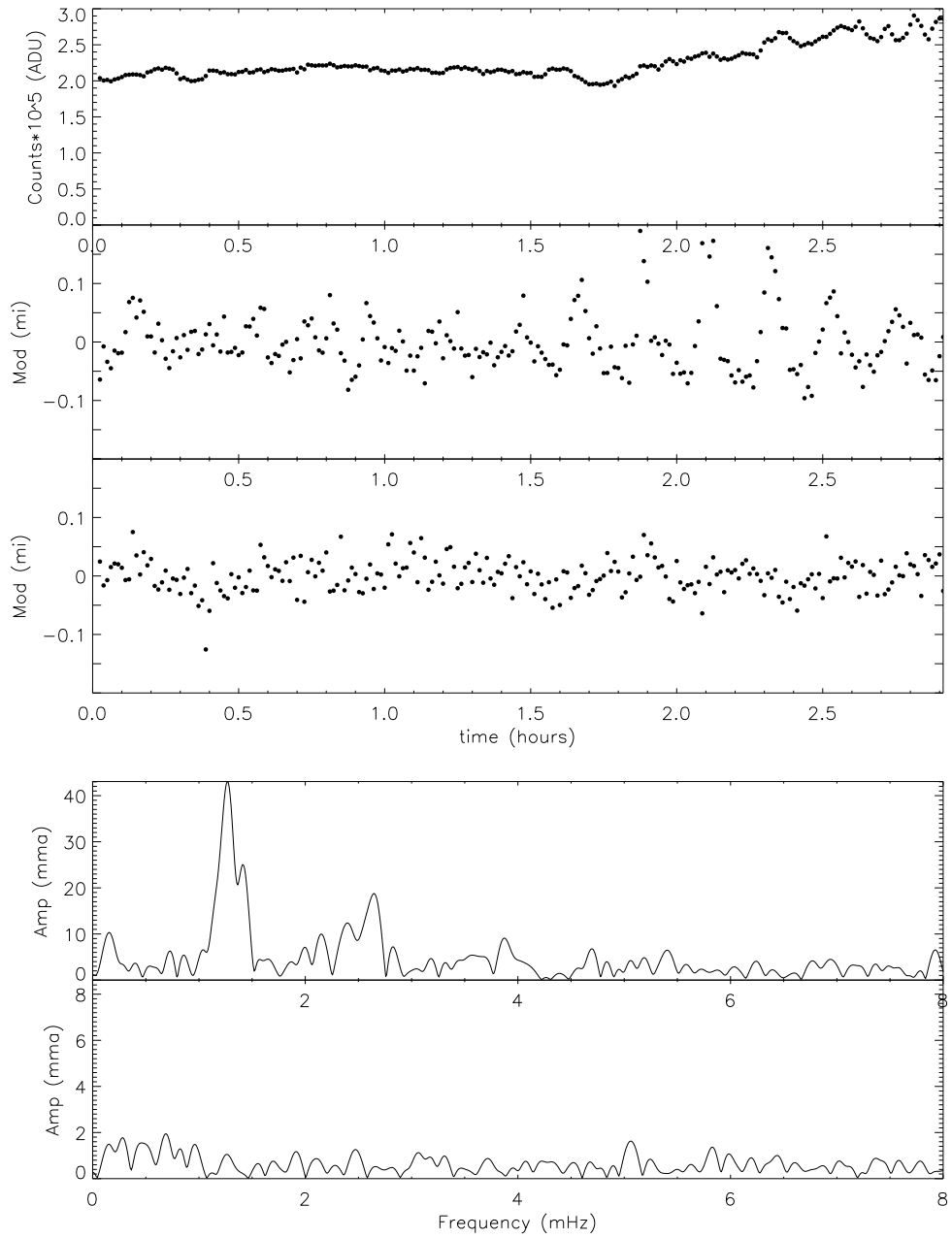


Figure 7.14: GD 358, 2302. From the top: Raw light curve, differential photometry of the target star, differential photometry of the constant star and amplitude spectrum of the target star and the constant star.

Periods of GD 358 observed 22.02.00

#	FREQ	AMPLITUDE	PERIOD	T_MAX	PHASE	WIDTH
1268.607		52.2561	788.27	139.10	-1.10877	104.2302
1522.042		20.0014	657.01	161.28	-1.54234	77.0746
1742.179		13.5032	573.99	189.57	-2.07516	69.6006
2169.890		14.6786	460.85	236.23	3.06242	95.3926
2508.885		16.9586	398.58	94.48	-1.48937	97.3759
2760.834		12.7362	362.21	120.87	-2.09668	83.

Periods of GD 358 observed 23.02.00

#	FREQ	AMPLITUDE	PERIOD	T_MAX	PHASE	WIDTH
1266.939		43.5539	789.30	478.38	2.47510	67.1142
1408.854		25.6521	709.80	537.01	1.52954	58.1462
1631.688		7.5278	612.86	450.27	1.66690	66.7285
1990.920		8.7928	502.28	469.06	0.41557	50.4432
2138.125		11.4882	467.70	136.33	-1.83151	54.4691
2416.651		11.2218	413.80	114.13	-1.73302	82.8767
2642.429		18.2481	378.44	368.67	0.16219	86.7610
3888.278		9.6834	257.18	100.65	-2.45888	82.3748
5402.018		6.2369	185.12	97.69	2.96748	67.0780
7925.963		8.6429	126.17	106.61	0.97414	53.5932

Table 7.3: Observed periods of GD 358 in Skibotn 22.02 and 23.00

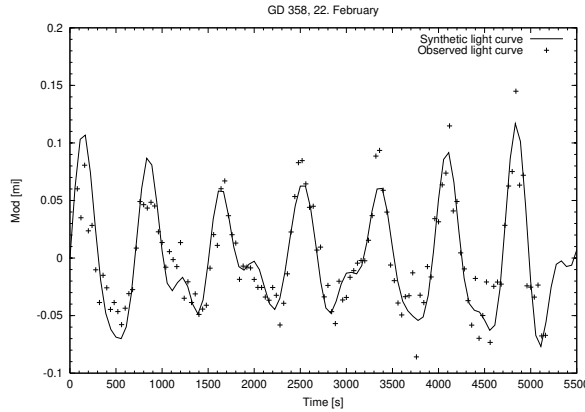


Figure 7.15: Differential photometry of GD 358, 2202. The observed light curve is with dots, and the solid line shows the synthetic light curve.

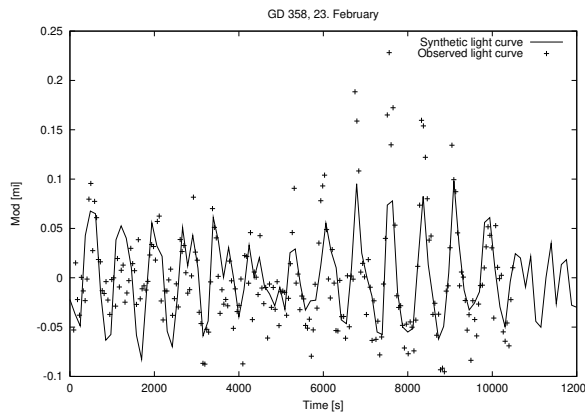


Figure 7.16: Differential photometry of GD 358, 2203. The observed light curve is with dots, and the solid line shows the synthetic light curve.

observed light curve. The first night the synthetic curve fits quite well to the observation. The second night the amplitude in the synthetic spectrum is too low. The reason for this can be that our run is too short to have the whole beat period.

The star has a beat period as we see in figure 7.12. The length of the period can be determined by taking the difference between the two largest peaks in the FT. In our data from the second day of observation of GD 358 the difference between the largest peaks are $142 \mu\text{HZ}$ which is approximately 2 hours.

In figure 7.17 and 7.18 we have marked the frequencies from table 7.2 on the amplitude spectra for the two nights.

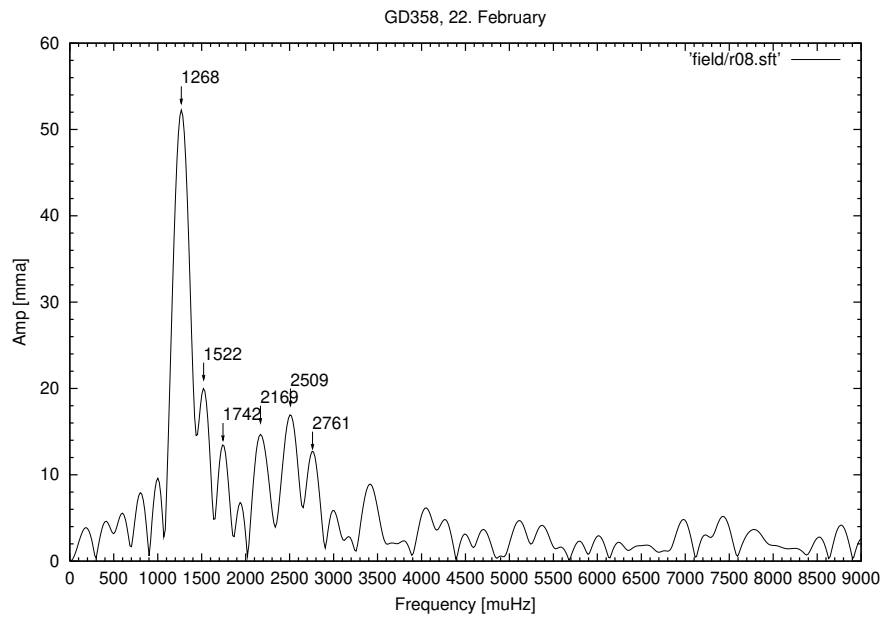


Figure 7.17: Fourier Transform of GD 358, 2302 with the identified periods marked.

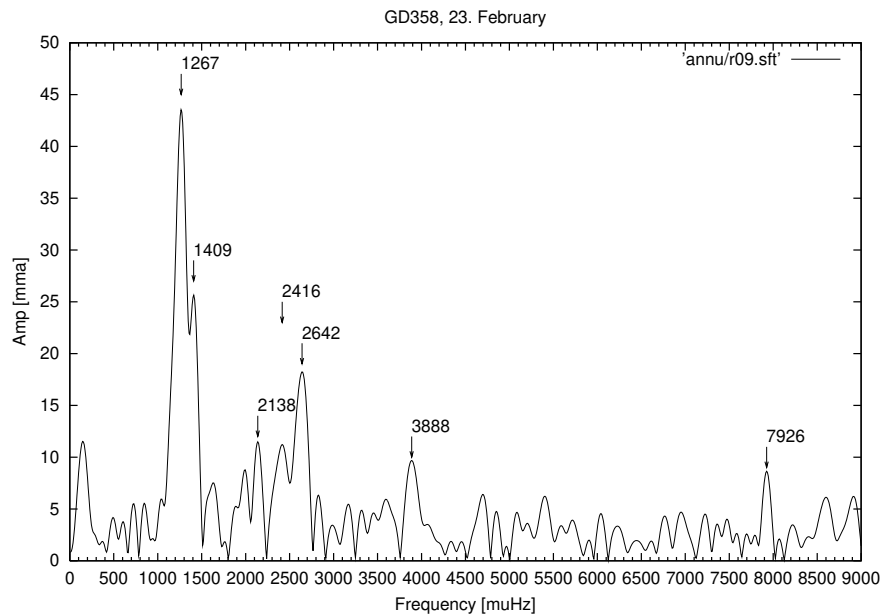


Figure 7.18: Fourier Transform of GD 358, 2302 with the identified periods marked.

Chapter 8

Conclusion

The TCP has been developed during the last years by the Astrophysics group in Tromsø, as a doctor project for Roy Østensen, and tested at NOT, Moletai and in Skibotn the last year. In these thesis, from the observations done in Skibotn, we have showed that the Tromsø CCD Photometer (TCP) is a very good instrument for high speed photometry on variable stars. It has improved the possibility of observation with the Skibotn telescope from 8 magnitude stars to 14 magnitude under auroral conditions.

Both hardware and software work good for the job they have been made for. It is fully portable, and with the possibility of getting the light curve in real time, it can be a instrument for the future for WET type of observations and in the work of discovering new short period pulsating stars.

The observation of AM CVn with 14.5 magnitude brightness and 10 mma main pulsation shows that with this instrument we can do real science with our 50 cm telescope under auroral conditions. In a single night the noise in the FT from the differential photometry, had a average of 1.5 mma. Combining several nights of observation of the same star lowered the noise level down to 1 mma. During the observations the background sky varied from 16.2 mag/−2 to 19.2 mag/−2. For comparison the sky brightness at Mauna Kea is 22.5 mag/arcsec−2 [Walker (1987)].

With the long light curves obtained for AM CVn, we can make FT on parts of the lightcurve. When comparing parts with and without aurora in the background, we found less differences than expected. The TCP corrected well even with strong aurora in the background. In less than three hours we could detect the 10 mma peak at 1902 μHz .

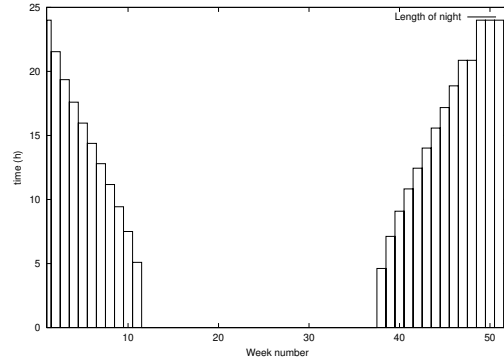
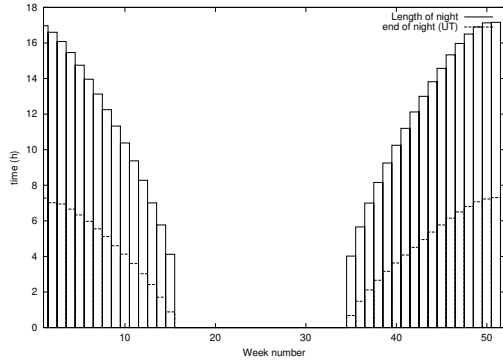


Figure 8.1: Length of observing night in Skibotn as a function of week number. Figure 8.2: Length of observing night on Svalbard as a function of week number.

Based on these results we may evaluate the use of the Arctic regions for high speed photometry. Two important parameters are needed to evaluate this: The length of the night and the number of clear nights available.

During the winter we have 6 observations that continued to the end of the night. From this we can calculate the sun elevation at the time we had to stop observation.

Date	Object	End time (UT)	Sun Altitude (degrees)
1502	AM CVn	05:12	-10:33
1602	AM CVn	05:10	-10:23
1702	AM CVn	05:12	-09:53
2202	GD358	04:35	-11:22
1403	LX Ser	03:32	-09:10
1603	LX Ser	03:11	-10:05

The average of Sun altitude is 10° below the horizon when we had to stop. This can be considered as a limit for the observing night. Because Skibotn is far north (69°), we have long nights in the winter and midnight sun in summer. If we take -10° as a limit, the length of each night during a year is represented graphical in figure 8.1. We did the same calculations for Longyearbyen, Svalbard, as seen in figure 8.2.

Using the long dark period for continuous photometry has many advantages. Only one telescope and one observer is needed to follow the object. When it is too bright to observe in the Arctic, the instrument can be moved to observatories at lower latitudes. This way a high cost instrument can be

used at observatories that can't afford to make their own instruments like this.

The system is newly developed, and this was one of the first tests of its performance. It is not finished, and we are still working with both the hardware and the software. On the hardware side, many improvements have already been made after the observations were finished this winter. A new shutter is made with a wider angle for the opening. To avoid reflections the new version of the filter and shutter unit will be made black inside. A possibility to change filters during the observations is implemented in the software.

Appendix A

Observation log

Here we list up the days spent in at the Skibotn Observatory not presented in chapter 5. An overview of the observations are put in the table below.

A.1 17.-20. January 2000

Monday 17.01.

After the last trip with Roy, I was ready to start my observations with the TCP. Frank and I went to Skibotn Monday 17. At 2330 the sky was clear, and we were ready to observe. Temperature -5° . Target GSC 1929+34. The almost full moon was dominating the background light, and there was no sign of aurora. After just short observation thin clouds came, and around 0030 UT the sky was completely cloudy. This first night of photometry with the TCP was only half an hour with observation, and no results will be shown.

NB: The dome is manually controlled from the control room. We needs a system to remind to move the dome, or even better an automatic system.

Tuesday 18.01.

The weather was very nice in the morning; cold and clear. I went skiing in the morning. Before it was dark, the sky were covered by clouds. It was cloudy during all observation time, and no observations were made..

date	start/stop	object	type	mark	sky/temp(chip/out)
0812		M74	bvri		good, -50.08/-13.9
0812	2131	SAO52680	bvri		-/-13.1
0812	2223	HS2333+3927	bvri		nice
0812		M42			
0812		flats	bvri		
1112		NGC7013			
1812	1436	sky	flats	test	
1812		dome	phot	test	
1912		dome	phot	test	
0701		test Tromsø	phot	test	
1001		test Tromsø	phot	test	
1701	2330	GSC 1929+34	phot	first real	-/-5
1901	2215	SAO75202	photometry	75 files	-/-11.3
2701	2130	SAO77170	phot.	311 files	1/2 cloud, -44/-6.6
0702					
0802		sky	flats	good	
0802		SAO92511	phot.	408 files	
0802		AM CVn	phot.		
0802		WDS4700			
0902	2130	M1	bvri	good	-/0.6
0902		WDS4200	picture		
0902		GS1310:2140	phot.		
1402		dome	bias/flat		
1502		moon			
1502		flats	B		
1502	1900/0612	AMCVn	phot.	good	-/-10.2
1602		flats	B		
1602	1907/0615	AMCVn	phot.	good	-/-11
1702	1930/0630	AMCVn	phot.	good	-/-7.0
1702		flats	B		
2202		flats	B		
2202		VV47	PNN		
2202	2040/2209	AMCVn	phot.		good, -/-8
2202	0408/0535	GD358	phot.	good	
2302		flats	B		
2302	0000/0306	GD358	phot.	good	-/-12
2402		dome	phot		
1403		M3	picture		-37/-8
1403		M92			
1403	0121/0332	LX Ser	phot.	good	-38/-10.4
1603		moon	bvri		
1603		sky	flats		
1603		M1	bvri	good	
1603		M92	bvri	good	
1603	2111	LX Ser	phot.	good	-39.6/-9

Wednesday 19.01.00

The night started good, but after only 86 frames of SAO75202 the clouds came and ruined the observation. No results will be represented.

A.2 26.-27. January 2000

We arrived at the Observatory at 1200 with Torfinn. The program for the trip was to learn Rimas how to use the TCP. It was snowing all day, so no observations were made.

The next day, at 2130 the sky was clear, and we started the observation. The target was a V-mag 9 star. We started with the B-filter but the comparison star was too weak, so we started again with no filter.

The data from this night was poor because of the clouds.

NB: The auto tracking was still not working, but we installed new software, CCD Track for Sbig4. We had a problem with the telescope moving. The slow speed on the hand controller in the dome, did not work. This was fixed later by Frank Johannessen.

A.3 07.-8. February 2000

We drove from Tromsø at 1600, and arrived at Skibotn 1800. It was cloudy, so we made no observations. The TCP had still starting problems. We took the camera off the telescope and put the filters in the right order (B, V, R, I, none, block). Then we changed the cover for one of the holes in the shutter from cardboard to plastic. (The cardboard got wet and touched some parts inside the photometer head.)

The next morning it was partly clouded. We mounted the TCP on the telescope. In the afternoon, we took flat-fields. There were problems with calibrating the filter wheel. No observations made this night.

Bibliography

- Bohm-Vitense, E.** *Introduction to stellar astrophysics*, volume 1. Cambridge, 1989.
- Bone, N.** *The Aurora, Sun-Earth interactions*. Ellis Horwood, 1991.
- Bradley, P. A.** White dwarf data tables. *Baltic Astronomy*, **7**, 355, 1998.
- Brekke, A.** *Physics of the Upper Polar Atmosphere*. John Wiley & Sons Ltd, 1997. ISBN 0-471-96018-7.
- Brekke, A.** Fysikk i den polare atmosfære og nordlyset. University of Tromsø, 1998. In Norwegian.
- Eather, R.** An aurora watcher's guide. *Sky& Telescope*, page 42, 2000.
- Egge, K. E.** Fotometri og analyse av formørkelser i kontaktbinærstjerner. Master's thesis, University of Tromsø, 1982. In Norwegian.
- Hoffmeister, C., G. Richter, and W. Wenzel.** *Variable Stars*. Springer, 1985.
- Høydalsvik, S.** Fotometriobservasjonar av stjerneokkultasjonar ved måneranda. Master's thesis, University of Tromsø, 1980. In Norwegian.
- Jones, A. V.** *The Aurora*. Dordrecht : D. Reidel, 1974.
- Kitchin, C. R.** *Astrophysical Techniques*. Adam Higler, 1991.
- Myrabø, H. K.** Stjernefotometri i nordlyssonen. Master's thesis, University of Tromsø, 1976. In Norwegian.
- Nather, R.** Gd 358 in 1994: A progress report. *Baltic Astronomy*, **4**, 321, 1995.
- O'Donoghue.** High speed ccd photometry. *Baltic Astronomy*, **4**, 519, 1995.

- Østensen, R. H.** *Time Resolved CCD Photometry; Development of a multi-windowing system and test on variable subdwarf stars.* PhD thesis, University of Tromsø, 2000.
- Østensen, R. H. and J.-E. Solheim.** Result from the tomsø ccd-photometry project. *Baltic Astronomy*, **9**, 411, 2000.
- Solheim, J.-E.** Whole earth telescope observations of an am canum venaticorum -discoseismology at last. *Astron, Astrophys*, **332**, (3), 939–957, 1998.
- Solheim, J.-E., R. Kamben, R. Østensen, and R. Thomassen.** Pulsating white dwarfs and dancing aurora. *Astronomy& Astrophysics*, 2000. in press.
- Thomassen, T.** Presisjons fotometri ved skibotn observatorium. Master's thesis, Universitetet i Tromsø, 1996. In Norwegian.
- Vuille, F.** Nonlinear behavior of the pulsating white dwarf gd 358. *Baltic Astronomy*, **9**, 33, 2000.
- Walker, G.** *Astronomical Observations, An Optical Perspective.* Cambridge University Press, 1987.